

AD-A131 084

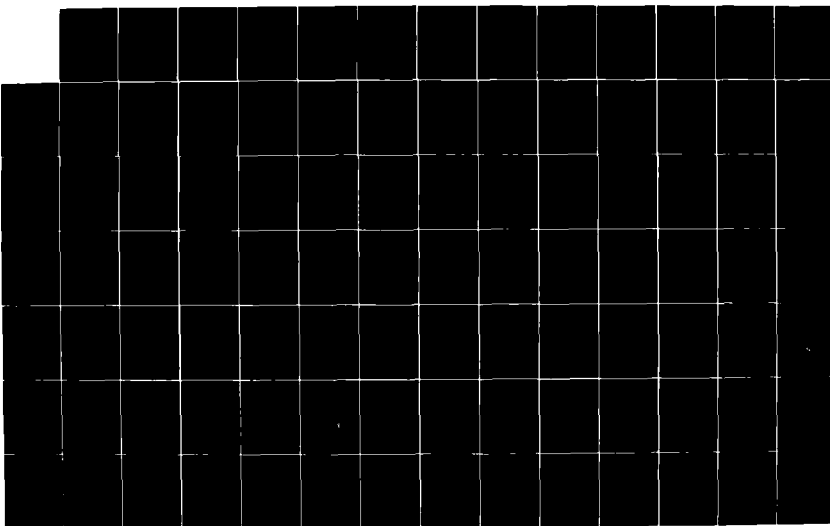
MICROBIAL FOULING AND ITS EFFECT ON POWER GENERATION  
(U) MONTANA STATE UNIV BOZEMAN DEPT OF CIVIL  
ENGINEERING AND ENGINEERING MECHANICS  
W G CHARACKLIS ET AL. JUL 83

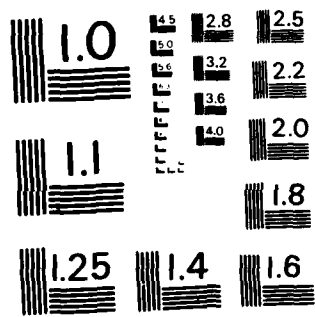
1/2

UNCLASSIFIED

F/G 13/10

NL





MICROCOPY RESOLUTION TEST CHART  
NATIONAL BUREAU OF STANDARDS-1963-A

ADA 131084

12

MICROBIAL FOULING AND ITS  
EFFECT ON POWER GENERATION

by

W.G. Characklis  
F.L. Roe  
M.H. Turakhia  
N. Zilver

Final Report  
July, 1983

Prepared for M.K. Ellingsworth, Program Monitor  
Power Program  
The Office of Naval Research  
Arlington, Virginia 22217

Under Contract N00014-80-C-0475

Approved for public release; distribution unlimited.  
Reproduction in whole or in part permitted for any purpose  
of the United States Government

Department of Civil Engineering  
Montana State University  
Bozeman, Montana 59717

Copy available to DTIC does not  
permit fully legible reproduction

DTIC FILE COPY

RECEIVED  
JUL 13 1983  
A

88 08 03 033

## **DISCLAIMER NOTICE**

**THIS DOCUMENT IS BEST QUALITY PRACTICABLE. THE COPY FURNISHED TO DTIC CONTAINED A SIGNIFICANT NUMBER OF PAGES WHICH DO NOT REPRODUCE LEGIBLY.**

SECURITY CLASSIFICATION OF THIS PAGE (When Data Entered)

REPORT DOCUMENTATION PAGE		READ INSTRUCTIONS BEFORE COMPLETING FORM
1. REPORT NUMBER N00014-80-C-0475	2. GOVT ACCESSION NO. AD-A131854	3. RECIPIENT'S CATALOG NUMBER
4. TITLE (and Subtitle) MICROBIAL FOULING AND ITS EFFECT ON POWER GENERATION		5. TYPE OF REPORT & PERIOD COVERED Final Report May 15, 1980 - May 14, 1983
		6. PERFORMING ORG. REPORT NUMBER
7. AUTHOR(s) W.G. Characklis		8. CONTRACT OR GRANT NUMBER(s) N0014-80-C-0475
9. PERFORMING ORGANIZATION NAME AND ADDRESS Dept. of Civil Engineering/Engineering Mechanics Montana State University Bozeman, MT 59717		10. PROGRAM ELEMENT, PROJECT, TASK AREA & WORK UNIT NUMBERS
11. CONTROLLING OFFICE NAME AND ADDRESS Office of Naval Research 800 N. Quincy St Arlington, VA 22217		12. REPORT DATE July 1983
		13. NUMBER OF PAGES
14. MONITORING AGENCY NAME & ADDRESS (if different from Controlling Office)		15. SECURITY CLASS. (of this report) Unclassified
		15a. DECLASSIFICATION DOWNGRADING SCHEDULE
16. DISTRIBUTION STATEMENT (of this Report)  Approved for public release; distribution unlimited		
17. DISTRIBUTION STATEMENT (of the abstract entered in Block 20, if different from Report)  Approved for public release; distribution unlimited		
18. SUPPLEMENTARY NOTES		
19. KEY WORDS (Continue on reverse side if necessary and identify by block number)  biofouling, biofilms, heat exchangers, corrosion, scaling, frictional resistance		
20. ABSTRACT (Continue on reverse side if necessary and identify by block number)  This report describes results of laboratory experiments conducted to determine the influence of fouling biofilm formation on heat transfer resistance and fluid frictional resistance. The research is directed at problems of power generation on ship board.		

DD FORM 1473  
1 JAN 73

EDITION OF 1 NOV 65 IS OBSOLETE

S N 0102-LF-014-6601

SECURITY CLASSIFICATION OF THIS PAGE (When Data Entered)

TABLE OF CONTENTS

	<u>Page</u>
I. INTRODUCTION-----	1
Fouling - A Definition-----	1
Types of Fouling Deposits-----	2
Problems Caused by Fouling-----	3
Consequences-----	3
II. MODELLING BIOFILM PROCESSES-----	5
The Iterative Nature of the Procedure-----	6
Rate and Stoichiometric Analysis-----	6
System Definition-----	8
Conservation Equations and Constitutive Properties-----	8
Fundamental Rate Processes-----	11
III. BIOFILM FORMATION: A PROCESS ANALYSIS-----	13
Transport to the Wetted Surface-----	13
Transport Mechanisms-----	14
Influence of Surface Roughness-----	15
Consequences of Transport Rates on Biofilm Development-----	16
Summary of Transport Processes-----	16
Adsorption of a "Conditioning" Film-----	17
Rate and Extent of Adsorption-----	17
Characterization of the Conditioning Film-----	18
Adhesion of Microbial Cells to the Wetted Surface-----	19
Hydrodynamic Effects-----	19
Physicochemical Forces-----	20
DLVO theory of adhesion-----	20
Interfacial free energy and adhesion-----	21
Other non-covalent forces-----	22
Extracellular Polymeric Substances (EPS)-----	22
Bacterial EPS-----	23
Microalgal EPS-----	25
Reactions within the Biofilm-----	27
Mass Transfer and Diffusion-----	28
Summary of Biofilm Reactions-----	30
Detachment of Biofilm-----	31
Hydrodynamic Influences-----	31
Chemical Treatment-----	32
Summary of Detachment Processes-----	32

Accession For

23

A



Table of Contents (Continued)		<u>Page</u>
IV.	PROPERTIES AND COMPOSITION OF BIOFILMS-----	33
	Physical Properties-----	33
	Chemical Properties-----	34
	Macromolecular Composition-----	34
	Cellular Densities-----	35
V.	FACTORS INFLUENCING FUNDAMENTAL RATE PROCESSES-----	36
	Physical Factors-----	36
	Chemical Factors-----	36
	Biological Factors-----	36
VI.	MEASUREMENT AND SIMULATION-----	38
	Laboratory Measurements-----	38
	Field Measurements-----	38
	Measurement Related to Fouling-----	39
	Monitoring the Progression of Fouling-----	39
	Characteristics of Fouling Deposits-----	40
	Important Environmental Factors-----	40
VII.	MODEL REACTORS-----	46
	Methods-----	46
	Geometries-----	48
	Tubular Reactor-----	49
	Annular Reactor-----	51
	Rotating Disk and Radial Flow Reactor-----	52
VIII.	BIOFILM PROPERTIES INFLUENCING TRANSPORT PROCESSES-----	54
	Friction Factor-----	54
	Laboratory Results-----	57
	Mechanisms-----	59
	Tube Constriction-----	59
	Biofilm Creep-----	59
	Filamentous Organisms-----	72
	Conclusions-----	75
IX.	BIOFILMS AND HEAT TRANSFER-----	76
	Fouling Measurement-----	76
	Frictional Resistance-----	76
	Overall Heat Transfer Resistance-----	78
	Deposit Thickness-----	81
	Overall Heat Transfer Resistance-----	81
	Fouling Resistance-----	84

Table of Contents (Continued)		<u>Page</u>
	Combined Heat Transfer and Friction Resistance-----	86
	Fouling Diagnosis Potential-----	86
	Field Observations-----	86
	Microbial Cell Accumulation in a Finned Tube-----	88
	Experimental System and Methods-----	91
X.	MICROBIALY-ASSISTED CORROSION-----	97
	Principles of Aqueous Metallic Corrosion-----	97
	Influence of Microbial Product Formation on Corrosion-----	98
	Extracellular Polymeric Substances (EPS)-----	98
	Role of Differential Aeration Cells-----	101
	Acid Production by Bacteria-----	101
	Sulfate Reducing Bacteria-----	104
	Biofouling, Biofouling Control, and Corrosion-----	106
	Biofouling Control Methods-----	107
	Corrosion-----	107
	Experimental Methods-----	109
	Recycle Tubular Loop (RTL)-----	109
	Feed Water-----	111
	Analytical Methods-----	113
	RTL Operation-----	113
	Results-----	115
	Control Experiments-----	115
	Microbial Cell Counts-----	115
	Scanning Auger Microprobe-----	115
	Chemical Analysis of Deposits-----	122
	Filtration of Influent Water-----	122
	Chlorination of Influent Water-----	122
	Discussion-----	129
	A Conceptual Model-----	129
	Influence of Substrate Loading Rate on Deposition-----	132
	Influence of Deposit Mass on Corrosion Rate of Cu-Ni-----	133
	Influence of Microbial Cell Numbers on Corrosion Rate of Cu-Ni-----	134
	Detachment of the Fouling Deposit and Corrosion Rate in Cu-Ni-----	135
	Chlorine Treatment and Corrosion of Cu-Ni Alloys-----	135
	Summary-----	136
XI.	BIOFOULING CONTROL-----	137
	Fundamental Fouling Processes-----	137
	Breaking the Chain-----	138
	Biofouling Control with Chlorine-----	139

Table of Contents (Continued)	<u>Page</u>
Transport of Chlorine-----	141
Water Phase-----	141
Biofilm-----	142
Reaction of Chlorine-----	142
Water Phase-----	142
Biofilm-----	143
Condenser Surface-----	143
Biofilm Removal and/or Destruction-----	144
Biofouling Control Through Disinfections-----	145
Biofilm Regrowth-----	145
Discussion-----	146
Research Needs-----	147
References-----	157

## I. INTRODUCTION

Fouling of surfaces in marine environments is a problem which affects a wide variety of systems from ship hulls to heat exchangers. System performance, as well as operating costs, suffer due to energy losses in the form of increased fluid frictional and heat transfer resistance. Most studies to date have avoided addressing fundamental questions concerning fouling in fluid flow and heat transfer systems and their effect on fluid frictional and heat transfer resistance.

The fouling process begins with transport of materials (soluble and particulate) to a surface and their adsorption or firm adhesion to the surface. The factors which affect these processes, such as surface material, surface active films, and shear stress, determine the rate and extent of deposit accumulation during the early stages of deposit accumulation.

The initial accumulation phase is followed by a rapid, frequently logarithmic, increase in the deposit thickness and/or mass. The extent and rate of growth are moderated by factors such as water quality and shearing forces at the fluid-deposit interface. Generally, a pseudo-steady state deposit accumulation develops where loss of deposit mass to the bulk fluid (primarily due to fluid shear forces) balances production of new deposit due to physical, chemical, and/or biological processes. This report will discuss the rate and extent of accumulation of biofouling deposits, inorganic deposits, and their combination.

Resulting frictional and heat transfer resistance are closely related to specific properties of the deposit. For example, viscoelasticity and roughness of the deposit affect fluid frictional and convective heat transfer resistance, while deposit thickness and thermal conductivity influence conductive heat transfer resistance. This report will discuss the contrasting influences of fouling biofilms and inorganic scale deposits on energy losses.

Corrosion is another important deleterious effect of fouling deposits. Under-deposit corrosion is considered as one of the most serious forms of deterioration. Experimental results are reported regarding the influence of biofouling on corrosion of titanium and copper-nickel 70-30.

This final report for our project period, 15 May 1980 through 14 May 1983, describes results of research projects related to fouling biofilm processes, the interaction between biofouling and precipitation (scaling) processes, and the interaction between biofouling and corrosion processes. The research also focused on the influence of alloys (titanium and copper-nickel 70-30) and to a lesser extent, biofouling control procedures (Cathelco and chlorine) on fouling, corrosion, and energy losses.

FOULING - A DEFINITION

Fouling refers to the formation of deposits on equipment surfaces which significantly decreases equipment performance and/or the useful life of the equipment.

#### TYPES OF FOULING DEPOSITS

Several types of fouling, and their combinations, may occur and have been conveniently classified (Epstein, 1979):

1. Biological fouling: the attachment and metabolism of macroorganisms (macrobial fouling) and/or microorganisms (microbial fouling).
2. chemical reaction fouling: deposits formed by chemical reaction in which the surface material (e.g., condenser tube) is not a reactant. Polymerization of petroleum refinery feedstocks is an important example of this type fouling.
3. corrosion fouling: the surface material itself reacts with compounds in the liquid phase to produce a deposit or degrade the surface material.
4. freezing fouling: solidification of liquid or some of its higher melting point constituents on a cooled surface.
5. particulate fouling: accumulation on the equipment surface of finely divided solids suspended in the process fluid. Sedimentation fouling is an appropriate term if gravity is the primary mechanism for deposition.
6. precipitation fouling: precipitation of dissolved substances on the equipment surface. This process is termed scaling if the dissolved substances have inverse temperature solubility characteristics (e.g.,  $\text{CaCO}_3$ ) and the precipitation occurs on a superheated surface.

In most operating environments, more than one type of fouling will be occurring simultaneously. For example, microbial fouling is not limited to processes related to biological activity. The term may also include the interaction of the microorganism and the associated slime layer with both the chemistry of the equipment surface and the bulk fluid. The interaction can enhance some of the more commonly observed phenomena such as particulate, sedimentation, and corrosion fouling.

The interactions between the various types of fouling are poorly understood and, consequently, provide a challenge to the water treatment chemist or engineer in terms of diagnosis and treatment.

## PROBLEMS CAUSED BY FOULING

The economic consequences of fouling are the essential reason for research interest in the fouling of heat transfer equipment. To assess the importance of a fouling situation, the economic and energy penalties arising from the operation of heat transfer and other equipment subject to fouling must be considered. The deleterious effects of fouling include the following:

1. energy losses due to increased fluid frictional resistance and increased heat transfer resistance.
2. increased capital costs for excess surface area in heat exchange equipment to account for fouling heat transfer resistance.
3. increased capital costs for premature replacement of equipment experiencing severe under-deposit corrosion.
4. unscheduled turnarounds or downtime, resulting in loss of production, to clean heat exchange equipment which fouled at an unanticipated rate.
5. reduced performance of sonar domes and periscope windows.
6. increased fuel consumption by ships due to fouling of the hull and propeller resulting in increased drag.
7. accelerated corrosion and impaired water quality in shipboard drinking water systems.
8. safety problems resulting from "leakers" caused by corrosion pits which penetrate the entire tube thickness in heat exchange equipment.

In summary, the anticipated presence of significant fouling can offset the size and other design features of operating equipment. The operation of this equipment subject to fouling is constrained by the need to formulate economically justifiable cleaning schedules.

Some progress is evident in the understanding of the specific types of fouling described above. However, the criticism most often directed at such research is that seldom does one specific type of fouling occur in any relevant, technical-scale application. This report will focus on the interaction between chemical, physical, and biological processes contributing to fouling deposition, measuring the deleterious effects of those deposits on heat exchanger performance, and evaluation of strategies for deposit control.

## CONSEQUENCES

Cooling water contains an endless variety of "impurities" which may lead to the formation of a fouling deposit including the following: dissolved organics and inorganics, particulates, and microorganisms. The fouling deposits are major causes of energy losses in the electric power industry, chemical process industry, and for the Navy. In fact, fouling has been referred to as the "major unresolved problem" in heat transfer (Taborek *et al.*, 1972). Lund (1981) estimate the annual fouling cost to the United States in 1980 at 1.8-2.9 billion dollars. These costs include increased capital costs for added heat transfer surface, energy losses, maintenance costs, and loss of production. Others have also estimated the dramatically high costs of fouling (Somerscales and Knudson, 1981; Garey, *et al.*, 1980; Chenoweth and Impagliazzio, 1981).

Generally, fouling is accounted for in engineering design of heat exchangers by adding extra surface area (i.e., fouling resistance) in addition to the "clean design area." The values for fouling resistance are selected from tables containing data of questionable accuracy and frequently obtained from unidentified sources. The extra surface area frequently is more than half of the total heat exchanger area and accounts for a significant fraction of the exchanger cost. Moreover, selection of a high fouling resistance does not guarantee prolonged operation of the heat exchanger. This design procedure also increases the size and weight of the exchanger unnecessarily, a problem of major concern to the Navy.

## II. MODELLING BIOFILM PROCESSES

Fouling is a complex phenomenon resulting from several processes occurring in parallel and in series. The rate and extent of these processes, in turn, are influenced by numerous physical, chemical, and biological factors in the immediate environment of the surface. Many laboratory experiments and field observations have resulted in volumes of data without deducing relationships of wide, general use. Much of the historical data available, in addition to future experimental fouling work would benefit from a conceptual framework for describing fouling processes. If the conceptual framework could be stated in mathematical terms, more benefits would accrue including the ability to mathematically simulate fouling processes on the computer...computer "experiments" frequently being cheaper than laboratory experiments.

A rational approach, as contrasted with an empirical approach, develops the conceptual framework by resorting to fundamental processes which are reasonably well understood. These fundamental processes can usually be described mathematically which is necessary for computer simulation. Consequently, such "models" can be used to extrapolate and generalize experimental results.

The difficulty in generalizing or extrapolating experimental fouling data is related to the complexity of the process which frequently involves heat transfer, mass transfer, momentum transfer, as well as physical, chemical, and biological processes at the surfaces. The rational approach attempts to elucidate each of the fundamental processes that contribute to the overall fouling process. Once these fundamental processes are properly understood, they are incorporated into a mathematical model of the overall fouling process. This requires experiments designed specifically to investigate particular fundamental processes rather than experiments which consider only the overall process. This approach is clearly more time consuming than research which only considers the overall fouling process, but it ultimately leads to results that can be applied with greater confidence to a wider range of fouling situations.

This type of "process analysis" has been described previously by Characklis (1981) for the specific case of microbial fouling. Burrill (1981) presents another illustration of the power of this technique in explaining a practical problem of fouling and the decisions necessary to minimize its effects.

These procedures can also lead to computer simulation "experiments" which can be used to test design concepts such as the influence of metallurgy, shear stress, heat flux, geometry, etc., on fouling processes and their influence on equipment performance. Simulation can also be used to test operating and maintenance procedures such as internal treatments and cleaning schedules. The process analysis technique may also lead to a more systematic method for developing and evaluating fouling control techniques,

regardless of whether they employ physical, chemical, or even biological methods. These ideas will be discussed below.

In summary, the rational approach to fouling entails a process analysis which identifies the contributing fundamental processes and determines the influence of process variables on process rate and extent. The approach requires experimental measurement techniques which permit the elucidation of the specific processes.

#### THE ITERATIVE NATURE OF THE PROCEDURE

Developing a rational understanding of the fouling process is an iterative process. Figure II-1 schematically describes some of the interrelationships between four of the important activities within this iterative process:

Cycle 1-EFFECTS OF FOULING are MEASURED by some appropriate instrument to test the performance of the equipment. The extent of the problem is determined and a FOULING CONTROL PREVENTION TREATMENT is applied. Any change in the EFFECTS OF FOULING are observed and the cycle is repeated.

Cycle 2-A process analysis is accomplished to determine the RATE AND STOICHIOMETRY of the process from which a model is developed. The influence of treatment procedures on rate and stoichiometry may be critical. The model is tested with a SIMULATION of the real system in which process variables can be carefully controlled. Reformulation or modification of the model may follow.

The overlap between the two cycles is MEASUREMENT AND SIMULATION. Simulating the process environment, in the laboratory or the field, is critically important to the rational approach and cannot be overemphasized. The usefulness of a model, and its ability to describe reality, is strictly dependent on the accuracy of the data used to develop and test the model.

#### RATE AND STOICHIOMETRIC ANALYSIS

The physical, chemical, and biological transformations resulting in fouling deposit accumulation are completed in a certain period of time. For example, some specific change may signal the shutdown of manufacturing operations and the beginning of cleaning operations. The time required for this specified change is inversely proportional to the rate at which the process occurs. Thus, the rate is the most important quantity in process analysis. If the process consists of a number of processes in series, the slowest

## DEVELOPING UNDERSTANDING...AN ITERATIVE PROCESS

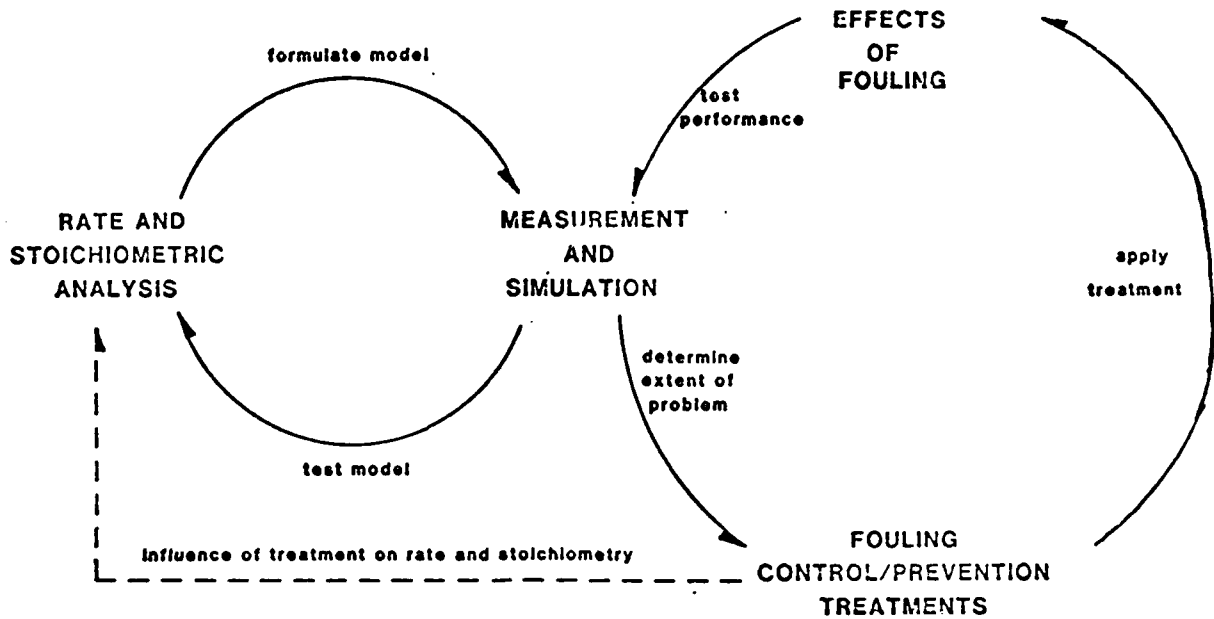
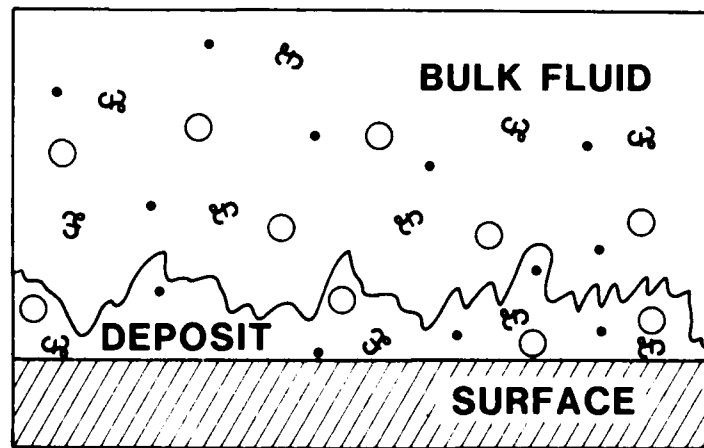


Figure II-1. The relationship between various aspects of research, analysis and testing related to fouling processes.



### "PHASE DIAGRAM"

Figure II-2. The fouling environment including microbial cells, macromolecules, and other particulate material in the bulk water and in the deposit.

step of the sequence exerts the greatest influence and controls the overall process rate. This step is called the "rate-determining process" or "rate-controlling process".

Stoichiometry is the application of the law of conservation of mass and the chemical laws of combining weights to chemical processes. Stoichiometry provides information about extent of reaction, composition, and yields.

Rate and stoichiometry are determined by measuring concentrations of reactants and products. In the case of fouling, the reactions take place in the microenvironment of the surface and interfacial concentrations are extremely difficult to measure. Consequently, rate and stoichiometric relationships must be developed as functions of concentrations in the bulk fluid environment. To do so requires a thorough understanding of the fluid flow regime, the nature of the surface, and, when applicable, the temperature gradient at the wall.

The remainder of this section will discuss the environment in which fouling reactions occur and provide an outline of methods for its description and analysis.

#### SYSTEM DEFINITION

Figure II-2 schematically describes the fouling environment. Important features include the following four "phases":

1. fluid phase
2. suspended particulates
3. solid or semi-solid fouling deposit
4. the substratum

The fluid phase contains dissolved organics and inorganics as well as the suspended particulates. The fouling deposit frequently contains a large percentage of water (e.g., as much as 80-98 percent in biofouling deposits) but is still considered a solid phase due to lack of fluid motion. The substratum is the equipment surface of concern (e.g., metal condenser tube). In many cases of interest, the fluid phase is in turbulent flow and the substratum is at an elevated (or reduced) temperature from that of the bulk fluid phase.

#### CONSERVATION EQUATIONS AND CONSTITUTIVE PROPERTIES

Analysis of this relatively complex system requires consideration of mass transfer, momentum transfer (i.e., fluid dynamics), and heat transfer as well as physical, chemical, and biological processes. Required tools include the equations for conservation of momentum, energy and mass which are a result of Newton's laws and the laws of thermodynamics.

Table II-1 indicates the intensive variable (i.e.,

variables independent of system mass or volume) and examples of thermodynamic properties that must be measured to utilize the conservation equations effectively. The intensive variables and thermodynamic properties are relatively easy to measure accurately.

Constitutive principles deal with the rates of physicochemical processes. Conservation and thermodynamic principles do not deal with mechanism, but constitutive principles do; constitutive principles deal with mechanism as it is influenced by the constitution of matter. Examples of constitutive principles are the laws that govern rates of transport and rates of chemical reactions.

Since conservation principles do not depend on the constitution of matter, a mathematical model expressing a conservation principle is "correct" if all flows, sources, and sinks have been included. The usefulness of the model, however, depends primarily on two things:

1. The choice of the system.
2. Availability of constitutive principles for description of unknown quantities which appear in the model (e.g., reaction rates).

Mechanisms and constitutions are often poorly understood. Therefore, constitutive relations present the most difficulty in modelling. Transport coefficients (Table II-11), for example, are difficult to measure and accuracy is generally poor, yet, transport coefficients are essential to determining rates of mass, heat and momentum transfer in fouling environments. Reaction rate coefficients ( $K_1$ ,  $u_{max}$ ,  $K_m$  in Table II-1) depend on many environmental factors. In fact, reaction rate coefficients are most often inferred from conservation equations by assuming a kinetic or rate model (e.g., power law or saturation rate equation). The stoichiometric coefficients ( $A_i$  and  $Y$  in Table II-1) are also constitutive properties and relate the rate of consumption or production of one reactant to another.

In modelling a fouling environment, it may be necessary to deal simultaneously with all three conservation equations as well as reaction kinetics. The interrelationships between these various processes often provide the greatest challenge to the investigator. A useful illustration is a recirculating cooling tower (RCT) system in which significant momentum, mass, and heat transfer is occurring in the condenser (heat exchanger) as well as the tower (Figure II-3). These aspects of the RCT system have been adequately described in a mathematical form by Sherwood et al (1975). However, the constitutive relationships describing fouling in the RCT system have received much less attention. The critical concern to equipment operators is the influence of fouling on heat and momentum transfer in the heat exchanger. With reasonably accurate constitutive relationships for fouling processes, these influences can be predicted and, thereby, avoided.

### CONSERVATION EQUATION

	MOMENTUM	ENERGY	MASS
INTENSIVE VARIABLE	$v$	$T$	$c$
THERMODYNAMIC PROPERTIES	$\rho$	$C_p$	$K_{eq}$

### CONSTITUTIVE PROPERTIES

-- TRANSPORT	$\nu$	$\alpha$	$D$
-- CHEMICAL REACTION	$\bullet$	$\bullet$	$K_i, A_i$
-- MICROBIAL REACTION	$\bullet$	$\bullet$	$\mu_{max}, K_s, Y$

Table II-1. The conservation equations and related variables and properties related to fouling in heat exchange systems.

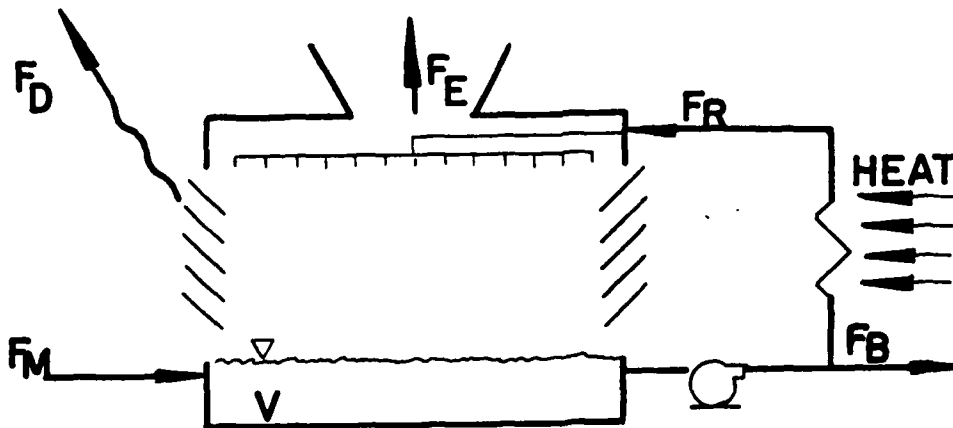


Figure II-3. A recirculating cooling tower system.  $F_M$ ,  $F_D$ ,  $F_E$ ,  $F_R$  and  $F_B$  are flow rates of make-up, drift, evaporation, recycle and blowdown streams, respectively.

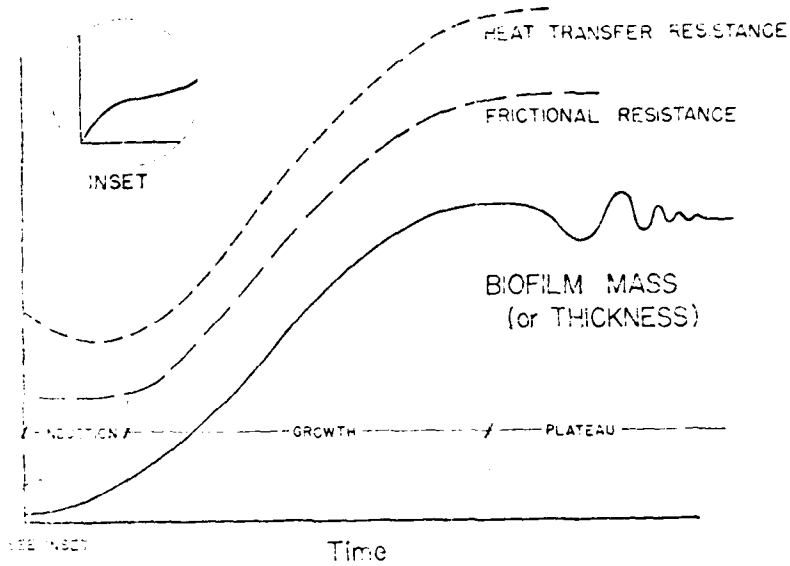
FUNDAMENTAL RATE PROCESSES. The constitutive fouling relationships can be classified into four rate processes which are fundamental to all types of fouling. Fouling deposit accumulation can be considered the net result of the following physical, chemical, and biological processes:

1. transport of soluble and particulate material to the wetted surface,
2. attachment of soluble or particulates to the wetted surface,
3. chemical or microbial reaction at the surface or within the deposit, and
4. detachment, sloughing, or spalling of portions of the deposit from the wetted surface.

The overall result is a progression of events characterized by three identifiable periods (Figure II-4):

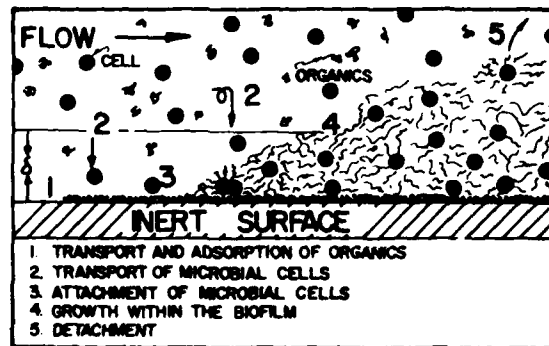
1. an induction period,
2. a rapid increase in accumulation, and
3. an asymptotic or plateau period.

Because fouling rate can be controlled by many process variables, one of the three periods may be negligible in duration compared to the other two.



Progression of Biofouling

Figure II-4. The sigmoidal shaped curve frequently characteristic of fouling progressions. Three periods have been identified.



BIOFOULING PROCESSES

Figure III-1. A summary diagram describing the fundamental processes contributing to the accumulation of a fouling biofilm.

### III. BIOFILM FORMATION: A PROCESS ANALYSIS

In this discussion, biofilm development will be considered to be the net result of the following physical, chemical, and biological processes (Figure II-1):

Transport of organic molecules and microbial cells to the wetted surface.

Adsorption of organic molecules to the wetted surface resulting in a "conditioned" surface.

Adhesion of microbial cells to the "conditioned" surface.

Metabolism by the attached microbial cells resulting in more attached cells and associated material.

Detachment of portions of the biofilm.

#### TRANSPORT TO THE WETTED SURFACE

When a clean surface is immersed in natural water, transport controls the initial rate of deposition. In very dilute suspensions of microbial cells and nutrients, transport of microbial cells to the surface may be the rate-controlling step for long periods of time. Biofilm development in open ocean waters or distilled water storage tanks may be illustrative of these cases. Transport of molecules and particles smaller than 0.01 - 0.1  $\mu\text{m}$  is described satisfactorily in terms of diffusion. In turbulent flow, the diffusion equation must be modified to include turbulent eddy transport (an eddy is a current or bundle of fluid moving contrary to the main current). Transport of such small molecules and particles is relatively rapid compared to transport of larger particles. Consequently, adsorption of an organic film is reported to occur "instantaneously" in many cases.

Transport processes are also significant in later stages of biofilm development. For example, mass transfer and diffusion of nutrients can influence the growth rate of cells within the biofilm (see Section below).

Larger particles develop a sluggishness with respect to the surrounding fluid. As the particle approaches the wetted surface, eddy transport diminishes and the viscous sublayer exerts a greater influence. For soluble matter and small particles, diffusion can adequately describe transport in the viscous sublayer (Lister, 1979; Lin et al, 1983; Wells and Chamberlin, 1967). For larger particles, other

mechanisms must be considered to explain experimental observations.

Within a turbulent flow regime, larger particles suspended within the fluid are transported to the solid surface primarily by fluid dynamic forces. Particle flux to the surface increases with increasing particle concentration. However, particle flux is also strongly dependent on the physical properties of the particles (e.g., size, shape, density) and is influenced by many other forces near the attachment surface.

Microbial cells (0.5 - 10.0  $\mu\text{m}$  effective diameter) can be transported from the bulk fluid to the wetted surface by several mechanisms including the following:

- diffusion (Brownian)
- gravity
- thermophoresis
- taxis
- fluid dynamic forces
  - inertia
  - lift
  - drag
  - drainage
  - downsweeps

**TRANSPORT MECHANISMS.** Particles in turbulent flow are transported to within short distances of the surface by eddy diffusion. Particles are propelled into the viscous (or laminar) sublayer under their own momentum. Turbulent eddies supply the initial impetus and frictional drag slows down the particle as it penetrates the viscous sublayer (Friedlander and Johnstone, 1957; Beal, 1970). For microbial cells, the inertial forces are very small because of their small diameter and density (in relation to water).

If the particle is travelling faster than the fluid in the region of the wall, the lift force directs the particle toward the wall (Rouhiainen and Stachiewicz, 1970). This would normally be the case if particle density is greater than fluid density and the particle is moving toward the wall. *Frictional drag forces* can be significant, especially in the viscous sublayer region. The drag force slows down the particle as it approaches the surface and is proportional to the difference between particle velocity and fluid velocity.

If the mass density of the particle differs substantially from the fluid density, the *gravity force* may be significant. For microbial cells in turbulent flow, the gravity force is generally negligible. *Thermophoresis* is only relevant when particles are being transported in a temperature gradient (Lister, 1979). If the surface is hot and the bulk fluid is cold, the

thermophoretic force will repel the particle from the surface. *Eddy diffusion* may be instrumental in dispersing particles in the turbulent core region, thus maintaining a relatively uniform concentration in that region. However, eddy diffusion will not be significant in transporting particles to the wall. *Brownian diffusion* contributes little to the transport of microbial cells ( $\approx 1.0 \mu\text{m}$  diameter) in turbulent flow. Certain microbes are capable of *motility* or *taxis* through their own internal energy independent of fluid forces. Velocities as high as  $50 \mu\text{m s}^{-1}$  have been observed. Taxis could possibly be a significant transport process in laminar flow or within the viscous sublayer. For particles in liquids, the *fluid drainage force* is significant (Lister, 1979). The drainage force describes the resistance the particle encounters near the wall due to the pressure in the draining fluid film between the two approaching surfaces. This force is quite large for a microbial cell as it approaches the wall.

Recent research on the structure of the viscous sublayer in turbulent flow indicates that "*downsweeps*" of fluid from the turbulent core penetrate all the way to the wall (Cleaver and Yates, 1974, 1976). Particles in the bulk fluid are transported all the way to the wall by these convective downsweeps. Aside from lift, this is the only fluid mechanic force directing the particle to the wall. Downsweeps are apparently quite important in terms of particle transport to the wall in turbulent flow.

For a tube 3 cm I.D. with fluid velocity  $100 \text{ cm s}^{-1}$  at a temperature of  $20^\circ\text{C}$ , the bursts resulting from the downsweeps have the following characteristics:

burst diameter	0.11 cm
average axial distance between bursts	0.50 cm
mean time between bursts	0.0006 s

Minimum transport rate of particles would be observed when particle diameter approximates  $0.1 \times 10^{-4} \text{ cm}$  under constant fluid flow conditions. At this diameter, *Brownian diffusion* starts exerting a significant effect. Particle flux from the bulk fluid to the pipe wall for a bulk fluid particle concentration  $10^4 \text{ particles cm}^{-3}$  is approximately  $0.1 \text{ particles cm}^{-2} \text{ s}^{-1}$ .

**INFLUENCE OF SURFACE ROUGHNESS.** Surface roughness significantly influences *transport rate* and *microbial cell attachment* for several reasons including the

following:

1. increases convective mass transport (i.e., mass transport due to fluid motion) near the surface
2. provides more "shelter" from shear forces for small particles
3. increases surface area for attachment

If surface roughness elements are larger than the viscous sublayer, the roughness can be measured quantitatively by hydraulic methods. If surface roughness elements are smaller than the viscous sublayer (i.e., microroughness), measurements of roughness are difficult to quantify and interpret (Thomas, 1982). Browne (1974) reports that particle deposition from gases is very sensitive to surface roughness too small to affect fluid frictional resistance.

#### CONSEQUENCES OF TRANSPORT RATES ON BIOFILM DEVELOPMENT.

When a "clean" surface first contacts water containing biological activity, organic substances and microbial cells must be transported to the surface before biofilm development can begin. Consequently, the rate of transport of these components determines the length of the "induction" period, i.e., the initial period during which no macroscopic effects of the biofilm are evident. In very dilute solutions (e.g., open ocean), the rate of transport may control the overall rate of biofilm development for long periods. Rate of transport is proportional to the concentration difference between the bulk fluid and the surface (Bryers and Characklis, 1981). In dilute solution, this difference is small. The flow regime (zero, laminar or turbulent flow) also significantly influences transport rates and should be defined carefully in any experimental system used for biofilm studies. Maintenance of surface characteristics is also critical in the reproducibility of the results and their application because as surface roughness increases so will transport and attachment rates. Which rate controls--that of transport or that of adhesion?

**SUMMARY OF TRANSPORT PROCESSES.** So little is known about rate of transport of particles (e.g., bacterial cells) in water under fluid flow or quiescent conditions that the cell "striking" rate at a surface cannot be determined. Consequently, net attachment, adsorption, or adhesion is the quantity generally reported. Determination of cell transport rate would permit calculation of a cell sticking efficiency, a useful criterion for comparing performance of coatings, chemicals, and other anti-fouling treatment. Particulate transport research could also determine the dominant transport mechanisms under different conditions and

lead to unique proposals for fouling prevention and/or control.

#### ADSORPTION OF A "CONDITIONING" FILM

Microorganisms select their habitats on the basis of many factors, including the nature of the wetted surface (material of construction and surface roughness). Adsorption of an organic monolayer occurs within minutes of exposure and changes the properties of the wetted surface. Investigations have shown that materials with diverse surface properties (e.g., wettability, surface tension, electrophoretic mobility) are rapidly conditioned by adsorbing organics when exposed to natural waters with low organic concentrations. These organic molecules frequently appear to be polysaccharides or glycoproteins.

**RATE AND EXTENT OF ADSORPTION.** Loeb and Neihof (1975) and DePalma et. al., (1979) have measured adsorption rates of organic molecules in seawater, and Bryers (1979) has observed adsorption rates in a laboratory system. Rate and extent of adsorption in these investigations are presented elsewhere (Characklis, 1981). Rates as high as  $0.45 \text{ nm min}^{-1}$  were observed but maximum accumulation from molecular fouling was always less than  $0.1 \text{ um}$ . The rate of molecular fouling can be considered instantaneous since it is much greater than the rate of microbial fouling. Based on "thickness" measurements, molecular fouling can have no significant effect on fluid flow or heat transfer. Nevertheless, the surface properties resulting from adsorption of an organic film may affect the sequence of microbial events which follow.

A unique aspect of diatom adhesion is that at least one organism may not require surface conditioning films to be present on the substrata before adhesion takes place. Cooksey (1981) found that a washed culture of the diatom *Amphora coffeaeformis* adheres to glass surfaces in less than five minutes. In these experiments, pre-adsorbed macromolecular films could arise from the washing procedure for the glassware, the analytical grade simple salts used in the suspending fluid, or from the cells themselves. Pre-conditioning the substrata with media from previous experiments did not alter the kinetics of the diatom attachment. (B. Cooksey, unpublished results).

Brash and Samak (1978) present experimental evidence that significant turnover occurs in molecular (proteinaceous) fouling films on polyethylene. Protein molecules in the bulk fluid are continuously exchanging with adsorbed proteins. This suggests that dispersed microbial cells and their associated extracellular material maybe

continually exchanging with biofilm material at the wall.

CHARACTERIZATION OF THE CONDITIONING FILM. These new, organically-conditioned interfaces influence considerably the adhesion of microbes. This conditioning film has been investigated by various means. For instance Loeb and Neihof (1975) found that the contact angle (Zisman, 1964) of the platinum-water or -methylene iodide interface increased considerably when the platinum had been exposed to natural sea water. Similar results have been obtained by DeFalma *et al* (1979) in natural systems. The phenomenon did not occur when the organic fraction of the sea water had been photo-oxidized with short-wave uv radiation. From this and some studies of the fluorescence of the adsorbed layer, Loeb and Neihof conclude that the film responsible for the decreased wetting of the platinum is organic and that humic acids may be implicated in its formation. Baier and various co-workers have characterized these acquired films as largely glycoprotein (Baier, 1980; Baier and Weiss, 1975; Marshall, 1979). These conclusions depend on the internal total reflectance infrared spectrophotometric analysis of the films adsorbed on pure germanium prisms. The technique has been described in detail by Harrick (1967). Marshall (1979), from results obtained in collaboration with Baier, implies that because the protein and polysaccharide I.R. absorption signals are detectable on the germanium prism before the onset of bacterial adherence, the formation of the conditioning film is an obligate first step in the attachment of organisms to surfaces. Baier (1980) has made the statement more emphatically. This is probably so in all natural systems because of the universal presence of organic macromolecules in natural waters and differential kinetics of the two processes. There appears to be no evidence, however, that microorganisms can *only* attach to conditioned surfaces. Indeed, some surfaces with adsorbed proteins inhibit bacterial adhesion. For example, Fletcher (1976) showed that the adhesion of a marine *Pseudomonad* to polystyrene was inhibited by albumin, gelatin, fibrinogen and pepsin. The influence of such compounds is certainly not clear-cut since Meadows (1971) found that although albumin was inhibiting in his system, casein and gelatin facilitated the process of adhesion. Adsorption of such molecules decreases the surface-energy of clean, high energy surfaces ( $70 \text{ dynes cm}^{-2}$ ) but has little effect on low energy surfaces ( $20 \text{ dynes cm}^{-2}$ ) (Baier, 1980). The concept of surface energy is discussed further below. One would expect that surfaces of initially differing energies, after conditioning with an adsorbed layer of protein, would influence the adhesion of cells similarly. This appears not to be the case. Baier (1980) has shown that the spread areas of mammalian cells, a parameter related to the

firmness of adhesion, is correlated with the initial energy of the surface, i.e., before conditioning has taken place. Thus, siliconized surfaces promoted adhesion of cells, even after protein conditioning of those surfaces. The configuration of the conditioning film, therefore, must be influenced by the initial surface state of the substratum (Baier, 1980). However, alternative explanations are possible (see below). These subtle modifications of surfaces by organic macromolecules are not reflected in changes of their surface charge. Neihof and Loeb (1972) showed the convergence of surface charge on various types (by means of microelectrophoresis experiments) of particles when exposed to natural sea water. Thus, it seems that the role of conditioning films in the adhesion of cells to surfaces is not yet clear. One of the problems in drawing conclusions from the published investigations in this area of research is related to the use of divergent experimental designs. For instance, various workers have used different microbial types, substrata, and conditioning macromolecules. One further problem lies in the fact that the ability of cells in laboratory culture to adhere sometimes changes with time (Costerton, *et al*, 1981).

#### ADHESION OF MICROBIAL CELLS TO THE WETTED SURFACE

Shortly following the conditioning of the substratum, bacterial adhesion begins. In most studies, adhesion has not been distinguished from colonization which includes the effects of subsequent growth of bacteria. Thus, numbers of bacteria reported on substrata may represent an integration of both processes.

Previous research (Marshall *et al*, 1971; Zobell, 1943) suggests the existence of a two-stage adhesion process: (1) reversible adhesion followed by, (2) an irreversible adhesion. Reversible adhesion refers to an initially weak adhesion of a cell which can still exhibit Brownian motion but is readily removed by mild rinsing. Conversely, irreversible adhesion is a permanent bonding to the surface, usually aided by the production of EPS. Cells attached in this way can only be removed by rather severe mechanical or chemical treatment. The forces influencing both reversible and irreversible adhesion will be discussed below.

**HYDRODYNAMIC EFFECTS.** Most of the research on cell adhesion has been conducted at very low fluid shear stress or in quiescent conditions which suggests sedimentation or diffusion may control the *rate of adhesion*. There is yet to be a demonstration of reversible adhesion in turbulent flow.

In turbulent flow, the *net rate of adhesion* is the quantity most easily measured. The net rate of cell

adhesion is the difference between the rate of cell adhesion and rate of cell detachment. Powell and Slater (1983) clearly show that any analysis which assumes that all cells contacting the surface become irreversibly attached, grossly overestimates the surface cell population. Cell detachment results from several forces including the following:

- fluid dynamic forces
- shear forces
- lift (upsweeps)
- taxis

Upsweeps are analogous to the downsweeps discussed in relation to transport. Downsweeps and upsweeps result in turbulent bursts which move to and away from the surface into the bulk flow. Upsweeps generate a lift force normal to the surface which can influence detachment. Drag or viscous shear forces act in the direction of flow on attached cells and are approximately 1000 times greater than the lift forces acting on attached cells. Note that although viscous shear may dislodge a particle, unless a lift force is present, the particle will presumably roll along the surface until another surface adhesion site is found.

**PHYSICOCHEMICAL FORCES.** The forces that reversibly bind a cell to a surface have been reviewed at various levels of mathematical complexity (Pethica, 1969, 1980; Baier, 1980; Daniels, 1980; Dolowy, 1980; Fletcher, 1980; Gingell and Vince, 1980; Rutter, 1980; Rutter and Vincent, 1980). Despite the large number of reviews and a considerable amount of work, theory does not explain the natural phenomena very well.

There are basically two theories of the initial interactions of cells and substrata. In the first, the electrostatic properties of the system (DLVO theory) are considered, whereas the second considers interfacial free energy of the system ('wettability' theory). DLVO theory of adhesion. The DLVO theory is named for Derjaguin and Landau (1941) and Verwey and Overbeek (1948). The positions of attraction have been called the primary minimum (at small separations) and the secondary minimum (at larger distances of separation). At a point between repulsive forces are maximal. Problems with this approach reside in the values used for the charges on the surfaces, the different geometry at the attachment site, and the varying dielectric constant of the liquid as the two surfaces approach. In addition, Hamaker's constant cannot be measured in these types of systems (Rutter, 1980). The theory predicts that reversible adhesion can take place at the secondary minimum (about 5-10 nm). This at least

appears true and has been described by Marshall *et al* (1971). Time spent at this distance may be sufficient for other adhesive forces to become effective, e.g., polymer bridging. It is unlikely that cells are able to approach a substratum sufficiently closely (e.g., less than 1 nm) to overcome the repulsive peak which exists between the primary and secondary minima. For instance, it has been calculated that the energy developed by a pseudomonad swimming at  $33 \text{ } \mu\text{m s}^{-1}$  is insufficient to overcome this barrier (Marshall *et al*, 1971). The mathematical expression of DLVO theory of particle interaction includes the radius of the particles. As the radius of the particles decreases, the repulsive energy barrier decreases. Thus, when cells are able to reduce their effective radius, as in the production of filopodia (e.g., mammalian cells) or fimbriae (bacteria), they may overcome the repulsive maximum and adhere at the primary attraction minimum (Rogers, 1979; Weiss and Harlos, 1977). All of the results mentioned above have been obtained in systems with little or no fluid shear stress--a situation that rarely obtains in the natural environment.

Interfacial free energy and adhesion. Theoretically, if the total free energy of a system containing a cell and an adjacent substratum is reduced by contact, then adhesion of the cell to the substratum will result. In many cases, adhesion of cells has been related to the critical wetting tension (mammalian tumour cells, Baier, 1980; bacteria, Dexter *et al*, 1979; diatoms, Cooksey, Cooksey, and Baier, see Figure). This parameter is, in turn, related to the contact angle between model liquids and the substrata being studied (Zisman, 1964). Harper and Harper (1967) showed that diatom adhesion to glass was stronger than to plastic. The activity of the surfaces was not reported but the glass probably had the higher surface energy. Diatom adhesion to substrata, as judged by experiments with *A. coffeaeformis*, exhibits the same relationship with substratum surface energy as has been described for other organisms, including minimal adhesion at approximately  $25 \text{ dynes cm}^{-1}$  (Grinnell *et al.*, 1972; Dexter, 1978; Baier, 1970, 1973, 1975).

Pethica (1980) finds the relationship between critical wetting tension and adhesion of particles (cells) to be qualitative at best. Pethica notes that the Young equation demands that particles be homogeneous and the surface be insoluble in the wetting liquid used to measure the contact angle. In practice, none of these requirements are rigorously obtained. Experimental results do allow us, however, some confidence in the use of contact angles for ranking both particles (cells) and the substrata.

Some of the objections related to the measurement of contact angles under one set of conditions, and their application in quite different experimental circumstances, have been overcome by Fletcher and Marshall (1982). They

measured contact angles of experimental surfaces both in the 'clean' and conditioned state in an aqueous system using an air bubble contact method. They found that the relative adhesion of bacteria to plastic substrata became modified by the adsorption of various proteins and these modifications were reflected in a change in measured contact angles.

Other non-covalent forces. Other forces that are responsible for cellular adhesion include hydrogen bonds, hydrophobic interactions, and ionic bonds (bridging). All of these act at short-range (i.e., approximately 1 nm).

EXTRACELLULAR POLYMERIC SUBSTANCES (EPS). Marshall (Marshall *et al.*, 1971; Marshall, 1980) has interpreted the physicochemical theories above in practical terms. Initially, cells are held close to a surface in a state of reversible or temporary adhesion. Cells in this state are often removed by gentle washing of the substratum, but those organisms undergoing gliding motility, although temporarily adhered, are not removed by this stress. If the cell resides at a surface for some critical time, it becomes irreversibly bound through the mediation of a cementing substance. This implies that such cells are no longer motile.

Zobell (1943), a pioneer in the field of microbial adhesion, suggested the participation of extracellular cementing substances in the adhesion of cells to substrata. Since then, considerable attention has been directed at these extracellular polymeric substances (EPS). However, much confusion exists over the terminology for the extracellular material intimately related to biofilms (Bowles and Marsh, 1982). Glycocalyx, slime, capsule, and sheath have all been used in referring to extracellular polymeric substances associated with individual cells, cell aggregates, or biofilms. EPS appears to be the least restrictive term. For example, glycocalyx is defined as "tangled fibers of polysaccharides or branching sugar molecules..." (Costerton *et al.*, 1978). However, in biofilm processes and in microbial adhesion in general, other macromolecules besides polysaccharides and sugars are found within the organic matrix including glycoproteins (Humphrey, *et al.*, 1979), proteins, and nucleic acids (Nishikawa and Kuriyama, 1968). Therefore, unless extensive identification has been performed, components of the organic matrix will be referred to as EPS (Geesey, 1982). EPS can conceivably contribute to biofilm processes in many ways including the following:

1. provide cohesive forces within the biofilm
2. adsorb nutrients
3. protect immobilized cells from rapid environmental changes including the influence of biocides

4. adsorb heavy metals from the environment
5. adsorb particulate material and other detritus
6. serve as a means of intercellular communication within the biofilm
7. provide short term energy storage via the cell membrane potential
8. enhance intercellular transfer of genetic material

EPS also significantly influences the physical properties of the biofilm including the diffusivity, thermal conductivity, and rheological properties. Presumably, water activity and/or osmotic pressure are elevated in a dense aggregate of EPS.

Bacterial EPS. As yet, we have little information concerning the structural analysis of purified adhesive EPS in microbial systems. This is in contrast to the expansive literature on the structure of one of the adhesive EPS of mammalian cells, fibronectin (Olden *et al*, 1980). For light microscopy, EPS can be stained with crystal violet, ruthenium red, and alcian yellow (or blue). Some of the stains have been used also for transmission electron microscopy (TEM). Conclusions concerning the chemical structure of EPS based on staining alone are tenuous (see below). In electron microscopic studies, especially where staining with ruthenium red or other dyes has been applied, bacteria attached to surfaces appear to be enmeshed in fibrillar material with certain of the fibrils bridging to the substratum (e.g. Corpe *et al*, 1976; Fletcher, 1980). The fibrillar nature of such polymers may be an artifact of fixation or drying in preparation for TEM examination, since in nature the EPS is highly hydrated (Geesey, 1982).

There are many qualitative analyses of bacterial EPS-- usually considered to be carbohydrate with acidic groups (Corpe *et al*, 1976; Fletcher and Floodgate, 1973), amino groups (Baier, 1975), and sometimes associated with proteins (Corpe *et al*, 1976). In most qualitative analyses, however, the possibility of multiple polymers of different structures and composition is rarely considered. Thus, the various functional groups may reside on separate polymers, e.g., detection of protein and carbohydrate in an EPS does not imply the presence of a glycoprotein unless the polymer is known to be single, covalently-linked entity. This problem has been recognized recently by Fletcher (1980). Based on electron microscopical histochemical evidence, she earlier postulated (Fletcher and Floodgate, 1973) that the attachment polymer of a marine pseudomonad NCMB 2021 was an acid polysaccharide. Hydrolysis of an extracellular carbohydrate fraction of these cells often showed the presence of neutral sugars (Sutherland, 1982) found in polymers of this type (glucose, mannose and galactose,

glucosamine, rhamnose and ribose), but no uronic acids. Carboxylic acid groups detected in the polymer by infrared spectroscopy were considered to be associated with protein since no uronic acids were detected after hydrolysis. Uronic acids were, however, detected in adhesive polymers from *Flexibacter* analyzed by Humphrey *et al* (1979). This analysis is probably one of the most detailed for a substance known to be involved directly in bacterial adhesion. These workers found that a partially purified extracellular slime contained both protein and carbohydrate, with glucose, galactose, fucose, deoxysugars besides uronic acids in the hydrolysate. Repeated attempts to remove the protein from the carbohydrate fraction were unsuccessful. Thus, it was concluded that the polymer could be glycoprotein. Calculations based on measurements and reasonable assumptions for the system showed that the force required to separate *Flexibacter* cells from surfaces was five times more than was needed for horizontal movement, i.e., the polymer really did possess Stefan adhesive properties. Polymers in EPS may well attach to substrata by ionic bonds (if they contain  $-COO^-$  groups) or hydrogen bonds. The possibility certainly exists that bacterial polymers could form heterocopolymers with surface-adsorbed materials. Thus, partially accounting for their adhesive nature (Rogers, 1979).

There is no clear picture concerning the participation of *fimbriae* in the formation of biofilms. Although the adhesion of *E. coli* to mammalian epithelial cells involves *fimbriae*, they are not involved in its attachment to glass. *Actinomyces* and *Bacteroides* species inhabiting the human mouth are *fimbriate* and these organisms are involved in the formation of dental plaque, most certainly a form of biofilm (Slots and Gibbons, 1978). One particularly interesting aspect of adhesion mediated by *fimbriae* has been described by Rosenberg *et al* (1982). These workers showed conclusively that *fimbriae* on the cell surface of *Acinetobacter calcoaceticus* were involved in its adhesion and subsequent growth on hexadecane at the hydrophobic liquid-liquid interfaces. Mutants lacking *fimbriae* were not adherent; revertants adhered and also acquired the ability to produce *fimbriae*. One aspect of adhesion mediated by *fimbriae* that does not seem to have been exploited in research on adhesion to inanimate objects is its specific inhibition by mannose and sometimes 2-deoxy glucose.

There seems to be no evidence for the participation of bacterial *flagella* in biofilm adhesion. They may be concerned in propelling cells to the secondary minimum, but we have not been able to find examples of cells attached only by their *flagella*. Conclusions implicating *flagella* in adhesion which depend on results obtained with chemically fixed microbial cells should be treated with caution (Ward

and Berkeley, 1980).

There are no documented cases of lectin mediation in adhesion of microorganisms to non-living surfaces. However, if one regards the dental pellicle as non-living, then bacteria possessing lectin-like ligands are known to attach with considerable specificity to receptors on its surface (Gibbons, 1980). Further examples of lectin-like interactions will likely be documented in the future as research workers study the specificity of adhesion both at the macro- and microbiological level.

Microalgal EPS. The most common microalgae to adhere to submerged substrata are diatoms. There are several methods by which these cells attach as discussed at length by Chamberlain (1976). Light microscopy shows cells attached by mucilage pads, stalks or, in some cases, they are found inside mucilage tubes attached to a substratum e.g., *Amphipleura rutilans*. A further method of attachment concerns the raphe canal. In these cases, light microscopy does not show the means of adhesion. The raphe system of a diatom is a single or double slit in the silica cell wall and runs along the long axis of the cell allowing direct communication of the cytoplasmic membrane and the extracellular environment. The raphe is clearly involved in gliding motility and, therefore, adhesion (Harper, 1977). Daniel *et al.*, 1980 have described a series of mucilage-containing intracellular vesicles in *A. veneta* which appear to arise from the cisternae of the dictyosome. These may be the same organelles described earlier by Drum and Hopkins (1966) as crystalloid bodies and postulated by them to be the source of diatom trail substance, and thus implicated in both adhesion and motility. We have electron micrographic evidence that indeed these vesicles are secreted into the raphe canal (Webster, *et al.*, 1982), and thus may be the source of the cellular adhesive. Since tunicamycin ( $1 \mu\text{g ml}^{-1}$ ), which is an inhibitor of the formation of the linkage between carbohydrate and protein in fibronectin, inhibits diatom adhesion, it might be speculatively implied that the vesicles contain glycoprotein (Cooksey and Cooksey, unpublished).

Several workers have made attempts at analysis of attachment polymers of diatoms. By means of histochemical tests, Chamberlain (1976) showed that the polar mucilage pads, investing mucilages, the polymers of the tube dwelling diatoms, and mucilagenous stalks were acidic polysaccharides. As has been mentioned previously (see ), analytical results based on staining reactions of unpurified materials must be regarded as properties of a mixture. Some hydrolyses have been performed, but in no case has an attempt been made to show that the polymeric material was a single molecular species. Thus, the capsule

of *Navicula pelliculosa* contains glucuronic acid (Lewin, 1955), that of the oval cells of *Phaeodactylum tricornutum* contains xylose, mannose, fructose, and galactose (Lewin, et al, 1958), the mucilage tubes of *Amphiplura rutilans* contain xylose, mannose, possibly rhamnose and some proteins (R. Lewin, 1958), and the stalks of *Gomphonema olivaceum* are composed of a B-linked sulfated polymer containing galactose and xylose (Huntsman and Slonecker, 1971). All the polymers analyzed so far are different from the diatom storage polymer chrysolaminarin, a B 1-3 linked glucan. Even less is known concerning the trail substance referred to earlier, probably because it appears to differ in physical properties from the enveloping polymers (capsules, etc.) described above. Trail substance is slowly water-soluble (unpublished results quoted in Edgar and Pickett-Heaps, 1982; Webster et al, 1982). In a detailed histochemical study where temporary and permanent adhesive polymers of *A. veneta* were not distinguished, Daniel et al, (1980) showed that the extracellular polymer contains uronic acids and sulfate groups but no protein or lipid.

**CATIONS.** Roux (1894) reported the necessity for divalent cations, notably  $\text{Ca}^{2+}$ , in cellular adhesion. Calcium has been shown to be necessary for adhesion of aquatic bacteria (Marshall, et al, 1971; Fletcher and Floodgate, 1973) and marine diatoms (Cooksey, 1981), although in this report it was found that strontium could substitute poorly for  $\text{Ca}^{2+}$ . The role of these cations in adhesion is presently unknown. It has been suggested that divalent ions, especially  $\text{Ca}^{2+}$ , can form bridges between negatively charged substrata and microorganisms, can stabilize the structure of EPS (Fletcher and Floodgate, 1973), or cause precipitation of EPS in the space between a cell and substratum (Rutter, 1980). Fletcher and Floodgate (1973) noted that lanthanum decreased bacterial adhesion and postulated an EPS-denaturing action for the ion. Lanthanum is known to inhibit  $\text{Ca}^{2+}$ -transport into cells and to displace calcium from cellular membranes (Weiss, 1974), so that the effect noted above may have been related to a diminution of the flux of  $\text{Ca}^{2+}$  to the intracellular space. Lanthanum inhibits diatom adhesion, a process which is Ca-dependent. Further evidence for the involvement of  $\text{Ca}^{2+}$  in the adhesive process comes from the use of complexing agents. Attachment of a marine bacterium was inhibited by EDTA, but the same agent did not remove cells already attached to substrata (Fletcher, 1980). Cooksey and Cooksey (1980) were able to remove the marine diatom *A. coffeaeformis* from glass with a more specific  $\text{Ca}^{2+}$ -chelant, EGTA. Attached diatom cells treated with this substance left behind substratum-attached material in the exact shape of the raphe canals. The material, which stained with acridine orange, was certainly involved in the

attachment of the organism. Similar more detailed experiments by Culp and his co-workers illustrate the dangers of adopting simplistic explanations of adhesion (Culp and Black, 1972; Terry and Culp, 1974; Rosen and Culp, 1977). These workers found that EGTA removed tissue culture cells from culture vessels but left behind 'substrate-attached material' (SA material). Based on this, it was thought that mammalian tissue cells attached to this substratum by ionic bridges. Recent papers by the same group (Culp *et al.*, 1979) have shown that the situation regarding attachment, detachment, and the formation of SA material is considerably more complex. SA material certainly exists, but not only does it contain glycoprotein, but also certain elements of the cytoskeleton such as actin. SEM studies suggest EGTA causes minimal changes in the adhesive 'footpads' which gave rise to the SA material. This caused the cells to 'round-up' and, in doing so, fibers of cellular material between the cells and the substratum were formed. The cytoskeleton within these fibers reorganized, the fibers broke, and the cells were liberated, leaving behind the footpads as SA material. There are no studies at this level of detail with microbiological biofilms.

#### REACTIONS WITHIN THE BIOFILM

FUNDAMENTAL AND OBSERVED RATE PROCESSES. Biofilm and biofouling studies thus far have relied on a relatively unstructured approach to analysis of the biomass component. The biotic component is generally characterized only in terms of cell numbers or cell mass with little attention given to the physiological state of the organisms although there have been some limited attempts at providing more structure (Trulear, 1983; Bakke, 1983). Within the restrictions of unstructured microbial process models, four *fundamental rate processes* can be identified:

- growth
- product formation
- maintenance and/or endogenous decay
- death and/or lysis

Any or all of these processes may be occurring in a biofilm at any time. Growth refers to cell growth and multiplication. The cells also form products some of which are retained in the biofilm (e.g., EPS) and some of which diffuse out into the bulk fluid. The cells also have to maintain their internal structure, another energy-consuming process. If nutrients are depleted or toxic substances are present, death and/or lysis ensues.

The rates of the fundamental microbial processes are

difficult to measure directly and are generally inferred from more easily *observed rate processes*. The more familiar observed rate processes include the following:

substrate consumption  
electron acceptor consumption  
biomass production  
product formation

Table III-1 presents the relationship between fundamental and observed process rates. The stoichiometry of the process is qualitatively represented by each row in the matrix (- refers to reactants and + refers to products). The columns of the matrix indicate the fundamental rate processes that may contribute to the observed rates (last row in the matrix). For example, substrate removal (column 1) is the net result of growth, maintenance, and product formation.

Trulear and Characklis (1982), Bryers and Characklis (1982), and Trulear (1983) have used process analysis techniques in experimental biofilm reactors to quantify the fundamental rate processes within a biofilm. Their results suggest the following:

1. The growth rate of cells in the biofilm can be estimated from their growth rate in chemostats when substrate concentration in the microenvironment of the cell is equal.
2. Product formation by biofilm cells is generally the same as dispersed cells and depends on substrate loading rates as well as substrate concentration.
3. Maintenance requirements are essentially negligible until the biofilm becomes very thick. Even then, the results of anaerobic metabolism deep within the biofilm may be mistaken for maintenance energy requirements.

Process analysis techniques may be useful in determining whether attached cells are more active than dispersed cells. Substrate removal rate alone is not a sufficient criterion for comparing their activity since substrate removal is the net result of several fundamental processes. Removing the cells from the surface obviates any relevance in subsequent measurements which purportedly describe the activity of attached cells.

**MASS TRANSFER AND DIFFUSION.** Analysis of biofilm process rate and stoichiometry are frequently complicated by significant mass transfer resistances in the liquid or diffusional resistances within the biofilm. Trulear and Characklis, (1982) have observed that substrate removal rate

	substrate (s)	nutrient (z)	e <sup>-</sup> acceptor (e)	cell mass (x)	product (p)	metabolite (a)
Growth	-	-	-	+	+	+
Maintenance/Decay	-	-	-	(-)		+
Product Formation	-	-	-		+	+
Death/Lysis				(-)	(+)	
	$q_s$	$q_z$	$q_e$	$\mu_n$	$q_p$	$q_a$

**FUNDAMENTAL**

**OBSERVED**

Table III-1. A matrix representation of the reactions occurring within a fouling biofilm.

increases in proportion to biofilm thickness up to a critical thickness beyond which removal rate remained constant. The critical or "active" thickness was observed to increase with increasing substrate concentration. This behavior has been observed by others (Mueller, *et al*, 1966; Baillo and Boyle, 1970; Williamson and McCarty, 1976; Matson and Characklis, 1976) and attributed to diffusional resistance within the biofilm. Once the biofilm thickness exceeds the depth of substrate penetration into the biofilm, the removal rate is unaffected by further biofilm accumulation.

The biofilm rate processes may also be controlled by mass transfer limitations in the bulk fluid phase (Trulear and Characklis, 1982). For example, substrate removal rate is dependent on fluid velocity past the biofilm. At low fluid velocities, a relatively thick mass transfer boundary layer can cause a fluid phase mass transfer resistance which decreases substrate concentration at the fluid-biofilm interface and, thereby, decreases substrate removal rate. Two factors may result in low mass transfer rates from the bulk fluid to the biofilm:

low fluid velocities  
dilute liquid phase concentrations of the  
material being transported

Much fouling biofilm research has been conducted at relatively low flows or in quiescent conditions. Mass transfer may be the rate-controlling step in the overall process in these studies and, without further analysis, may be confused with the rates of more fundamental processes such as growth rates, adsorption rates, etc. In highly turbulent systems, mass transfer in the liquid phase is rarely a significant factor.

**SUMMARY OF BIOFILM REACTIONS.** The microbial processes occurring in a biofilm are more complex than suggested by the four fundamental processes defined above. However, this classification has been useful in determining, to some extent, the flow of substrate energy through the biofilm. Mathematical description of the kinetic expressions has also been accomplished (Trulear, 1983). Further structuring of biofilm processes may await more sophisticated methods for observing the processes within the biofilm (as opposed to the influence of the processes on the overlying liquid phase) and more specific identification of the products being formed.

Bakke (1983) has observed a remarkable biofilm phenomenon which demands more attention. He increased the supply of growth substrate step-wise to a biofilm and observed the following:

- a. immediate detachment of biofilm material
- b. biofilm cell numbers remained constant
- c. specific substrate removal rate and product formation rate increased instantaneously

These observations cannot be described with unstructured models but suggest that the biofilm organisms may slough their EPS in response to the "shock". In addition, the attached cells seem to possess a "reaction potential" which is expressed in response to instantaneous increase in substrate loading. The experiments clearly indicate the need to observe microbial physiology while the organisms are attached in their growth environment (*in situ*). More attention must be directed to transients because of their relevance to natural and technological phenomena.

#### DETACHMENT OF BIOFILM

Detachment of microbial cells and related biofilm material occurs from the moment of initial attachment. However, the macroscopic observation of biofilm detachment is easier as the biofilm becomes thicker.

Detachment phenomena can be arbitrarily categorized as shearing or sloughing. Shearing refers to continuous removal of small portions of the biofilm which is highly dependent on fluid dynamic conditions. Under these circumstances, rate of detachment increases with increasing biofilm thickness and fluid shear stress at the biofilm-fluid interface (Trulear and Characklis, 1982). Sloughing refers to a random, massive removal of biofilm generally attributed to nutrient or oxygen depletion deep within the biofilm (Howell and Atkinson, 1976) or some dramatic change in the immediate environment of the biofilm (see previous section). Sloughing is more frequently witnessed with thicker biofilms developed in nutrient-rich environments. Shearing is probably occurring under the same conditions under which sloughing is occurring but no such direct measurements have been attempted.

**HYDRODYNAMIC INFLUENCES.** Both Powell and Slater (1982) and Timperley (1981) conducted studies to determine the influence of fluid dynamics on detachment. Both investigators observed an increase in detachment with an increase in Reynolds number, i.e., fluid velocity. Timperley also considered different tube sizes and, within that context, concluded that mean fluid velocity was more significant in determining cleaning effectiveness than Reynolds number.

As fluid velocity increases, the viscous sublayer thickness decreases. Consequently, the region near the tube wall subject to relatively low shear forces (i.e., the viscous sublayer) is reduced. As a result, there may be some upper limit to the effectiveness of any cleaning operation based on fluid shear stress. The viscous sublayer may provide a valuable *a priori* criterion for predicting the maximum effectiveness (the minimum thickness attainable) of any cleaning technique dependent on fluid dynamic forces.

Detachment processes must also be significant in the processes of cell turnover in the biofilm. As a biofilm develops, succession in species is observed. Trulear (1983) developed a biofilm of *Pseudomonas aeruginosa* in conditions of relatively high shear stress and then challenged it with *Sphaerotilus natans*. The *Sphaerotilus* quickly became the dominant species within the biofilm. Detachment, influenced strongly by fluid shear stress, may serve to "wash out" organisms from the biofilm.

CHEMICAL TREATMENT. Detachment may occur for reasons other than hydrodynamic forces. Bakke (1983) has observed massive detachment when substrate loading to the biofilm was instantaneously doubled. He hypothesizes that cell membrane potential plays a key role in the phenomena. Turakhia, (unpublished results) and (Characklis, 1980) have observed dramatically increased detachment upon the addition of chelants (EGTA and EDTA, respectively) suggesting the importance of calcium to the cohesiveness of the biofilm.. Many other chemical treatments have been used to detach biofilm material with varying success including:

- chlorine (Characklis *et al*, 1980; Characklis and Dydek, 1976; Norrman *et al*, 1977)
- bromine chloride (Bongers *et al*, 1977)
- bromo-chloro-dimethylhydantoin (Matson and Characklis, 1983)
- surfactants

SUMMARY OF DETACHMENT PROCESSES. Detachment processes must play a major role in the ecology of the biofilm. Detachment from and absorption into the biofilm of microorganisms provides the means for interaction between dispersed (planktonic) organisms and the biofilm. Detachment of biofilm is the major objective of many anti-fouling additives used in manufacturing processes.

Very little is known regarding the kinetics of detachment and the factors affecting the removal. Such kinetic expressions would be useful for modelling purposes and for serving as comparative criteria in testing of anti-fouling treatments.

#### IV. PROPERTIES AND COMPOSITION OF BIOFILMS

Microorganisms, primarily bacteria, adhere to surfaces ranging from the human tooth and intestine to the metal surface of condenser tubes exposed to turbulent flow of water. The microorganisms "stick" by means of extracellular polymeric fibers, fabricated and oriented by the cell, that extend from the cell surface to form a tangled matrix of extracellular polymer substances (EPS). The fibers may conserve and concentrate extracellular enzymes necessary for preparing substrate molecules for ingestion, especially high molecular weight or particulate substrate frequently found in natural waters.

The biofilm surface is highly adsorptive, partially due to its polyelectrolyte nature, and can collect significant quantities of silt, clay and other detritus in natural waters.

Physical, chemical, and biological properties of biofilms are dependent on the environment to which the attachment surface is exposed. The physical and chemical components of the microenvironment combine to select the prevalent microorganisms which, in turn, modify the microenvironment of the surface. As colonization proceeds and a biofilm develops, gradients develop within the biofilm and average biofilm properties change. Changes in biofilm properties that occur during biofilm development must be considered when attempting to predict the influence of biofilms on the immediate environment. These changes have been largely ignored in past studies.

##### PHYSICAL PROPERTIES

Relevant *thermodynamic properties* of biofilm are its volume (thickness) and mass. In turbulent flow systems, wet biofilm thickness seldom exceeds 1000  $\mu\text{m}$  (Picologlou et al., 1980). The biofilm dry mass density can be determined from the wet biofilm thickness if the biofilm mass and the wetted surface area are known. The dry mass density reflects the attached dry mass per unit wet biofilm volume and measured values in turbulent flow systems range from 10 - 50  $\text{mg}/\text{cm}^{-3}$ . Biofilm density increases with increasing turbulence and increasing substrate loading (Picologlou et al. 1980; Trulear and Characklis, 1982). The increase in biofilm density with increasing turbulence may be caused by one of the following phenomena:

1. selective attachment of only certain microbial species from the available population
2. microbial metabolic response to environmental

stress

3. fluid pressure forces "squeeze" loosely bound water from the biofilm.

The relatively low biofilm mass densities compare well with observed water content of biofilm (Characklis, 1980; Characklis, 1973).

The *transport properties* of biofilm are of critical importance in quantifying effects of biofilms on mass, heat and momentum transfer. Diffusion coefficients for various compounds through microbial aggregates have been reported in the literature (Matson and Characklis, 1976), mostly for floc particles. Matson and Characklis (1976) report variation in the diffusion coefficient for glucose and oxygen with growth rate and carbon-to-nitrogen ratio. In biofilms, the diffusion coefficient is most probably related to biofilm density. *In situ* rheological measurements indicate that the biofilm is viscoelastic with a relatively high viscous modulus (Characklis, 1980). Reported biofilm thermal conductivities are not significantly different from water (Characklis *et al.*, 1981).

#### CHEMICAL PROPERTIES

**ELEMENTAL COMPOSITION.** Inorganic composition of biofilms undoubtedly varies with the chemical composition of the bulk water and probably affects the physical and biological structure of the film. Calcium, magnesium, and iron probably affect intermolecular bonding of biofilm polymers which are primarily responsible for the structural integrity of the deposit. In fact, chelants are effective, in detaching biofilm (Characklis, 1980; Turakhia, unpublished results). In heat exchangers, corrosion products and inert suspended solids can adsorb to the biofilm matrix and influence its chemical composition. Characklis (1981) reports a range of inorganic compositions observed in selected biofilms.

**MACROMOLECULAR COMPOSITION.** The organic composition of the biofilm is strongly related to the energy and carbon sources available for metabolism. Classical papers (Herbert, 1961; Schaecter *et al.*, 1958) have demonstrated the effect of environment and microbial growth rate on the composition of the cells and their extracellular products. For example, nitrogen limitation can result in production of copious quantities of microbial extracellular polysaccharides. Characklis (1981) presents data on the composition of biofilms developed in the field and in the laboratory. In terms of macromolecular composition, Bryers (1979) has measured protein-to-polysaccharide mass ratios ranging from

0 to 10 (polysaccharide concentration in terms of glucose and protein concentration based on casein) with increasing biofilm accumulation. Other chemical analyses of biofilm have been reported by Bryers and Characklis (1979).

#### CELLULAR DENSITIES

The organisms which colonize the attachment surface will strongly influence biofilm development rate and biofilm chemical and physical properties. However, organism-organism and organism-environment interactions undoubtedly shift population distributions during biofilm accumulation. Several investigators have observed succession during biofouling. The first visible signs of microbial activity on a surface are usually small "colonies" of cells distributed randomly on the surface. As biofilm development continues, the colonies sometimes grow together forming a relatively uniform biofilm. The viable cell numbers are relatively low in relation to the biofilm volume ( $10^4 - 10^8 \text{ cm}^{-3}$  biofilm) occupying only from 1-10 percent of the biofilm in dilute nutrient solutions (Characklis, 1980; Trulear, 1983). Jones *et al* (1969) present photomicrographs which corroborate these data. Areal densities have been observed as high as  $10^{13}$  cells  $\text{m}^{-2}$  (Zelver, *et al*, 1982). Many surfaces, presumably clean but untreated in any rigorous way, contain as many as  $10^4$  cells  $\text{m}^{-2}$  (Zelver, unpublished results). Sometimes it is not obvious that the precautions described by DiSalvo (1973) have been taken when withdrawing substrata from the aqueous phase through the air-water interface. This interface, which is rich in bacteria, will contaminate surfaces drawn through it and lead to over-estimations of the numbers of bacteria attached on experimental substrata.

In many cases, filamentous forms emerge as the biofilm develops further. *Hyphomicrobium*, *Sphaerotilus* (Trulear and Characklis, 1982) *Caulobacter* (Corpe, 1970) *Saprospira* (Lewin, 1965) and *Beggiatoa* (Heukelekian, 1956) are frequently identified. The filamentous forms may gain an ecological advantage as the biofilm develops since their cells can extend into the flow to obtain needed nutrients or oxygen which may be depleted in the deeper portions. Obtaining representative cell numbers from filamentous biofilms is very difficult.

## V. FACTORS INFLUENCING FUNDAMENTAL RATE PROCESSES

Physical, chemical, and biological factors influence the fundamental rate processes. These factors influence the rate as well as the extent to which fouling deposits accumulate.

### PHYSICAL FACTORS

The most important physical factors affecting the fundamental processes are shear stress, temperature (bulk fluid and surface), and surface (micro) roughness. All three factors influence transport, interfacial phenomena, detachment and reactions at the interface. Only temperature will influence reactions within the deposit. Other factors influence fouling processes at the macroscopic system level including geometry or configuration of the heat exchanger, residence time, and physical treatment methods (e.g., Amertap, MAN brushes).

### CHEMICAL FACTORS

The chemical factors influencing the fundamental rate processes are too numerous to list. However, some of the more important are pH,  $Ca^{++}$ ,  $Fe^{+++}$ , Si, dissolved oxygen, and organic carbon. These factors do not affect transport rates but may affect interfacial phenomena and certainly influence reaction rate and extent in the deposit and at the metal surface. Another chemical factor influencing fouling processes is the metal alloy. There have been numerous tests which have evaluated the fouling and/or corrosion potential of various alloys. The influence of surface (micro) roughness versus surface chemical composition, however, is not always clear. Internal chemical treatment programs to minimize fouling provide a multitude of other chemical compounds which influence fouling processes. Chemical treatment programs depend on the type of deposit and, in some cases, treatment for one condition may be antagonistic to control of another. For example, phosphorous compounds added to minimize precipitation fouling may enhance biological fouling. Many chemical compounds exert a significant influence on fouling processes at relatively low concentrations which further complicates analysis.

### BIOLOGICAL FACTORS

Biological factors have their greatest influence on

biochemical reactions within the deposit where bacterial cell numbers, physiological state of the cells, and microbial community structure determines the influence of the deposit on equipment performance (Characklis, 1981). However, biological factors may also influence interfacial adsorption/adhesion as well as detachment. For example, microbial deposits contain significant quantities of extracellular polymer substances (EPS) which increase the adsorptive capacity of the wetted surface and trap particulates (Trulear, 1983). Microbial activity within the deposit may also increase the cohesiveness of the deposit (Zelver et al., 1982) forming an organic matrix which provides resistance to fluid shear forces. Biological factors probably influence the effectiveness of chemical treatment programs in minimizing other types of fouling (e.g., precipitation and corrosion fouling) although the author has found no literature documentation for this statement.

## VI. MEASUREMENT AND SIMULATION

### NEED AND PURPOSE

The experimental investigation of fouling is a necessary and important route to obtaining an understanding of the fundamental processes. If reliable fouling data could be obtained on full-scale heat exchange equipment using the actual fluids, other measurements and simulation would be unnecessary. However, many of the parameters of interest vary considerably throughout the equipment and, in addition, vary with time. As a result, measurements in the laboratory and in field locations are necessary at specified and constant values for critical parameters.

**LABORATORY MEASUREMENTS.** The laboratory provides the proper environment for conducting mechanistic studies which lead to useful models in terms of simulating real systems. These tests are a "starting point." Physical, chemical, and biological factors can be controlled at desired levels. Valuable information can be obtained related to design concepts such as influence of alloy (Characklis *et al.*, 1983), fluid velocity, tube geometry (*e.g.* enhanced heat transfer surfaces), and temperature profiles (Characklis, 1979). The effect of water quality (chemical and biological) on these factors can also be evaluated. Operation and maintenance procedures can be evaluated. For example, laboratory tests can evaluate the effectiveness of a treatment (chemical or physical) procedure applied at varying frequency (Norrman *et al.*, 1977; Zilver *et al.*, 1981). These tests frequently identify the operating conditions which are best for a given treatment procedure. Laboratory experimentation frequently results in development of measurement techniques useful for field tests and monitoring (Characklis *et al.*, 1981).

Aside from mechanistic data and testing, laboratory tests are generally less expensive than field tests based on value of the information obtained.

**FIELD MEASUREMENTS.** Measurements at the operating plant are essential because no system can be simulated perfectly. But the purpose of field measurements is generally monitoring equipment performance and/or warning of impending problems. Field measurements which simulate the equipment environment could be used to evaluate the effectiveness of internal chemical treatment programs but this activity, for reasons unknown, has been rare. Field tests have been used to evaluate the influence of physical factors and a limited number of chemical factors on fouling and corrosion. For example, the performance of different alloys is presently being tested at a power plant site using an instrument which simulates the heat exchange equipment (Zilver *et al.*, 1982). Field tests are also useful in evaluating the performance of contemplated changes in treatment programs

and/or process modifications (Characklis, et al., 1981; Natson and Characklis, 1982). Of all factors influencing fouling, biological variables are most difficult to control in the field as is also frequently the case with some chemical components generally contributing to water quality.

Laboratory and field measurements are intimately related within the iterative procedure described in Figure 11-1.

Laboratory observations under carefully controlled conditions provide the framework for evaluating and interpreting field results where control of all parameters is not possible. On the other hand, field results indicate inconsistencies in the models and provide the impetus and experimental hypotheses for further laboratory work.

#### MEASUREMENT RELATED TO FOULING

Measurements related to fouling processes include methods for monitoring the progress of the fouling process, methods for characterizing the fouling deposit, and methods for describing and/or controlling the fouling environment. In some cases, methods for monitoring progress can also be used to characterize the deposit.

**MONITORING THE PROGRESSION OF FOULING.** Methods available for monitoring the progress of fouling processes can be conveniently classified as follows (Characklis et al., 1982):

1. direct measurement of deposit quantity
2. indirect measurement of deposit quantity
  - a. specific constituent within the deposit
  - b. for biofilms, microbial activity within the deposit

Direct measurement includes deposit mass and deposit thickness and is essential for several reasons. Calibration of any indirect method involves comparison with actual quantity of accumulated deposit. Direct measurements are a necessity when using mass conservation equations to determine process rates and stoichiometry. Direct methods are also useful in relating deposit accumulation to fluid frictional resistance and heat transfer resistance in a rational way.

Indirect methods provide significant benefits including increased sensitivity. For example, organic carbon analysis of biofilm is as much as 25 times as sensitive as biofilm mass measurements (Characklis et al., 1982). In this case, the specific constituent of the deposit (i.e., organic carbon) provides an excellent measure of accumulation. However, if the deposit contains a large amount of silt and

sediment, organic carbon may not be representative.

Indirect methods include monitoring the influence of deposits on heat transfer and fluid frictional resistance as discussed above. These techniques have been discussed in more detail by others (Characklis *et al.*, 1981) and indicate that the influence of deposits on heat and momentum transfer depends strongly on deposit characteristics (e.g., composition, thermal conductivity, roughness).

**CHARACTERISTICS OF FOULING DEPOSITS.** Fouling deposits can exhibit a wide range of chemical and microbial composition. Not surprisingly then, two deposits of equal thickness can influence heat and momentum transfer in drastically different ways. The reason for this behavior is widely varying deposit thermal conductivity and roughness as indicated in Table VI-1. Characterization of deposits is a necessary preliminary to choosing control strategies.

Presuming an *in situ* deposit thickness measurement is possible, effective deposit thermal conductivity and roughness, can be determined through measurements of conductive and convective heat transfer resistance, fluid frictional resistance, and engineering correlations. This *in situ* diagnostic method is presently being incorporated into an on-line fouling monitor. Such a diagnostic tool would find advantage as a feedback control device in an operating plant or on shipboard. As more data accumulates, deposit composition could be estimated from thermal conductivity and roughness determinations in much the same way as chemical composition is determined from "libraries" of spectral data associated with gas chromatography/mass spectrometry. Field data of this type would also contribute to empirical relationships useful for predicting fouling processes as a function of environment. . . . providing that the appropriate environmental factors are known or measured. A library file of deposit properties and compositions of this type exists and is being expanded at regular intervals.

**IMPORTANT ENVIRONMENTAL FACTORS.** There are many factors which influence the rate and extent of fouling processes but the primary ones certainly include bulk water quality (chemical and biological), temperature (bulk water and surface), fluid shear stress at the surface, and the nature of the surface (alloy). Superimposed on these factors is any chemical or physical treatment program regularly employed to minimize the effects of fouling.

Fouling is a heterogeneous process in that it requires both a liquid and solid phase. Consequently, concentrations and compositions at the liquid-solid interface determine the processes which control deposition. Unfortunately, interfacial conditions are extremely difficult to measure except under controlled laboratory conditions and interfacial processes must be related to the bulk water environment. Under these limitations, data interpretation must proceed with caution and a thorough process analysis must be accomplished before valid conclusions can be drawn.

Type Deposit	Thermal Conductivity (watt m <sup>-1</sup> C <sup>-1</sup> )
Biofilm	0.63
Calcium Carbonate	2.26-2.93
Combined Biofilm/Scale	1.61

Type Deposit	Deposit Thickness (cm)	Relative Roughness (dimensionless)
Biofilms	0.0040	0.003
	0.0165	0.014
	0.0300	0.062
	0.0500	0.157
CaCO <sub>3</sub> Scale	0.0165	0.0001
	0.0224	0.0002
	0.0262	0.0006
Combined Biofilm/Scale	0.0118	0.006
	0.0363	0.04

Table VI-1. Properties of various fouling deposits. Calcium carbonate thermal conductivities from Drew Chemical Corporation (1979).

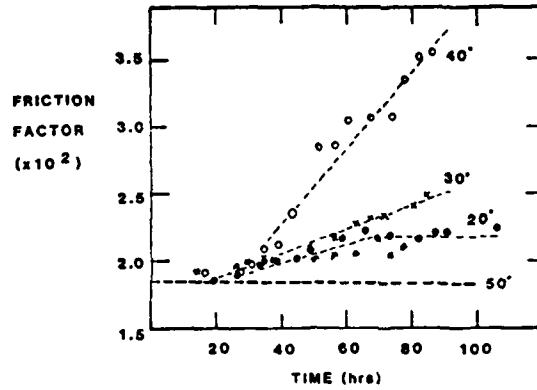


Figure VI-1. Progression of fluid frictional resistance (as represented by friction factor) as a function of bulk water temperature (Stathopoulos, 1981).

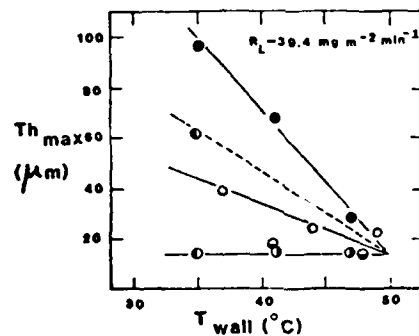


Figure VI-2. The influence of wall temperature and nutrient loading rate on maximum biofouling deposit thickness in a laboratory system. Fluid velocity was  $1.1 \text{ m s}^{-1}$ , tube alloy was stainless steel. Tube I.D. was 1.27 cm and bulk temperature was  $35^\circ\text{C}$  (Characklis, 1979).

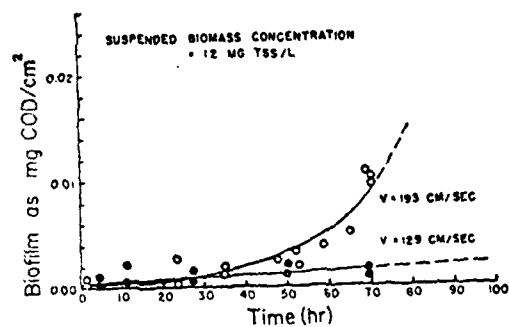


Figure VI-3. Influence of fluid shear stress on biofilm development (Bryers and Characklis, 1981).

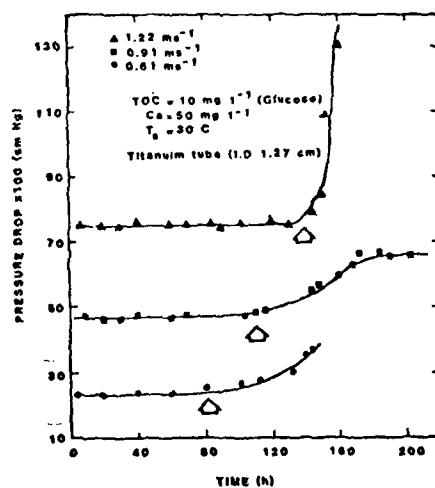


Figure VI-4. Influence of fluid shear stress on fluid frictional resistance due to biofilm development.

As an illustration, consider biofouling in an open recirculating cooling tower (RCT) system. It was believed for many years that biofouling was related to the colony-forming units (CFU) measured by a plate count procedure. Recently, data was presented (Characklis *et al.*, 1981) which indicated no relationship between CFU's in the bulk water and fouling as measured by heat transfer or fluid flow measurements. The lack of correlation can be attributed to the number of processes contributing or removing organisms from the bulk water phase. Organisms enter the cooling tower bulk water through the make-up water, by growth and reproduction within the bulk water, from the air, and by detachment from biofouled surfaces. Organisms leave the RCT system bulk water in the blowdown and drift, by adsorption to surfaces within the RCT system, and by "death," at least partially due to biocide application. Obviously, the number of CFU in the cooling water is not strictly related to the extent of biofouling in the RCT system.

Key chemical constituents which influence fouling processes include  $\text{Ca}^{++}$ ,  $\text{Mg}^{++}$ ,  $\text{Fe}^{+++}$ ,  $\text{Fe}^{++}$ ,  $\text{Si}$ ,  $\text{O}_2$ ,  $\text{PO}_4^{3-}$ ,  $\text{CO}_2$  (and related forms),  $\text{SO}_4^{2-}$ ,  $\text{Cl}^-$ , and organic carbon.

Bulk temperature influences most chemical and biochemical reaction processes as well as transport rate processes. Fouling processes are no exception as indicated in Figure VI-1 which indicates the progression of fluid frictional resistance as a function of bulk water temperature in a biofouling environment (Stathopoulos, 1981). The most deleterious effects are observed at 40°C (104° F). Surface temperature also influences fouling processes as indicated in Figure VI-2 which indicates the maximum biofouling deposit thickness attained as a function of surface temperature and nutrient loading rate (Characklis, 1980). One important observation from these data is the significant interaction between variables, in this case, surface temperature and nutrient loading rate.

Fluid shear stress is critical in fouling environments since it strongly influences transport and detachment rates. Figure VI-3 indicates the influence of fluid shear stress on biomass accumulation rates (Bryers and Characklis, 1981). Accumulation rates are higher at the higher flow rate suggesting that transport dominates over detachment in this system during the early stages of deposit formation. Figure VI-4 indicates the influence of shear stress on fluid frictional resistance changes caused by biofilm accumulation (Turakhia, unpublished results).

Finally, the composition of the surface material influences the rate of deposition. Figures X-5 and X-6 depict the progress of biofouling deposition on titanium and copper-nickel in a laboratory sea water system (Characklis *et al.*, 1983). If only total deposit mass is considered, the copper-nickel alloy fouled to a much greater extent than titanium. However, consideration of volatile deposit mass suggests that "biofouling" was essentially the same in the

two alloys. Other analyses indicated that much of the total deposit mass on copper-nickel could be attributed to corrosion products (Characklis et al., 1983).

## VII. MODEL REACTORS

Model reactors used in the laboratory provide the capability of investigating fouling phenomena with complete control of water quality. In contrast, field studies frequently provide no control of the chemical, biological and physical water quality parameters which critically influence the fouling process. Critical water quality parameters include:

### CHEMICAL

- inorganic concentration
- organic concentration
- pH
- dissolved oxygen
- biocide type
- biocide concentration

### BIOLOGICAL

- organism type(s)
- organism numbers

### PHYSICAL

- water temperature
- hydraulic residence time

In order to study the effect of any one of these parameters on the rate and extent of fouling or on the removal of a fouling deposit, control of all other parameters is required. Fluctuation of these parameters in the field exclude the use of field monitoring for developing fundamental models of the fouling process. In addition, there are practical reasons for conducting fouling studies in the laboratory including the following:

- Eliminate expensive transportation costs to field sites.
- Shorten experiments by operating under conditions designed to promote rapid fouling.

## METHODS

Figure VII-1 shows a schematic of the continuous stirred tank reactor (CSTR) concept employed in our research. Figure VII-1 also indicates the environmental control capabilities of the CSTR system. Methods have also been developed for measuring characteristics of a fouling deposit including:

- thickness
- mass
- extent and distribution of area covered (patchiness)
- numbers and types of microorganisms
- organic and inorganic constituents

## CSTR WATER SUPPLY SYSTEM

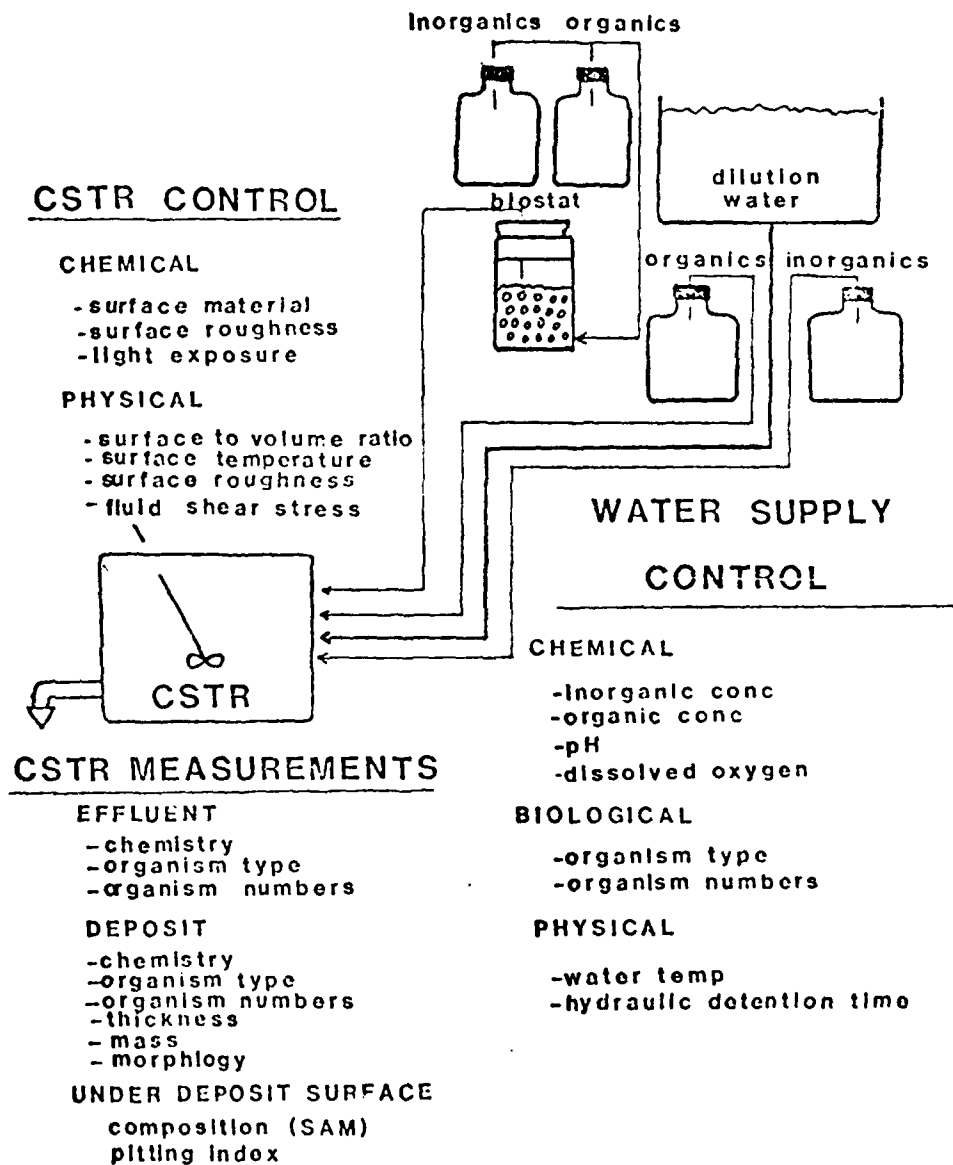


Figure VII-1. A schematic diagram of the continuous stirred tank reactor (CSTR) concept used in this research.

-deposit morphology

The CSTR system consists of a 1) a water supply system where water quality is controlled and 2) the CSTR where conditions at the fouling surface are controlled. Chemical and physical factors which describe conditions at the surface include:

#### CHEMICAL

- surface material
- light exposure

#### PHYSICAL

- surface area to volume ratio
- surface temperature
- surface roughness
- fluid shear stress
- surface roughness

Reaction time in the CSTR bulk water is dependent on the hydraulic residence ( $\theta$ ) which equals liquid volume divided by water supply flow rate ( $\theta = \text{volume} / \text{flow rate}$ ). Control of  $\theta$  provides a number of benefits compared to operating with a once-through flow:

1. Growth rate of bacteria in suspension (non-attached) is equal to  $\theta$ . If only wall growth is desired, the CSTR can be operated with a  $\theta$  significantly less than the maximum specific growth rate and suspended bacteria will wash-out before reproducing.
2. Operating with a long hydraulic residence time requires less water supply and consequently less water supply chemicals compared to operating a once-through system.
3.  $\theta$  can be varied during an experiment if an approximation of a once-through system is desired. For example, an experiment may be operated at  $\theta = 30$  minutes during development of the biofilm and operated with a  $\theta \ll$  one minute while a biocide is applied.

#### GEOMETRIES

A number of different reactor geometries have been used to study fouling phenomena because of their relative advantages in particular applications:

1. A tubular system is used because it is the prevalent geometry in heat exchangers and also because a wide variety of alloys are available in this form. Fluid dynamics in this geometry

are well-defined.

2. A rotating annular reactor is used because of its compactness and ease of operation. Such a reactor also permits non-destructive sampling of the fouling deposit.
3. A radial flow reactor is used because it provides a defined range of fluid shear stress conditions simultaneously at the fouling surface.
4. A rotating disk reactor also is used because it provides a defined range of fluid shear stress conditions at the fouling surface while maintaining a uniform mass transfer boundary layer over the entire surface..

Each of the model reactors may be operated as a CSTR with the desired water supplied as indicated in Figure . Typically when large volumes of dilution water are required, tap water treated to remove residual carbon and suspended solids is used. Nutrients, glucose, microorganisms and, in some cases, a synthetic growth media are added to the CSTR to provide the necessary mineral, energy, and carbon requirements for microbial growth.

**TUBULAR REACTOR.** The tubular reactors are CSTR's with internal recycle as indicated in Figure VII-2. This system is typically used when modelling heat transfer tubing or water supply conduits. Often, the experimental system may contain the alloy and actual tube diameter being simulated. Advantages of the tubular configuration include the following:

1. At high recycle rates employed (recycle flow rate  $\gg$  dilution water flow rate), the reactor contents are completely mixed and no concentration longitudinal gradients exist in the liquid phase. This simplifies mathematical descriptions and sampling. It also provides a relatively uniform biofilm in the recycle section while allowing simple control of pH and temperature. From a practical standpoint, this system minimizes the consumption of water, microbial nutrients and other chemical additives.
2. A short hydraulic residence time can be maintained which minimizes biomass activity in the bulk fluid and restricts microbial activity in the system to the reactor surfaces.
3. Fluid shear stress at the wall in the recycle loop is independent of mean residence time in

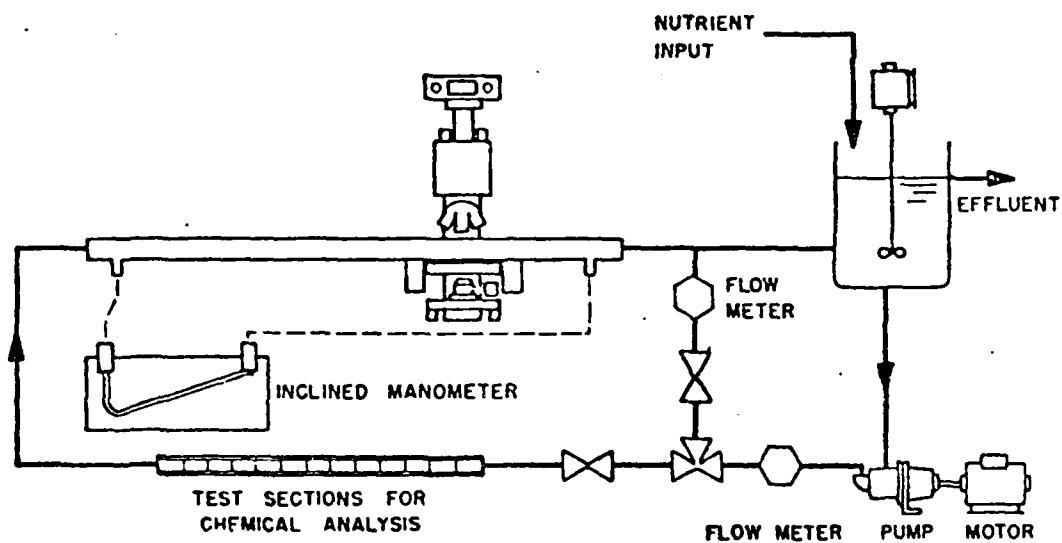


Figure VII-2. The tubular reactor system.

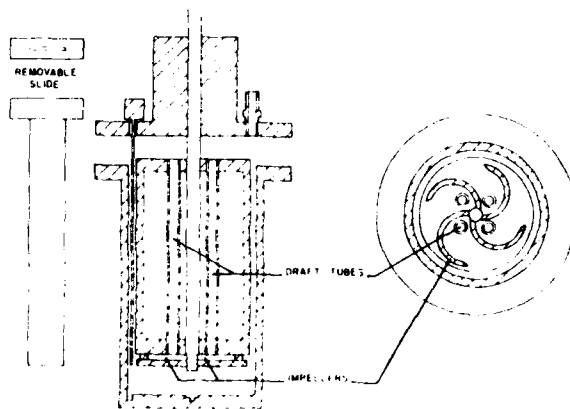


Figure VII-3. The annular reactor.

the reactor system.

Each tubular reactor system may incorporate one or more of the following types of tubular sections:

1. A tubular test section in which pressure drop is monitored by a manometer or pressure transducer during biofilm development. Fluid frictional resistance can be calculated from flow rate and pressure drop measurements.
2. A test heat exchanger section in which changes in heat transfer resistance are monitored as a function of biofilm development.
3. A tubular section or sleeve which contains removable sample tubes. Sample tubes are removed periodically for determining biofilm thickness, biofilm mass, or biofilm chemical analysis.
4. A glass tubular section for visual or microscopic observations. Periodic micrographs or video recordings of biofilm development may be obtained using a transparent section.
5. A rectangular duct section may be used when samples of biofilm developed on a flat-plate are desired. This is particularly desirable when periodic access to a deposit is required, for instance, using probes to obtain chemical profiles within a deposit.

**ANNULAR REACTOR.** The annular reactor is a potential method for monitoring biofilm development because of its sensitivity, particularly to changes in fluid frictional resistance. Furthermore, changes in the fouling deposit can be monitored continuously and non-destructively.

The annular reactor consists of two concentric cylinders, a stationary outer cylinder and a rotating inner cylinder (Figure VII-3). A torque transducer, mounted on the shaft between the cylinder and the motor drive, monitors the drag force on the surface of the inner cylinder. Fluid frictional resistance is calculated from rotational speed and torque measurements. A removable slide, which forms an integral fit with the inside wall of the outer cylinder, is used to determine biofilm thickness, biofilm mass, and provide samples for determining biofilm chemical composition. The reactor is completely mixed by either an external recycle or by draft tubes in the inner cylinder which are designed for fluid mixing. The fluid shear stress at the wall can be varied independently of mean residence time.

ROTATING DISK AND RADIAL FLOW REACTOR. These two reactor designs are useful for studies when a range of fluid shear stress values are desired simultaneously (i.e. investigating effect of fluid shear stress on efficiency of a biocide).

*RADIAL FLOW REACTOR* The radial flow reactor, as designed by Fowler (1980), consists of two parallel disks separated by a narrow spacing (Figure VII-4. Culture fluid is pumped into the center of one of the disks at a constant volumetric flow rate and flows out radially between the disks to a collection manifold. As the cross sectional area available for flow increases with increasing radius, the linear velocity and fluid shear stress decreases. Thus, high shear forces are present near the inlet and lower shear forces are present toward the outlet.

*ROTATING DISK REACTOR* The rotating disk reactor consists of a rotating disk placed in a solution of fluid. The rotating disk has been used to study the effect of fluid shear stress on biofilm development because fluid shear stress varies with the radius of the disk with the highest fluid shear stress at the outer edge of the disk and lower fluid shear stress values towards the disk center.

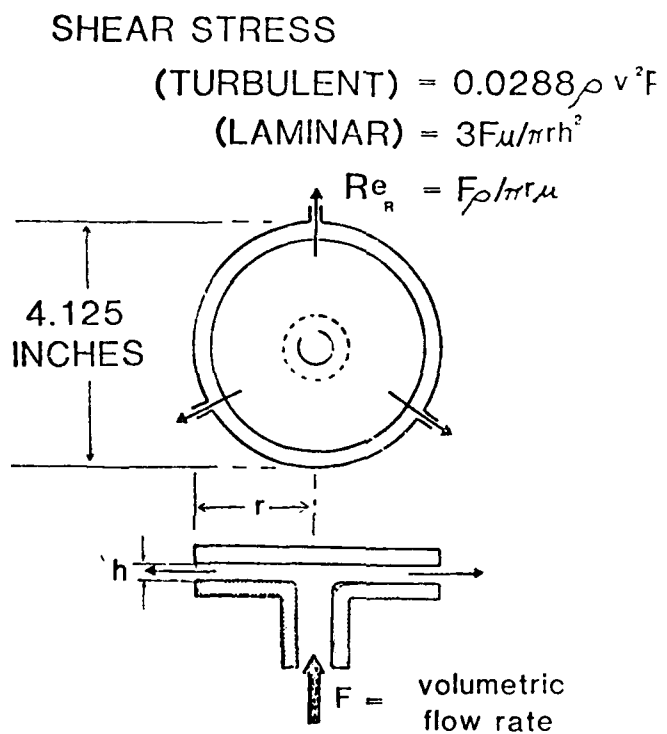


Figure 211-4. The radial flow reactor.

### VIII. BIOFILM PROPERTIES INFLUENCING TRANSPORT PROCESSES

Biofouling of surfaces in contact with flowing water is known to cause serious increases in fluid frictional resistance (FFR). This results in increased pressure drop and pumping requirements in conduits that require constant flow or, conversely, loss in flow capacity if head loss is held constant (e.g. gravity feed systems). Biofouling of ship hulls results in reduction of peak ship speed.

A typical example of an increase in FFR in a power plant water conduit is shown in Figure VIII-1. The O.8 in copper-nickel conduit exhibited a 30 percent increase in frictional resistance after 15 days of operating with brackish water. Table VIII-1 documents other case histories of biofouling in water conduits. Characklis and co-workers have conducted numerous laboratory studies on the effect of biofouling on FFR using both salt water and fresh water (Zelver, 1979; Picologlou et al., 1980; Characklis et al., 1981a; Characklis et al., 1981b; Trulear and Characklis, 1982; Characklis et al., 1982; and Characklis and Zelver, 1983). These studies document the dramatic increases in FFR due to biofouling. In addition, explanations are proposed for mechanisms by which biofouling increases FFR.

#### FRICITION FACTOR

FFR is determined by a dimensionless friction factor ( $f$ ) which is calculated from fluid velocity and pressure drop through the conduit (Olson, 1973):

$$f = 2.0 \frac{d}{L} \frac{\Delta P}{\rho_f v^2} \quad (\text{Eq. VIII-1})$$

where,

$d$	= tube diameter	(L)
$\Delta P$	= pressure drop	(M L <sup>-1</sup> t <sup>-2</sup> )
$\rho_f$	= fluid density	(M L <sup>-3</sup> )
$v$	= fluid velocity	(L t <sup>-1</sup> )

**NOTE:** Some texts use a constant of 0.5 instead of 2.0 in the friction factor calculation.

At any given velocity, if pressure drop increases, friction factor increases in direct proportion. A number of factors may be responsible for fluid energy losses which lead to increased pressure drop:

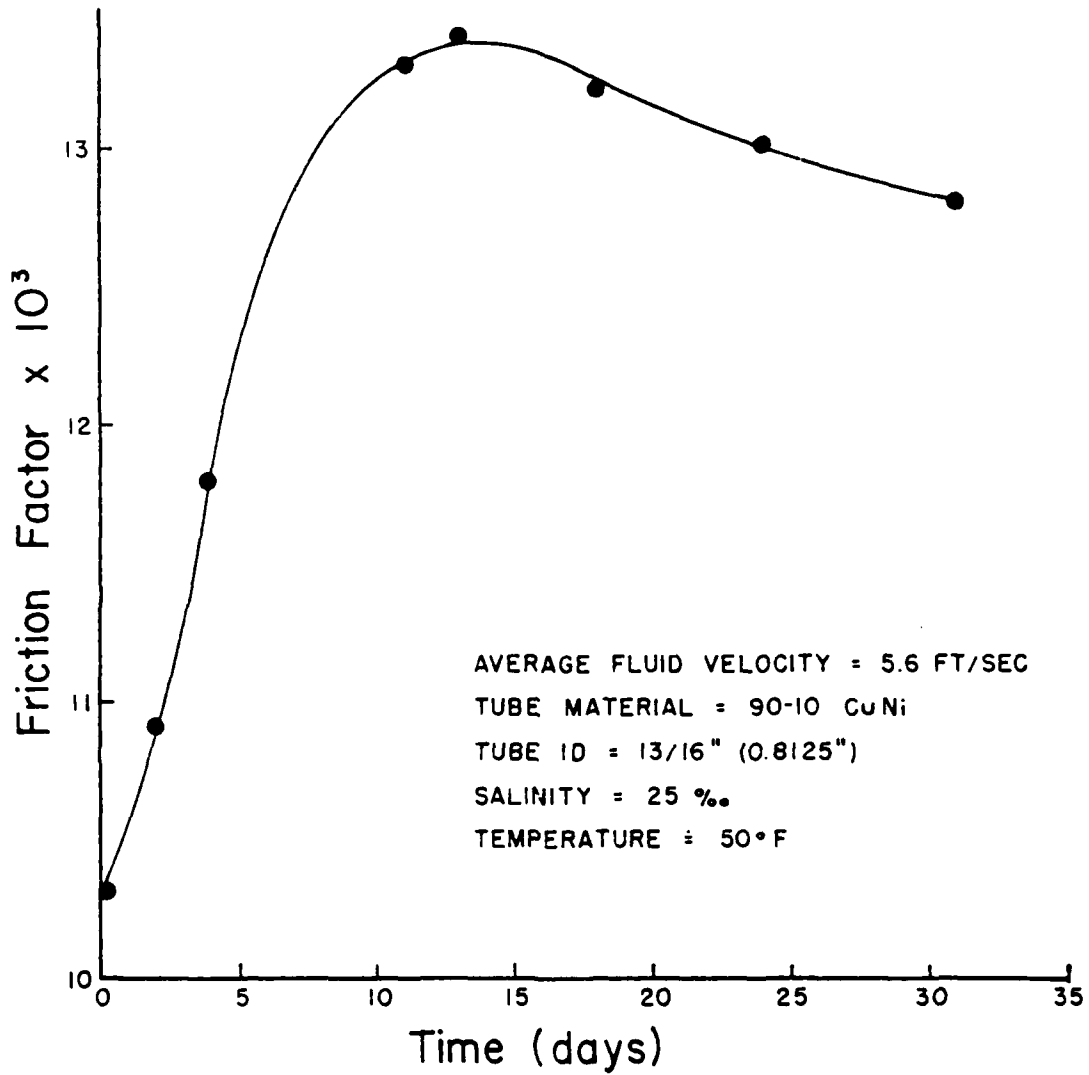


Figure VIII-1. Increase in frictional resistance due to biofouling in the field (DeHart, 1979).

Table VIII-1. Data Summary from Case Histories of Closed Conduits Experiencing Frictional Losses Due to Biofilms

Reduction in Design Flow Capacity	Biofilm Thickness ( $\mu\text{m}$ )	Conduit Diameter (cm)	Conduit Length (km)	Conduit Surface
1 12% in 2 yrs	800	105	13	Cement
2 23% -----	1600	90	13	Concrete
3 16% in 3 wks	3000	90	41	Steel
4 55% in 3 yrs	635	60	93	Steel
5 3.5% in 1 yr	-	36	2.5	Steel

1 Minkus (1954)

2 Minkus (1954)

3 Arnold (1963)

4 Wiederhold (1949)

5 Derby (1947)

- o *Increase in Fluid Viscosity.*
- o *Constriction of Tube Diameter*
- o *Viscous Dissipation due to Creeping Action of a Surface Coating.* Brauer (1963) performed experiments on form stability of the interior of asphalt-lined pipes as a function of the flowing water. At higher temperatures, the asphalt coating assumed a rippled surface structure that was accompanied by an unusual increase in frictional resistance. Brauer explained the phenomenon as an actual flow of the coating under the action of fluid shear stresses. Energy is dissipated by the asphalt being dragged along the pipe surface.
- o *Viscous Dissipation within a Surface Coating due to an Oscillatory Response to Turbulent-Flow Excitation.* The possibility exists for a visco-elastic surface to absorb energy from the flowing fluid, such energy being eventually dissipated through viscous action.
- o *Increased Surface Roughness.* When the roughness of an inside tube wall surface is sufficiently coarse, eddy currents develop which result in energy losses.

#### LABORATORY RESULTS

Characklis and co-workers (Zelver, 1979; Picologlou, et al., 1980; Trulear, 1980; Trulear and Characklis, 1982) have documented the effects of biofouling on FFR using Tubular Reactors (TR) having a 0.127 cm inside diameter and a hydraulically smooth surface. These systems were inoculated with a wide spectrum of fouling bacteria and run with fresh water with addition of inorganic and organic nutrients. Monitoring capabilities included measuring pressure drop, flow rate, biofilm mass and biofilm thickness. In some cases, biofilm morphology was examined microscopically. Results of these experiments were as follows:

1. *Increase in FFR due to biofilm accumulation during an experiment with constant flow-rate.* Figure VIII-2 shows the increase in pressure drop in the fouled TR operated at a constant flow rate of  $150 \text{ cm sec}^{-1}$ . Within 60 hours pressure drop had doubled.
2. *Loss of flow capacity due to biofilm accumulation during an experiment with constant head (pressure*

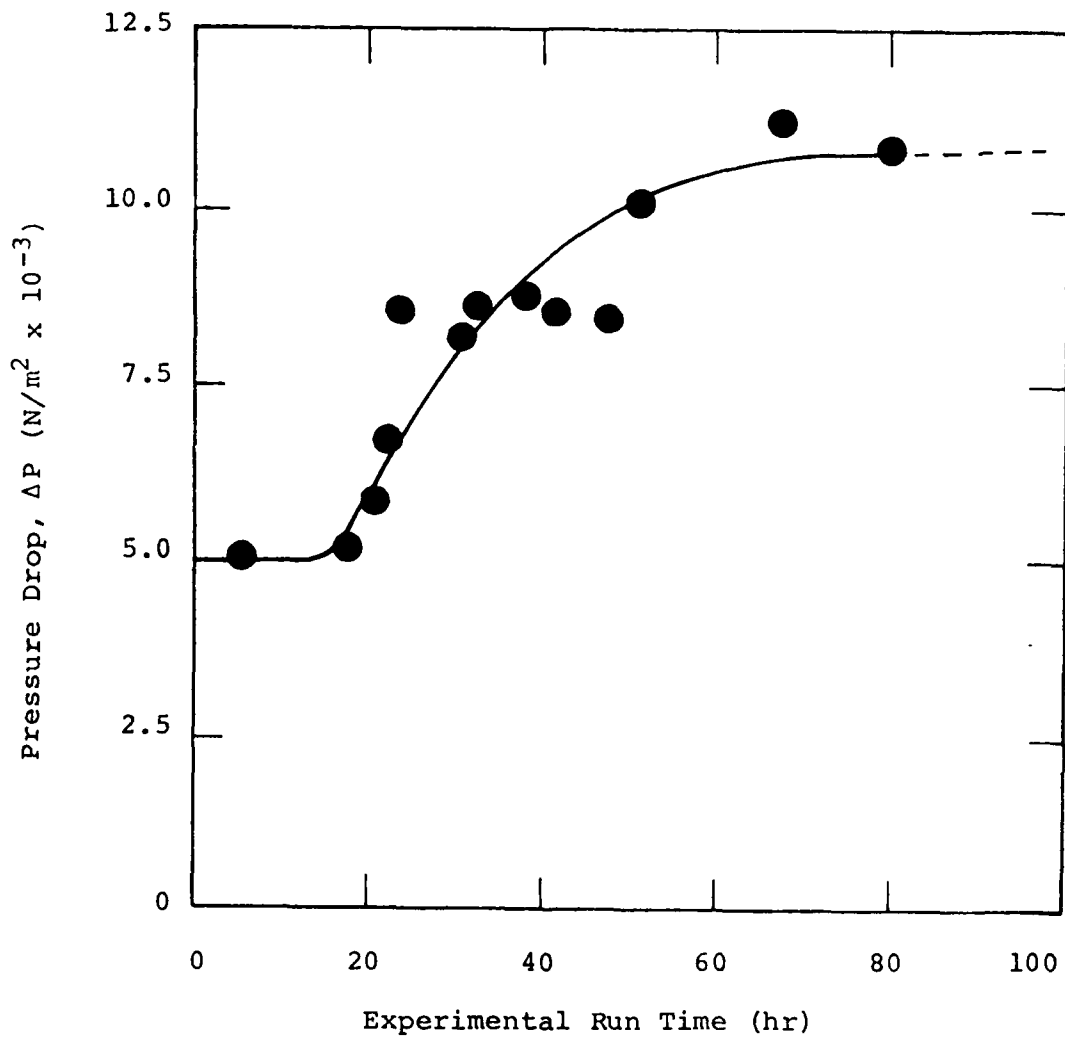


Figure VIII-2. Change in pressure drop with time for a constant flow experiment.

drop). Figure VIII-3 shows flow capacity was halved within 60 hours of operating with an initial flow velocity of  $185 \text{ cm sec}^{-1}$ .

3. *Relationship of Biofilm Thickness to Frictional Resistance.* Figure VIII-4 shows friction factor increases with biofilm thickness with the exception of a beginning lag. This lag is typical. FFR is not evident until biofilm thickness reaches a critical thickness (in this case approximately  $30 \mu\text{m}$ ).

#### MECHANISMS

Any or all of the mechanisms discussed above could account for the dramatic increase in FFR. Each will be discussed in order.

**FLUID VISCOSITY.** Fluid viscosity did not change during a TR experiment. Fluid viscosity from TR experiments under different conditions was measured using a capillary viscometer. Fluid viscosity varied no more than 2.0 percent from water for any experiment.

**TUBE CONSTRICTION.** Figure VIII-5 indicates: (1) The increase in pressure drop and biofilm thickness with time for a typical experiment; and (2) the increase in pressure drop for a decrease in radius equal to the measured biofilm thickness. Pressure drop attributed to biofilm thickness is calculated by the Blasius equation for a smooth tube (Olson, 1973):

$$f = \frac{0.316}{\left(\frac{dv}{v}\right)^{0.25}} \quad (\text{Eq. VIII-2})$$

where,

$$\begin{aligned} d &= \text{tube diameter} && (\text{L}) \\ V &= \text{fluid velocity} && (\text{L/t}) \\ \nu &= \text{kinematic viscosity} && (\text{L}^2 \text{ t}^{-1}) \end{aligned}$$

Constriction of the tube accounted for no more than a 10 percent increase in pressure drop whereas pressure drop due to biofilm accumulation increased approximately 110 percent. Clearly, the effect of a reduction in tube diameter by biofilm accumulation was minimal.

**BIOFILM CREEP.** Transport of biofilm in the TR system seems an unlikely explanation for the high frictional resistance in the fouled TR system because the biofilm coating always appeared uniform throughout the tubing (biofilm transport

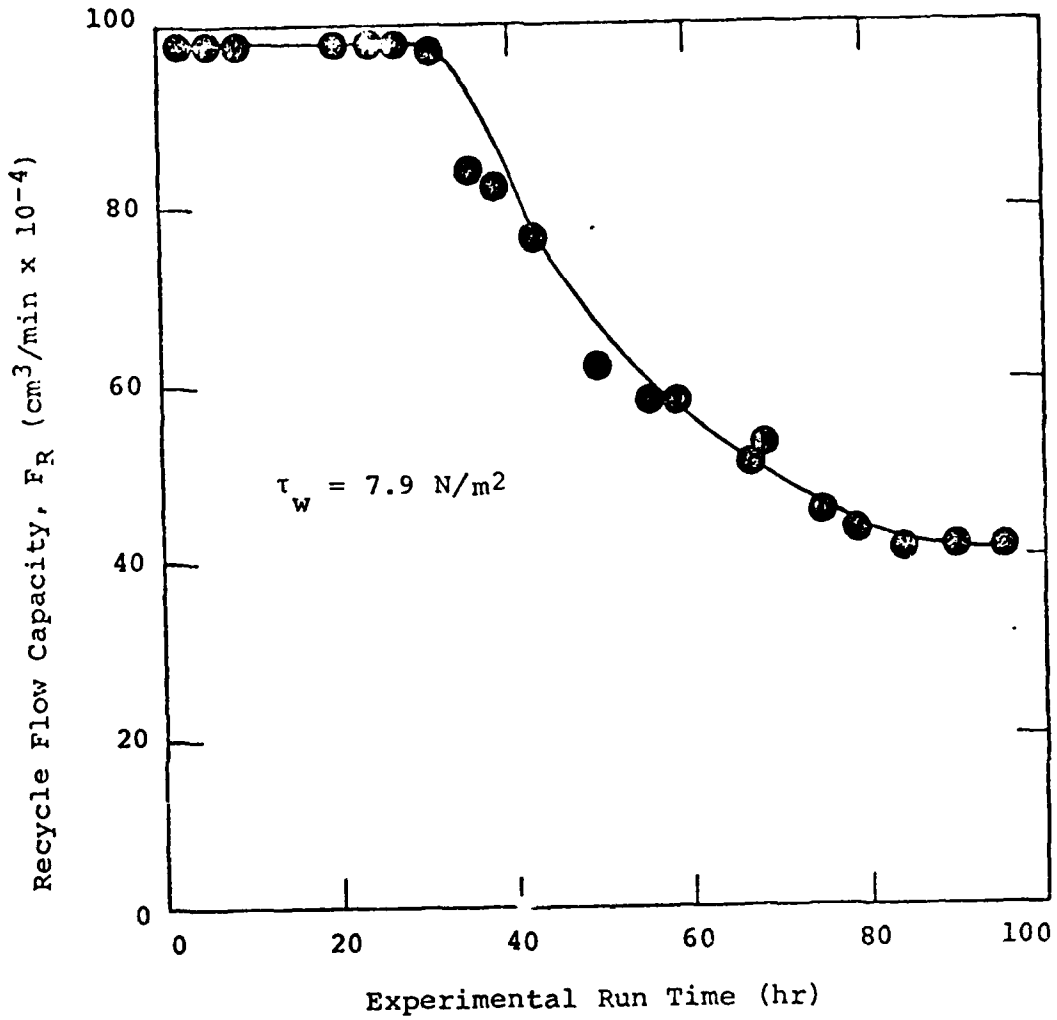


Figure VIII-3. Change in flow capacity with time for a constant pressure drop experiment.

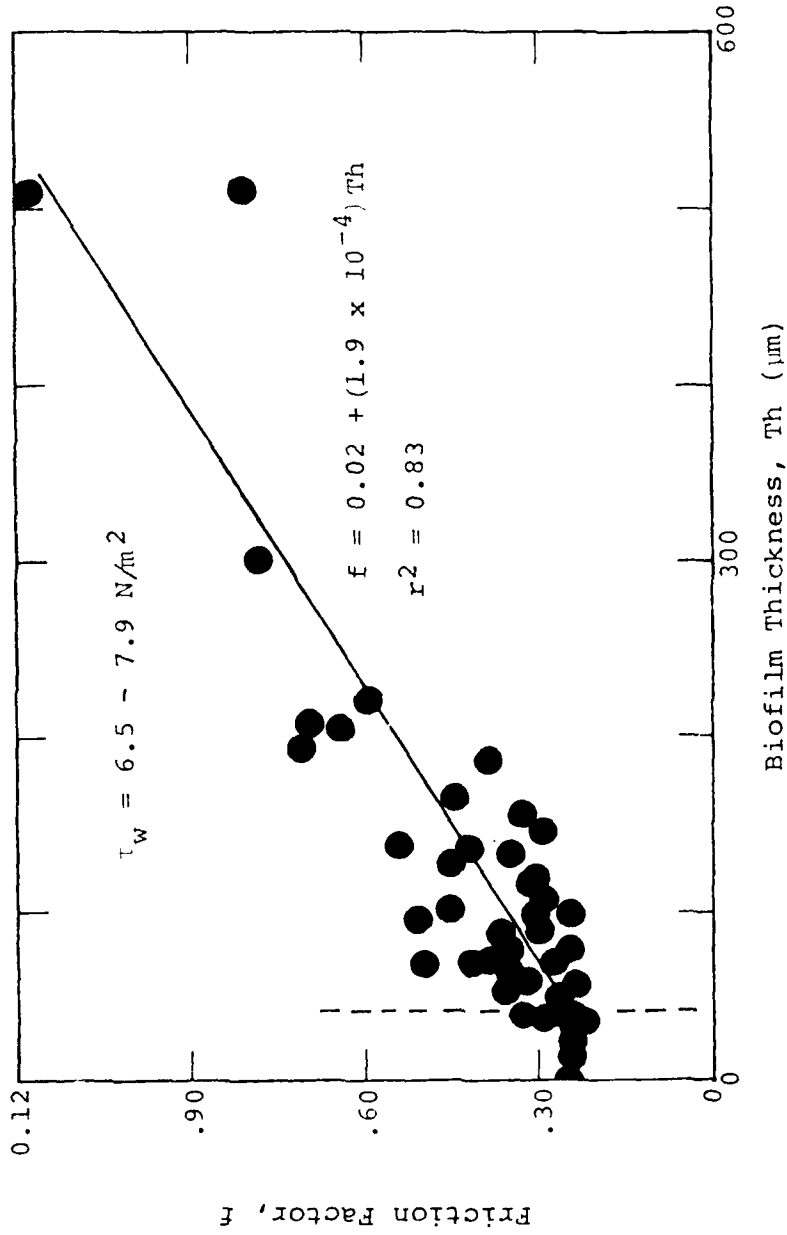


Figure VIII-4. Change in friction factor with biofilm thickness.

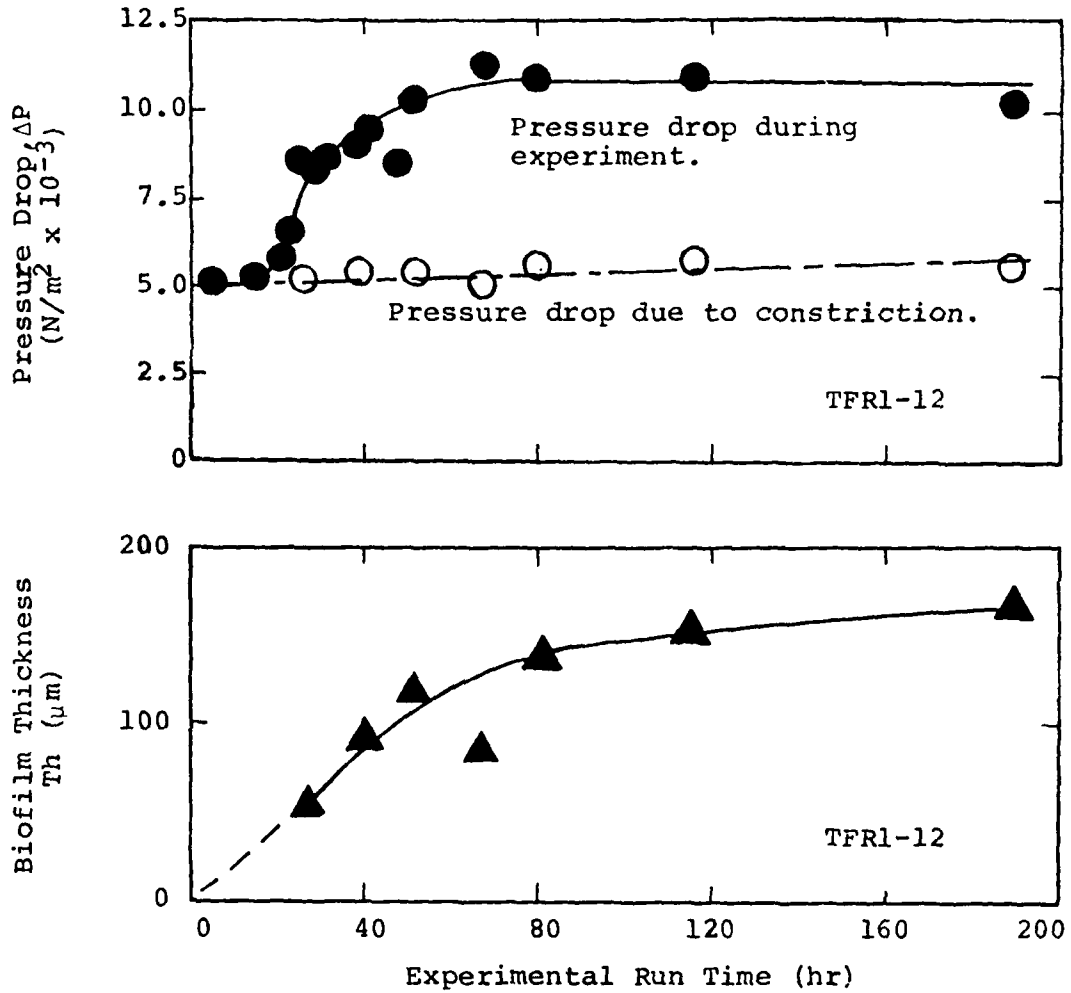


Figure VIII-5. Progression of actual pressure drop compared to the calculated pressure drop due to a decrease in tube radius equal to the biofilm thickness.

would require a steady supply of film or the wall coating would disappear).

**BIOFILM OSCILLATION.** Rheological measurements performed on biofilm grown on platens of a Weissenberg Rheogoniometer established the viscoelastic nature of the biofilm (Zelver, 1979). As a result of the relatively large viscous modulus (the viscous modulus was larger than the elastic modulus at all frequencies tested between 7 Hz and 12 Hz), the possibility exists that the biofilm draws energy from the flow, such energy being eventually dissipated through viscous action. The situation is quite complex and defies analysis, particularly since there is a nonlinear coupling between the structure of the turbulent flow and the biofilm response.

**RIGID ROUGHNESS.** FFR caused by biofouling has been compared to the classical relationships developed for FFR due to *rigid roughness* in tubes (Zelver, 1979 and Picologlou et al., 1980). Extensive work on flow within rough pipes was done by Nikuradse (1932) using known-size sand grains fixed to the inside of tubes. Nikuradse's work describes the relationship of friction factor to Reynolds Number (Re) for a range of sand roughness diameters where Re is a product of fluid velocity, tube diameter and fluid kinematic viscosity:

$$Re = \frac{v d}{\nu} \quad (\text{Eq. VIII-3})$$

where,

$$\begin{aligned} v &= \text{fluid velocity} && (\text{L/t}) \\ d &= \text{tube diameter} && (\text{L}) \\ \nu &= \text{kinematic viscosity} && (\text{L}^2/\text{t}) \end{aligned}$$

The relationship between friction factor and Re for a range of biofilm thicknesses in the fouled TR system (Zelver, 1979) is presented in Figure VIII-6. The dependency of friction factor on Re is the same as for a tube with a rigid rough surface between the range of Reynolds numbers investigated (5,000-48,000). These data were obtained by reducing in steps the shear stress from its initial value in a given experiment and calculating friction factor and Re at each step. Reduction, rather than increase of the shear stress from the initial condition, minimized sloughing of biofilm during an experiment.

The friction factor is related to Re and the equivalent sand roughness,  $k_s$ , through the empirical Colebrook-White

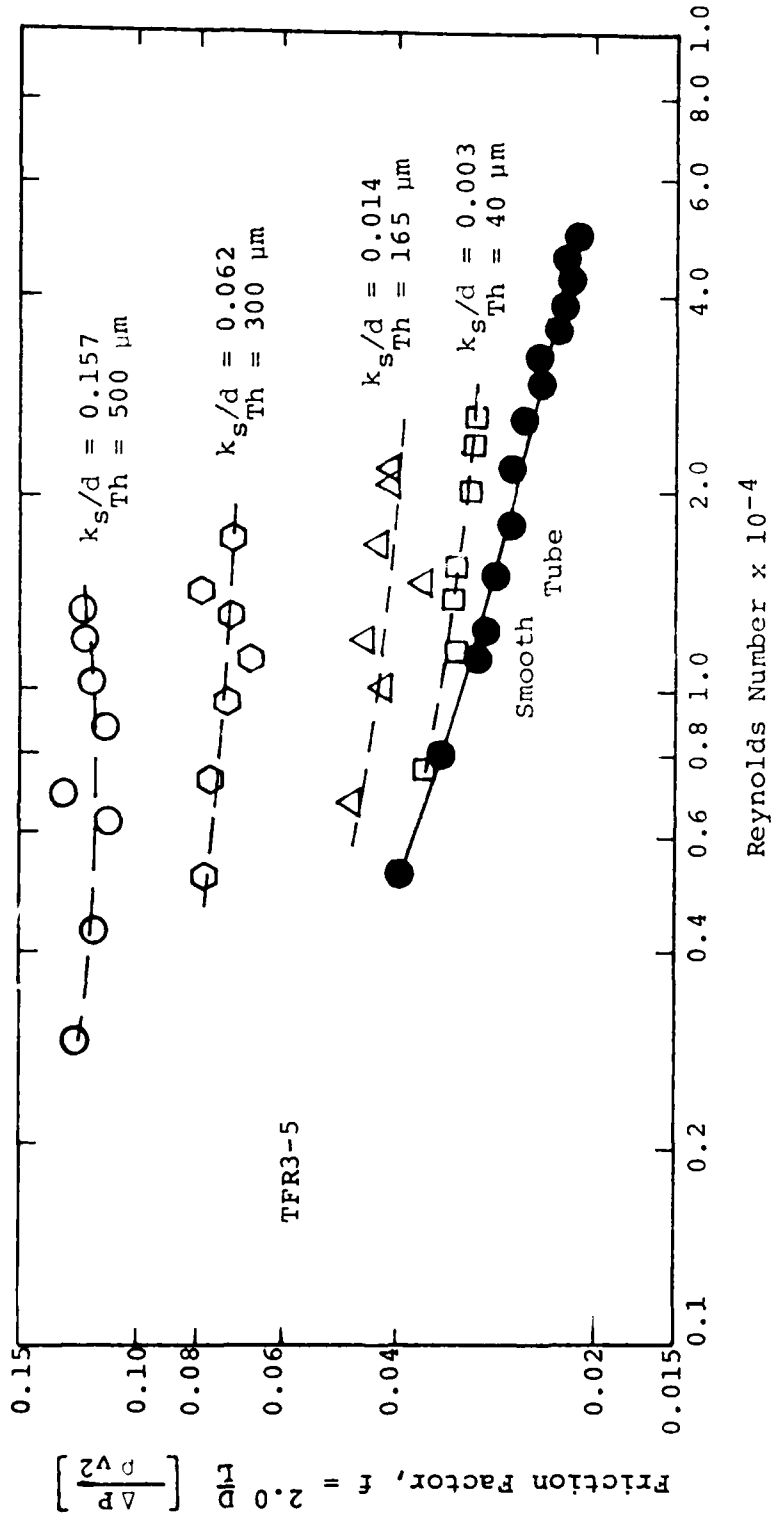


Figure VIII-6. Change in friction factor with Reynolds number for the fouled TR system.

equation (Schlichting, 1968). This equation provides good correlation for friction versus Re for various "commercially rough" tubes:

$$k_s = \frac{d}{2} \left( 10^{(0.87 - 0.50f^{-1/2})} - \frac{18.70}{\text{Re } f^{1/2}} \right) \quad (\text{Eq. VIII-4})$$

where,

d = tube diameter (L)  
 f = friction factor (-)  
 Re = Reynolds Number (-)

This expression can be used to compute an equivalent sand roughness for the biofilm from a measurement of the flow rate (F) and pressure drop ( $\Delta P$ ). Figure VIII-7 shows the progression of  $k_s$  with time for a typical experiment. Figure VIII-8 indicates the dependence of  $k_s$  on biofilm thickness for a range of shear stress values ( $6.5 \text{ N m}^{-2}$  -  $7.9 \text{ N m}^{-2}$ ). The data imply that the equivalent sand roughness of the biofilm can be greater than the actual film thickness. Furthermore, scatter in the  $k_s$  data cannot be attributed to change in nutrient feed or temperature. The difficulty in determining the dependency of  $k_s$  on biofilm thickness may be due to one or all of the following reasons:

1. The biofilm thickness measurement is an average thickness measurement and does not measure actual height of roughness peaks. The average biofilm thickness could be less than any roughness peaks of the biofilm.
2. Drainage of the sample tube prior to the biofilm thickness measurement may decrease the effective biofilm volume and thus decrease the biofilm thickness; the effective biofilm thickness may be greater with the sample tube *in situ* and the biofilm saturated with water.
3. As mentioned previously, the equivalent sand roughness depends on the roughness peaks, but it is not numerically equal to their size. It is not unusual for the equivalent sand roughness to be greater than the roughness peaks (Schlichting, 1968)
4. If the biofilm indeed increases the effective roughness of the tube wall, a dependency of calculated equivalent sand roughness on biofilm surface morphology should be expected. It has been well established that different surface roughness configurations having identical sizes of

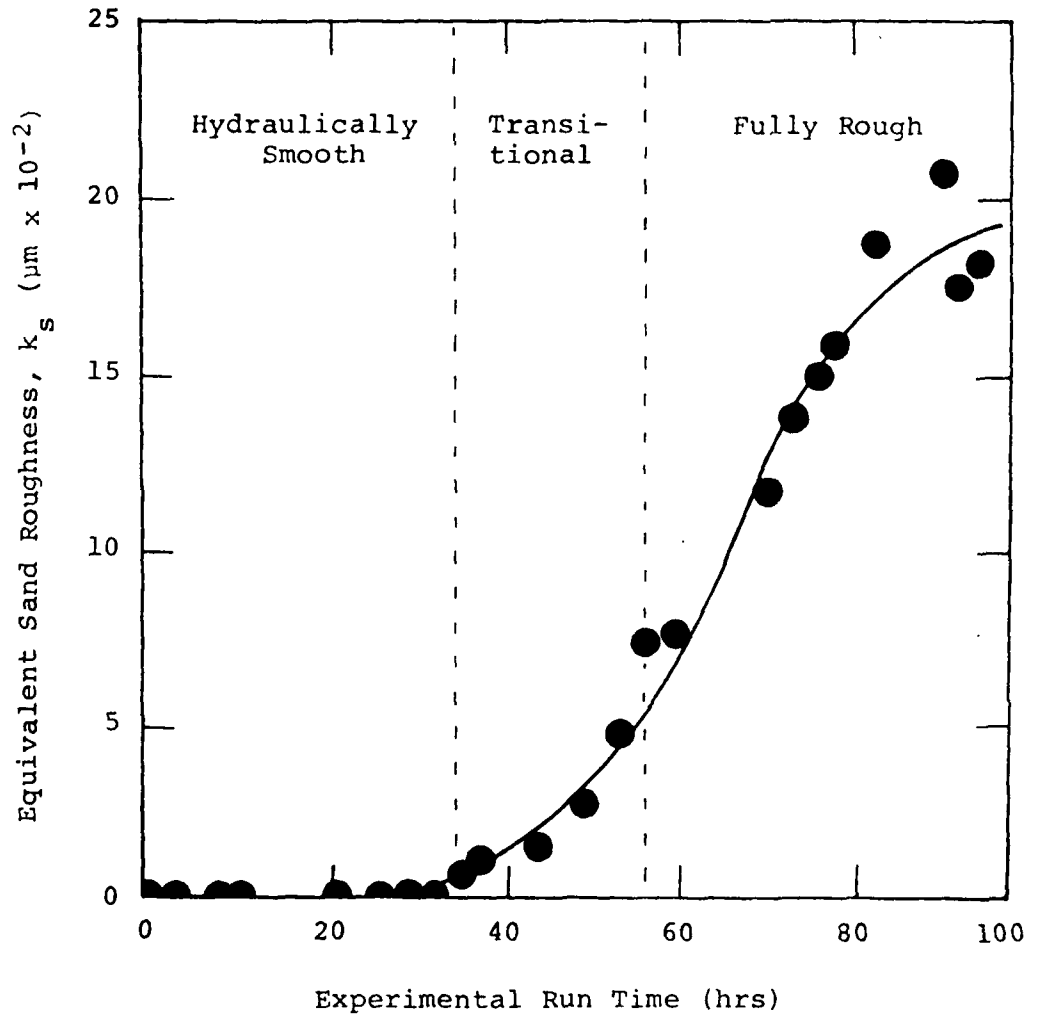


Figure VIII-7. Change in equivalent sand roughness with time.

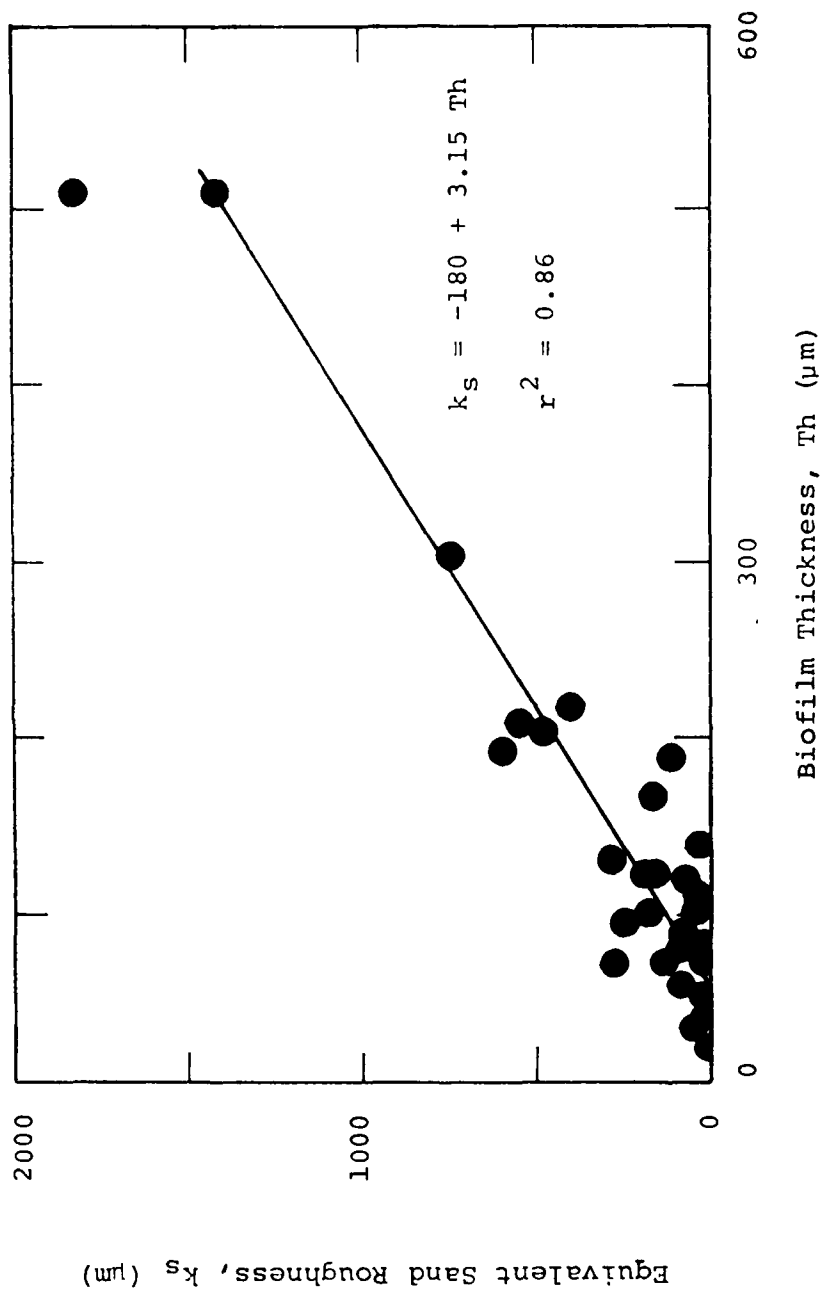


Figure VIII-8. Change in calculated equivalent sand roughness with biofilm thickness at a fluid shear stress of  $6.5\text{--}7.9 \text{ N m}^{-2}$ .

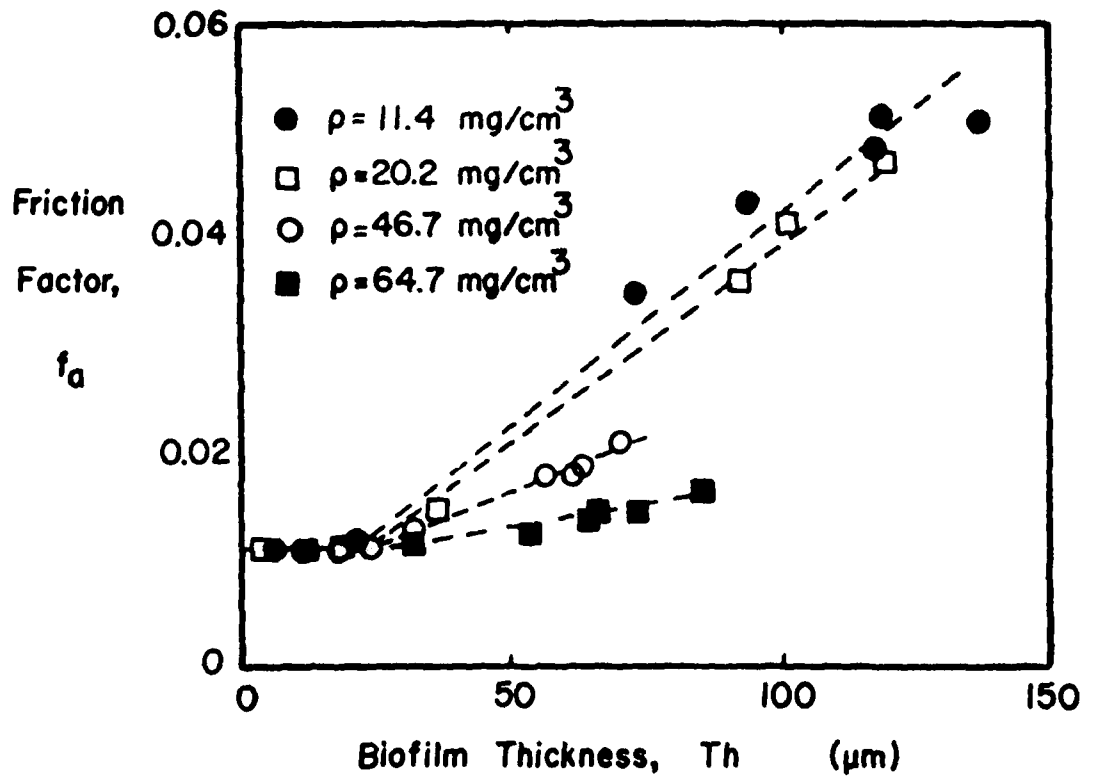


Figure VIII-9. Relationship between friction factor and biofilm thickness as a function of biofilm density ( $\rho$ ) in an annular reactor.

roughness peaks results in different equivalent sand roughness (Schlichting, 1968). Figure VIII-9 shows the relationship between friction factor and biofilm thickness as a function of *biofilm* density in an Annular Reactor (Trulear, 1980). There is no doubt that varied biofilm morphology (density) results in different FFR. In this case, the decrease in biofilm density resulting in increased FFR was attributed to development of filamentous biofilm.

Determination of the flow regime (smooth, transitional, or fully rough) depends on the magnitude of  $k_s$  relative to the size of the viscous sublayer ( $\delta$ ): is given by Schlichting (1968):

$$\delta = \frac{10d}{Re} \left( \frac{f}{2} \right)^{-0.5} \quad (\text{Eq. VII-5})$$

where,

$d$  = tube diameter (L)  
 $Re$  = Reynolds Number (-)  
 $f$  = friction factor (-)

More specifically, when  $k_s < \delta$ , the pipe is considered hydraulically smooth; when  $14\delta > k_s > \delta$ , the flow is in the transitional regime; when  $k_s > 14\delta$ , the flow is in the fully rough regime (Schlichting, 1968). Figure VIII-7 shows the typical progression of a TR experiment where the tube is initially hydraulically smooth and proceeds to the transitional and fully rough regimes.

As indicated in Figure VIII-4, friction factor is dependent of biofilm thickness only *after* a critical thickness is attained which is approximately equal to the thickness of the viscous sublayer. The critical film thickness corresponds to the stage of biofilm development of which surface irregularities protrude through the viscous sublayer. Until this stage, the roughness peaks are smaller than the viscous sublayer thickness ( $k_s < \delta$ ) and the friction factor does not increase (the tube is hydraulically smooth). For a wall shear stress of  $6.5 - 7.9 \text{ Nm}^{-2}$  the viscous sublayer is approximately equal to  $40 \mu\text{m}$ ; this corresponds well with the observed critical thickness ( $30 - 35 \mu\text{m}$ ) for the same wall shear stress range. This is shown in Figure VIII-10 which expands the initial fouling stage of Figure VIII-4. Figure VIII-11 shows the relationship between the viscous sublayer and biofilm thickness at the start of increase in friction factor for experiments run at a range of Reynolds numbers. For this series of  $Re$  biofilm thickness is always very close to the viscous sublayer depth.

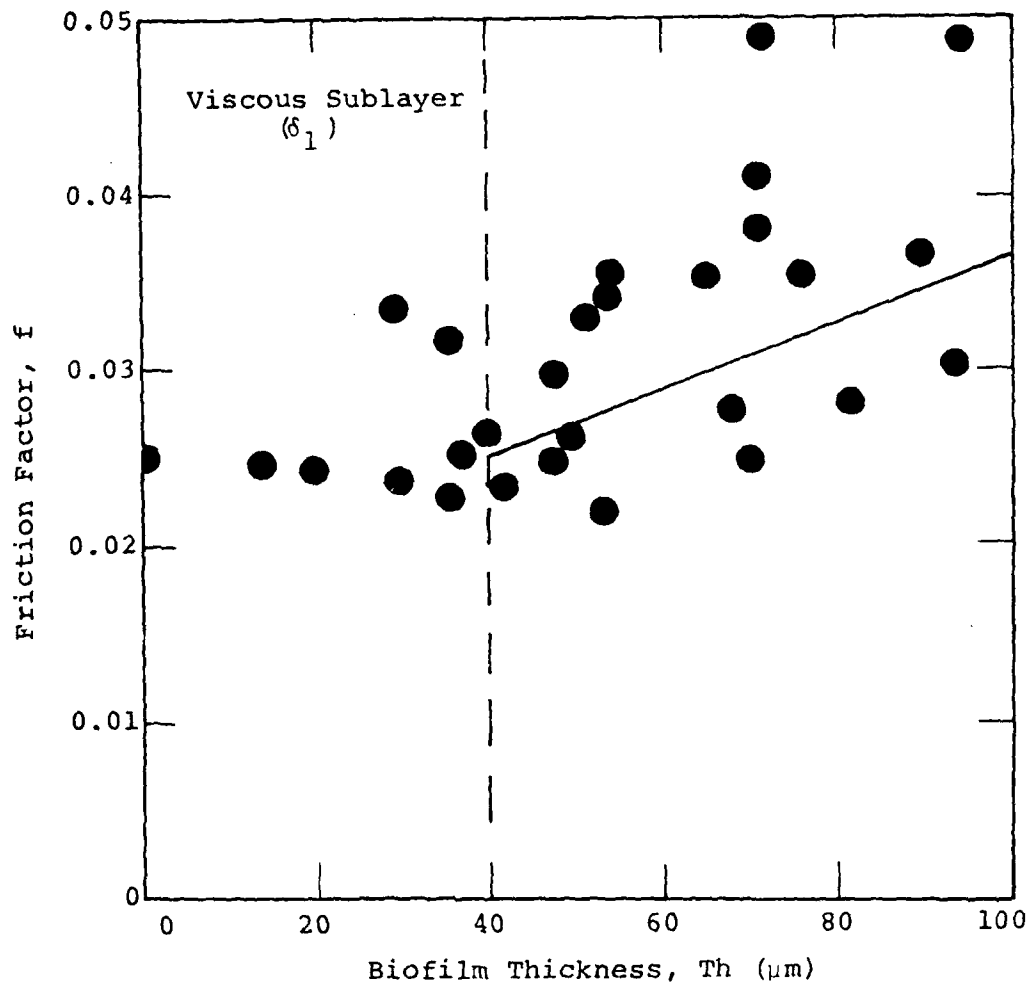


Figure VIII-10. Change in friction factor with biofilm thickness. The critical film thickness where friction factor begins to increase is approximately 30 to 35  $\mu\text{m}$ .

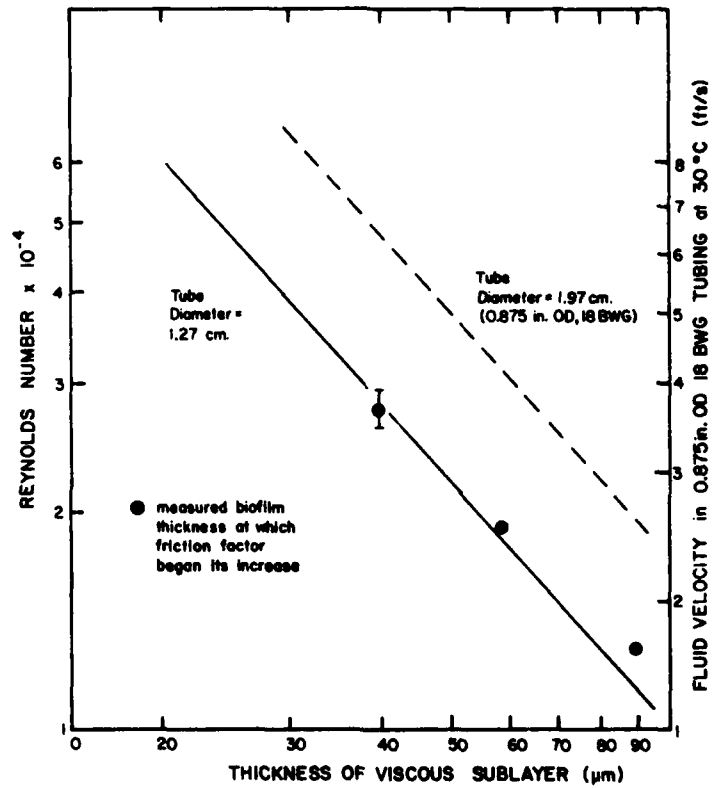


Figure VIII-11. Relationship between the viscous sublayer and biofilm thickness at the start of increase in friction factor for experiments run at a range of Reynolds numbers.

In turbulent flow in conduits with compliant boundaries, the possibility exists that when  $Re$  exceeds a certain value, rippling of the compliant boundary takes place accompanied by drastic changes in friction factor (Schuster, 1971). Such a phenomenon would manifest itself, according to the preceding analysis, as a significant change in the equivalent sand roughness for the biofilm. Such transitions were not observed in our experiments for the range of  $Re$  numbers investigated. A single equivalent sand roughness was sufficient to correlate the friction factor and the  $Re$ .

Although the frictional resistance effects of biofilm can be adequately described by formulas suitable for rigid rough surfaces, the conclusion should not be made that, indeed, the biofilm presents a rigid rough surface to the flow. Such a notion is an oversimplification and cannot account for all experimental observations, e.g., Figure VIII-12 compares two TR experiments with identical conditions except for the roughness of the inner tube surface. The surface of TR3-6 was initially hydraulically smooth ( $k_s/\delta = 0.20$ ) while the surface of TR3-11 was initially fully rough ( $k_s/\delta = 36$ ). The fully rough condition was due to sand grains (average diameter of 0.22mm) immobilized on the inside surface. The following results are evident:

1. Initial friction factor ( $f$ ) is greater in the rough tube and frictional resistance remains greater at all times
2. Frictional resistance is reduced slightly during the first 30 hours in the rough tube.

The decrease in frictional resistance at the beginning of TR3-11 suggests that the biofilm developed between the sand grains and provided a less rough surface up to approximately 30 hours.

The friction factor increases relative to the clean conditions ( $f - f_c$ ) for each experiment are superimposed in Figure VIII-13 and indicate little difference. The additional pronounced frictional resistance in the preroughned tube indicates that the effect of the biofilm on frictional resistance is not due to a simple increase of rigid surface roughness. A possible explanation may lie with the fact that a significant amount of the frictional loss is due to the presence of the biofilm filaments. If so, growth of biofilm filaments on a fully rough pipe will increase the losses and increase the friction factor to the same extent observed in an initially smooth pipe.

**FILAMENTOUS ORGANISMS.** As indicated previously, the presence of filaments appears to increase FFR. The filaments of the biofilm were observed to flutter with a frequency that is a function of the average fluid velocity. It was also observed that frictional resistance increased

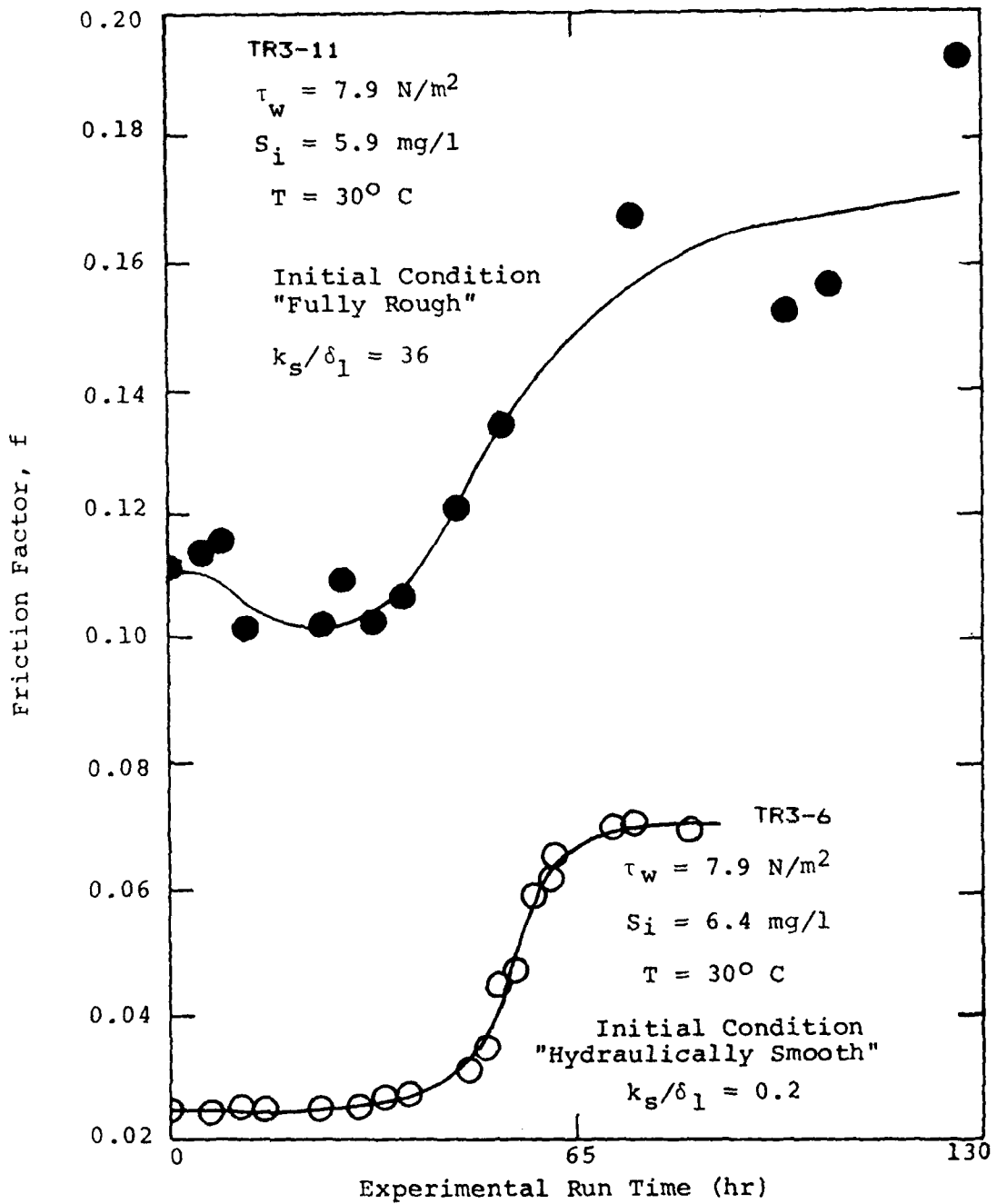


Figure VIII-12. Comparison of friction factor progression in a pre-roughned tube (TR3-11) with friction factor progression in a smooth tube (TR3-6).

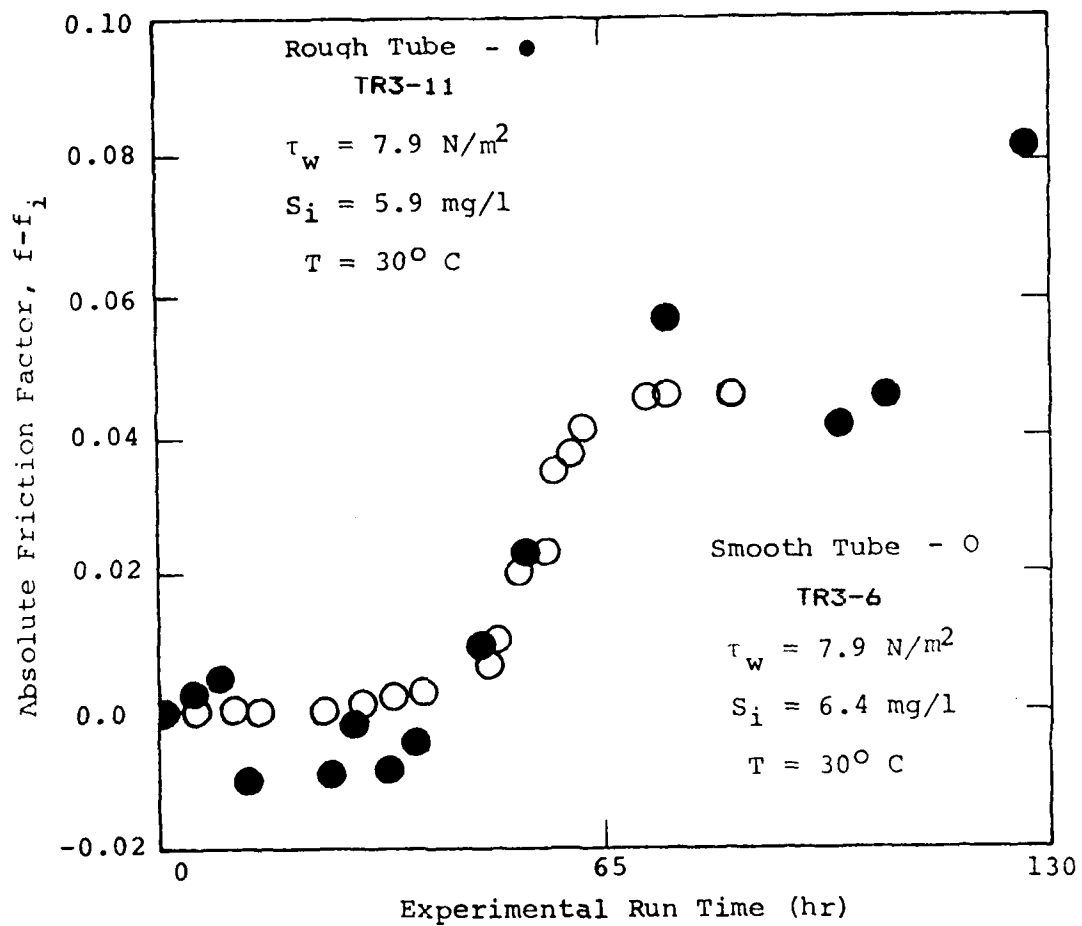


Figure VIII-13. Absolute friction factor progression ( $f-f_i$ ) in a pre-roughened tube (TR3-11) and in a smooth tube (TR3-6).

with increasing filament length. Such increases are analogous to increased drag in streams due to bottom vegetation. Similar phenomena occur in the study of atmospheric boundary layers due the presence of grassy vegetation.

#### CONCLUSIONS

The following conclusions can be derived from the preceding description and analysis of laboratory experiments investigating biofouling and FFR:

1. Increase in frictional resistance corresponds to an increase in biofilm thickness or biofilm mass.
2. Increase in the calculated equivalent sand roughness corresponds to an increase in biofilm thickness.
3. Increase in frictional resistance is characterized by an induction period at small biofilm thicknesses followed by a rapid increase after biofilm thickness reaches a critical value. The critical biofilm thickness corresponds to the viscous sublayer thickness.
4. Constriction of the tube due to biofilm production accounts for only approximately 10 percent of the frictional resistance.
5. The effect of Reynolds Number on friction factor for a tube with an attached biofilm is similar to a tube with a rigid rough surface in the range of Reynolds Numbers investigated (5,000 to 48,000).
6. The filamentous nature of the biofilm contributes to the increase in frictional resistance.

## IX. BIOFILMS AND HEAT TRANSFER

Overall heat transfer resistance is the sum of conductive and convective resistances. Convective heat transfer will decrease as fouling progress due to increased turbulence resulting from deposit formation. Conductive heat transfer resistance will increase as the insulating fouling deposit accumulates. The relative contribution of convective and conductive resistance to overall heat transfer resistance due to biofilm deposition in a laboratory experiment (Characklis *et al.*, 1981a; Nimmons, 1979) is shown in Figure IX-1. The low convective resistance is due to pronounced relative roughness of the biofilm which causes increased turbulence. Recent experiments in our laboratory indicate relative roughness of calcium carbonate scale deposit is small as compared to that of biofilms (Table VI-1) resulting in negligible changes in convective heat transfer resistance.

Present research for the Office of Naval Research includes evaluation of the effect of surface material (metallurgy) and fouling treatments on both biological fouling and corrosion fouling of shipboard heat exchangers. Closed looped systems of heat exchanger tubing has been built in the laboratory to simulate full scale systems. The tubing is interchangeable so that various metals can be tested, in these tests fouling on titanium is compared to fouling on 70:30 Cu/Ni tubing. Treatment by chlorine and cathelco method are being compared on both types of metal surfaces (see section Control).

### FOULING MEASUREMENT

Fouling in the tubular reactor system (TR), described in a previous section, is measured by monitoring the changes in the following parameters:

1. frictional resistance
2. overall heat transfer resistance
3. deposit thickness

The first two methods are the effect of deposition while the latter is a direct measure of the deposit accumulation.

**FRICTIONAL RESISTANCE.** Fouling deposits can cause increased fluid frictional resistance by decreasing the effective diameter of the tube and increasing the tube roughness. Frictional resistance is determined from pressure drop and flow measurements in the tube and is calculated by (Picologlou *et al.*, 1980):

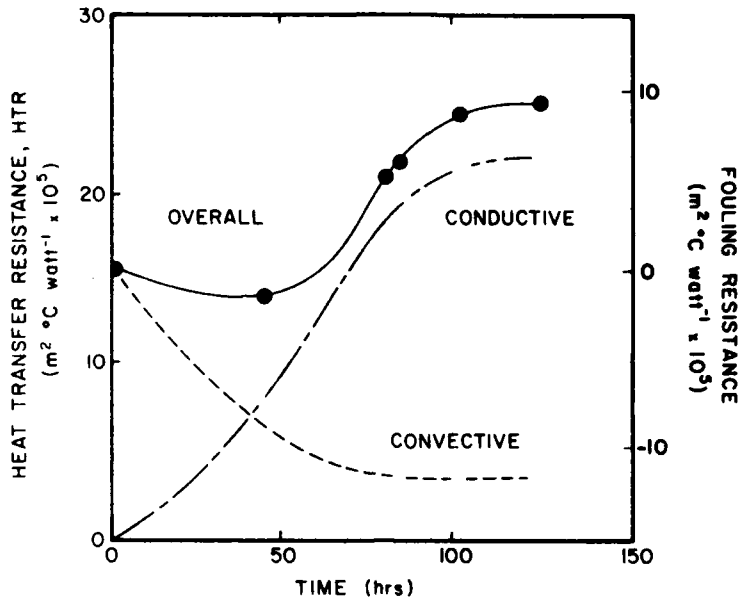


Figure IX-1. Relative contribution of convective resistance and conductive resistance to overall heat transfer resistance due to biofilm deposit in a laboratory experiment.

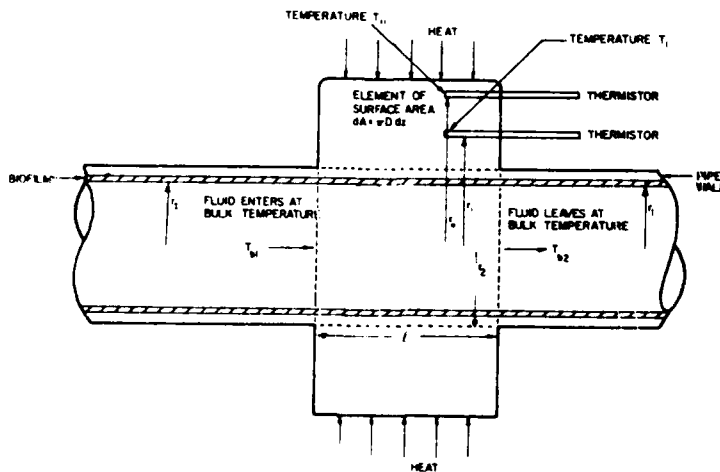


Figure IX-2. Schematic cross-sectional diagram of TWHF.

$$f = \frac{4 r_1 \Delta P}{L \rho_f v^2} \quad (\text{Eq. IX-1})$$

where,

$f$	= frictional resistance	(dimensionless)
$r_1$	= inside radius of the tube	(L)
$\Delta P$	= pressure drop across length L	(ML <sup>-1</sup> t <sup>-2</sup> )
L	= distance between pressure ports	(L)
v	= mean fluid velocity	(Lt <sup>-1</sup> )
$\rho_f$	= fluid density	(ML <sup>-3</sup> )

OVERALL HEAT TRANSFER RESISTANCE. Constant heat is supplied to a thick walled heat exchanger (TWHE) to measure the overall heat transfer resistance. Figure IX-2 is a schematic cross sectional diagram of the TWHE. The TWHE consists of a metal annulus clamped firmly to a heat exchanger tube. The heat transferred through the TWHE can be obtained by measuring the temperature at two radial positions within the metal block.

$$q = \frac{2 \pi k_M l (T_{ii} - T_i)}{\ln(r_{ii}/r_i)} \quad (\text{Eq. IX-2})$$

where,

q	= heat input to metal block	(ML <sup>2</sup> t <sup>-3</sup> )
$k_M$	= thermal conductivity of metal block	(MLt <sup>-3</sup> T <sup>-1</sup> )
l	= length of metal block	(L)
$r_i$	= radial distance to inner thermistor	(L)
$r_{ii}$	= radial distance to outside thermistor	(L)
$T_{ii}$	= temperature at $r_{ii}$	(T)
$T_i$	= temperature at $r_i$	(T)

The contact resistance between the metal block and the tube alloy can be determined using a graphical technique developed by Wilson (1915). If the contact resistance is zero, the temperature on the outside of tube wall,  $T_2$ , can be determined as:

$$T_2 = T_i - \frac{q \ln(r_i/r_2)}{2 \pi k_M l} \quad (\text{Eq. IX-3})$$

where,

$r_2$  = outside radius of tube (L)

$T_2$  = temperature at  $r_2$  (T)

The overall heat transfer resistance can be obtained as:

$$U^{-1} = \frac{2 \pi r_2 l (T_2 - T_{B(AVG)})}{q} \quad (\text{Eq. IX-4})$$

where,

$T_{B(AVG)}$  = average bulk fluid temperature (T)

$U^{-1}$  = overall heat transfer resistance (M<sup>-1</sup>t<sup>3</sup>T)  
at any time t

The overall heat transfer resistance ( $U^{-1}$ ) is the sum of conductive and convective resistances. For a fouled tube  $U^{-1}$  is :

$$U^{-1} = \frac{r_2}{(r_1 - Th)h} + \frac{r_2 \ln(r_2/r_1)}{k_T} + \frac{r_2 \ln(r_1/(r_1 - Th))}{k_D} \quad (\text{Eq. IX-5})$$

convective resistance      conductive resistance  
 (tube alloy)      (fouling deposit)

where,

$h$  = convective heat transfer coefficient (Mt<sup>-3</sup>T<sup>-1</sup>)

$k_T$  = thermal conductivity of tube (MLt<sup>-3</sup>T<sup>-1</sup>)

$k_D$  = thermal conductivity of deposit (MLt<sup>-3</sup>T<sup>-1</sup>)

$Th$  = deposit thickness (L)

For a clean tube, the conductive resistance of the deposit is zero. The convective heat transfer coefficient can be calculated using the Colburn analogy (1933):

$$h = 0.125 f C_p^{0.33} \mu^{-0.67} k^{0.67} \rho_f v \quad (\text{Eq. IX-6})$$

where,

$$\begin{aligned} C_p &= \text{specific heat of fluid} && (\text{L}^2 \text{t}^{-2} \text{T}^{-1}) \\ \mu &= \text{fluid viscosity} && (\text{ML}^{-1} \text{t}^{-1}) \\ k &= \text{fluid thermal conductivity} && (\text{MLt}^{-3} \text{T}^{-1}) \end{aligned}$$

The convective heat transfer resistance,  $R_{\text{CONV}}$ , can be calculated as:

$$R_{\text{CONV}} = \frac{r_2}{(r_1 - Th)h} \quad (\text{Eq. IX-7})$$

where,

$$R_{\text{CONV}} = \text{convective heat transfer resistance} \quad (\text{M}^{-1} \text{t}^3 \text{T})$$

The conductive heat transfer resistance of the deposit,  $R_{\text{COND}}$ , can be calculated rearranging equation IX-5:

$$R_{\text{COND}} = U^{-1} - \frac{r_2}{(r_1 - Th)h} - \frac{r_2 \ln(r_2/r_1)}{k_T} \quad (\text{Eq. IX-8})$$

where,

$$R_{\text{COND}} = \text{conductive heat transfer resistance of deposit} \quad (\text{M}^{-1} \text{t}^3 \text{T})$$

The thermal conductivity of the deposit can be estimated from the conductive heat transfer resistance of the deposit and the deposit thickness.

$$k_D = \frac{r_2 \ln(r_1/(r_1 - Th))}{R_{\text{COND}}} \quad (\text{Eq. IX-9})$$

DEPOSIT THICKNESS. The thickness of the deposit in the test section is estimated from the volume of the deposit. A detailed description of the method for estimating the deposit volume is presented elsewhere (Zelver, 1979). Deposit thickness is determined by dividing deposit volume by the surface area of the tube.

#### OVERALL HEAT TRANSFER RESISTANCE

Fouling can be monitored by measuring the increase in overall heat transfer resistance which is the major concern in heat exchangers/condensers.

The overall heat transfer resistance is the sum of conductive and convective heat transfer resistance. For a clean tube, at time  $t = 0$ , the *conductive resistance of the deposit* is zero so that the convective resistance is equal to the overall heat transfer resistance (clean tube). At any time,  $t > 0$ , the relative contribution of conductive and convective resistance to overall heat transfer resistance will depend on the type of deposit accumulated on the heat transfer surface.

Experiments have been conducted in our laboratory to determine the influence of different types of deposit on heat transfer resistance. In this study, the tube alloy (70:30 Cu/Ni), bulk water temperature (35°C), flow velocity ( $0.91 \text{ m s}^{-1}$  or 3 fps), calcium content ( $250 \text{ mg l}^{-1}$ ), and the pH of the water (8-8.2) were held constant in all the experiments. The influence of three different types of deposit on heat transfer resistance was determined.

In the case of a combined biofilm/scale, the experiment was initiated by inoculating the fermenter with a mixed population of microorganisms and operating in the batch mode for 8-10 hours. The system was then continuously supplied with  $10 \text{ mg l}^{-1}$  glucose. In the case of silicate scale, the system was continuously supplied with  $200 \text{ mg l}^{-1}$  of sodium silicate while in the case of a pure calcium carbonate scale the system was not supplied with glucose or sodium silicate. The following observations were noteworthy:

1. Different types of deposit were found to exhibit a different rate and extent of fouling as measured by the increase in overall heat transfer resistance.
2. In the case of "pure scale" (Figure IX-3), the increase in overall heat transfer resistance was largely due to the increase in conductive resistance. This type of deposit was found to exhibit a low relative roughness and the convective resistance was essentially constant.
3. The calcium carbonate/silicate scale (Figure IX-4) exhibited a higher increase in overall heat transfer resistance as compared to a calcium carbonate scale.
4. For the combined biofilm/scale (Figure IX-5), the increase in conductive resistance of the deposit was largely offset by the decrease in convective

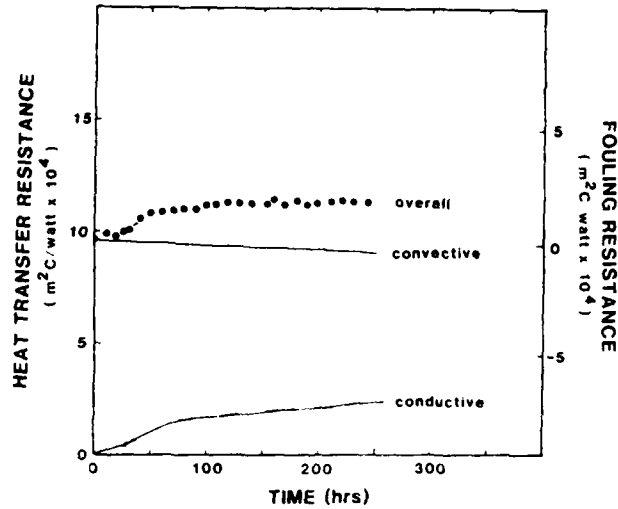


Figure IX-3. Progression of heat transfer resistance due to the deposition of calcium carbonate for a constant flow of  $0.91 \text{ m s}^{-1}$  (tube alloy 10:30 Cu/Ni and  $\text{Ca}^{++} = 250 \text{ mg l}^{-1}$ ).

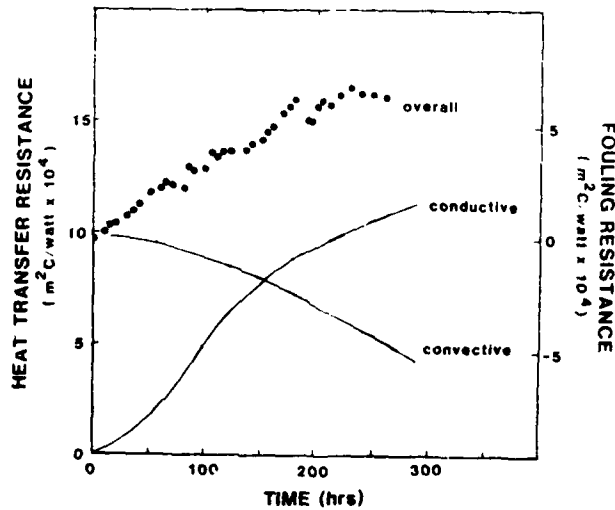


Figure IX-4. Progression of heat transfer resistance due to the deposition of calcium carbonate/silicate scale for a constant flow of  $0.91 \text{ ms}^{-1}$  (tube alloy 70:30 Cu/Ni,  $\text{Ca}^{++} = 250 \text{ mg l}^{-1}$ ,  $\text{Na}_2\text{SiO}_3 = 200 \text{ mg l}^{-1}$ ).

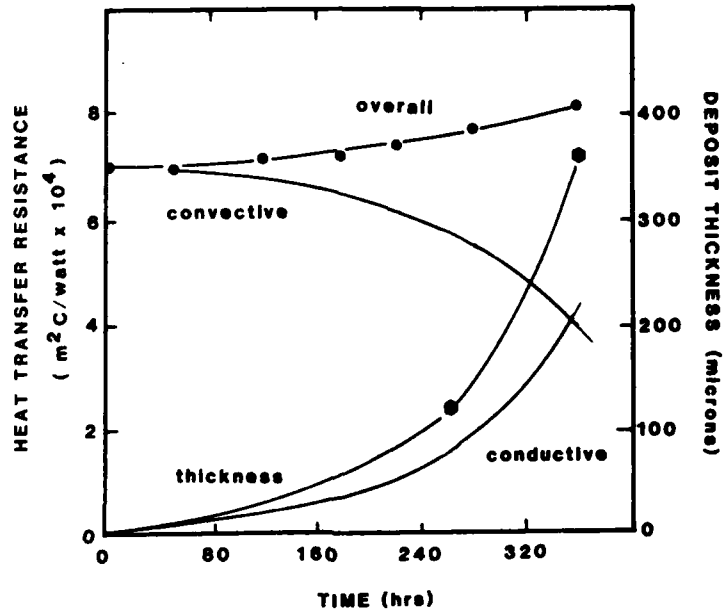


Figure IX-5. Progression of heat transfer resistance due to the deposition of combined biofilm/scale for a constant flow of  $0.91 \text{ m s}^{-1}$  (tube alloy 70:30 Cu/Ni,  $\text{Ca}^{++} = 250 \text{ mg l}^{-1}$ , total organic carbon =  $10 \text{ mg l}^{-1}$  (Glucose)).

resistance (due to deposit roughness).

#### FOULING RESISTANCE

Fouling data are customarily reported in terms of *fouling resistance* or *fouling factor* ( $R_f$ ) which is defined as follows:

$$R_f = U^{-1} - U_o^{-1} \quad (\text{Eq. IX-10})$$

where,

$$R_f = \text{fouling resistance or fouling factor} \quad (\text{M}^{-1} \text{t}^3 \text{T})$$

$$U_o^{-1} = \text{overall heat transfer resistance at} \quad (\text{M}^{-1} \text{t}^3 \text{T})$$

$$t = 0$$

The term *fouling resistance* is sometimes misleading and does not yield any valuable diagnostic information:

1. The influence of fouling on heat exchange rate in engineering design is generally determined as a *fouling resistance* describing the *thermal* (conductive) resistance of the deposit (Kreith, 1973). In fact, the term *fouling resistance* represents the *net* increase in heat transfer resistance (conductive plus convective resistance) and not thermal (conductive) resistance of the deposit.
2. The values for *fouling resistance* are generally selected from tables (e.g., TEMA standard) of questionable accuracy with vague information as to the operating condition (shear stress) and the type of deposit (scale, biofilm, etc.) for which *fouling resistance* values were determined.
3. The conductive resistance of the deposit, in *most* cases, will be higher than the *fouling resistance*. The extent to which it is greater than *fouling resistance* will depend on the roughness characteristics of the deposit accumulated on the heat transfer surface. Figure IX-1 shows the increase in heat transfer resistance due to accumulation of biofilm inside a tube in a laboratory experiment (Characklis et al., 1981a). In terms of *fouling resistance*, an increase in heat transfer resistance of 0.00009  $\text{m}^2 \text{ }^\circ\text{C/watt}$  (0.00051  $\text{ft}^2 \text{ h }^\circ\text{F/BTU}$ ) was observed, but the increase in conductive resistance was 0.00023  $\text{m}^2 \text{ }^\circ\text{C/watt}$  (0.0013  $\text{ft}^2 \text{ h }^\circ\text{F/BTU}$ ), 2.5 times higher than *fouling resistance*.
4. The calculation of *fouling resistance* depends on the overall heat transfer resistance (i.e., convective resistance) at clean condition. For

example, velocity of water past the heat transfer surface will influence the convective resistance at clean condition and hence the calculation of *fouling resistance*.

5. Most mathematical models (Kern and Seaton, 1968; Taborek et al., 1972; Watkinson and Epstein, 1969) describing the influence of fouling processes on heat transfer are generally based on the following relationship:

$$\frac{dR_f}{dt} = \phi_d - \phi_r \quad (\text{Eq. IX-11})$$

where,

$$\frac{dR_f}{dt} = \text{net rate of fouling accumulation} \quad (\text{M}^{-1}\text{t}^2\text{T})$$

$$\phi_d = \text{deposition rate} \quad (\text{m}^2\text{K/J})$$

$$\phi_r = \text{removal rate} \quad (\text{m}^2\text{K/J})$$

This relationship expresses the deposition rate and removal rate of fouling deposit in terms of energy units rather than in term of mass flux.

Based on Equation IX-11, at constant *fouling resistance*, the deposition rate equals removal rate (or thickness remains constant). However, constant *fouling resistance* can also result when the increase in conductive resistance (or thickness) of the deposit equals the decrease in convective resistance (due to deposit roughness).

6. The *fouling resistance* model (Equation IX-11) defines fouling resistance as:

$$R_f = Th/k_D \quad (\text{IX-12})$$

where, Th = thickness of deposit (L)  
 $k_D$  = thermal conductivity of deposit (MLt<sup>-3</sup>T<sup>-1</sup>)

This relationship is *only valid* when the convective resistance remains constant and *fouling resistance* equals conductive resistance of deposit. Fouling, in most cases, is associated with an increase in pressure drop (or decrease in convective resistance).

7. The model (Equation IX-11) cannot predict a negative value of  $R_f$ . Yet, negative *fouling resistance* can result during initial biofilm accumulation (Figure IX-1), when the increase in *conductive resistance* (or thickness) of the deposit is *less* than the decrease in convective resistance. Negative *fouling resistance* in the early stages of biofilm accumulation has also been

- observed in the field when new surfaces are initially exposed to a fouling environment.
8. Asymptotic *fouling resistance* can only result when conductive and convective resistance of the deposit remain constant (special case  $\alpha_d = \alpha_r$ ).
  9. At constant deposit (biofilm) thickness, change in density or composition of the deposit can influence the conductive resistance (*fouling resistance*) of the deposit.

#### COMBINED HEAT TRANSFER AND FRICTIONAL RESISTANCE

Heat transfer resistance or frictional resistance measurements alone cannot be effectively used to monitor fouling since, in such cases, the deposits are rarely homogenous. However, frictional resistance, in combination with heat transfer measurements, can yield valuable information on the progress of fouling.

#### FOULING DIAGNOSIS POTENTIAL

Fouling monitoring methods frequently do not measure effects of deposition and do not yield information regarding the composition and type of deposit. Information regarding deposit type would be useful in selecting an appropriate treatment procedure.

Recent experiments in our laboratory indicate a significant difference in fouling deposit properties as shown in Table IV-1. These properties can be estimated using a fouling monitor which measures the increase in deposit thickness, heat transfer resistance, and frictional resistance. A summary diagram of such a monitoring program is shown in Figure IX-6. The type of deposit occurring inside a heat exchanger/condenser can be determined by estimating its thermal conductivity and relative roughness using a fouling monitor if an apparent deposit thickness is known. If an apparent deposit thickness could be determined *in situ*, the *in situ* estimation of deposit thermal conductivity and deposit relative roughness can be used as a diagnostic decision variable for internal control of fouling. Characklis et al., (1982) have described a method for obtaining apparent deposit thickness *in situ* and *automatically* at regular intervals. A schematic diagram illustrating the apparatus required for this method is shown in Figure IX-7.

#### FIELD OBSERVATIONS

The fouling monitor system has been successfully used (Characklis et al., 1981b; Zilver et al., 1982) to monitor fouling in a brackish water cooling system. The goal of one such project (Zilver et al., 1982) was to determine the fouling potential of AL-6X stainless steel heat exchanger tubing. An inside tube wall temperature was chosen for optimum fouling indicated by previous laboratory studies (Stathopoulos, 1981). Results show a rapid build-up of a microbial matrix containing considerable silt

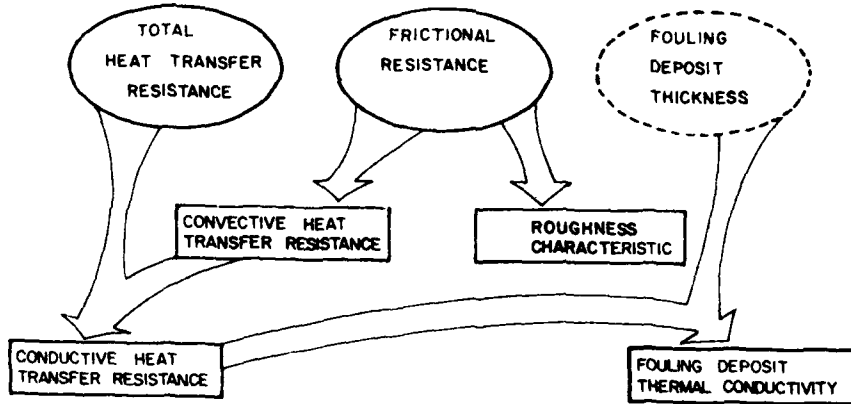


Figure IX-6. Summary of fouling monitoring method.

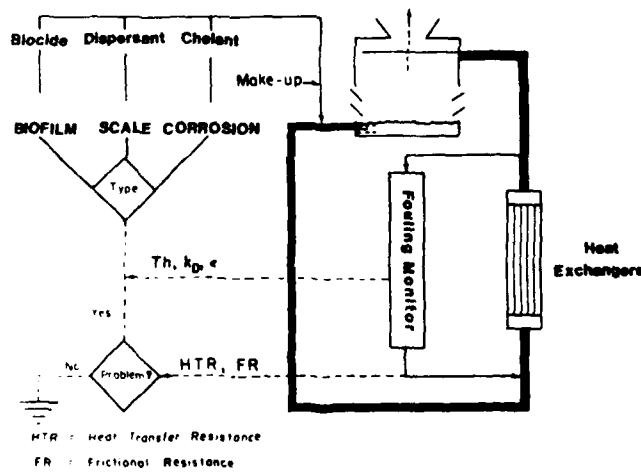


Figure IX-7. An illustration of the use of a diagnostic, on-line fouling monitor as a feedback control device in an open, recirculating cooling tower system.

debris. Heat transfer fouling appears to plateau at approximately  $0.0012 \text{ m}^2 \text{ C/watt}$  ( $0.0068 \text{ ft}^2 \text{ °F hr/BTU}$ ) within 40 to 60 days regardless of seasonal variation or flow velocity from  $0.30 \text{ m s}^{-1}$  (1.0 fps) to  $0.50 \text{ m s}^{-1}$  (1.7 fps).

*Test conducted at  $0.30 \text{ m s}^{-1}$  (1.0 fps).* Figure IX-8 presents the progression of heat transfer resistance and the fouling factor for the first 100 days of testing at a constant flow velocity of  $0.30 \text{ m s}^{-1}$  and a constant inside tube wall temperature of  $35 \text{ °C}$  ( $95 \text{ °F}$ ). In addition to the obvious increase in heat transfer with time, several other features are noteworthy:

1. On day 24 and day 62, momentary flow excursions occurred which increased flow to  $0.90 \text{ m s}^{-1}$ . These flow excursions were associated with sudden drops in heat transfer resistance as a result of the fouling deposit sloughing off.
2. On day 30, the AL-6X was replaced with a new AL-6X tube of identical dimension (test 2). The fouling factor returned to within 3 percent of its original value. Figure IX-9 shows the progression of heat transfer resistance for the first 30 days (test 1) superimposed on test 2 results. Progression of heat transfer resistance was almost identical for both test despite seasonal variation resulting in change in bulk water temperature from  $17 \text{ °C}$  to  $27 \text{ °C}$ .

Figure IX-10 presents the progression of fluid friction resistance as friction factor for test 1 and test 2 at a low velocity of  $0.3 \text{ m s}^{-1}$ . A similar progression as heat transfer resistance is observed. Of particular interest, is the drop in the frictional resistance at day 62 corresponding to the drop in heat transfer resistance attributed to the  $0.90 \text{ m s}^{-1}$  flow excursion.

*Test conducted at  $0.50 \text{ m s}^{-1}$  (1.70 fps).* Figure IX-11 shows the progression of heat transfer resistance and the fouling factor with time for a flow velocity of  $0.50 \text{ m s}^{-1}$  and a constant inside wall temperature of  $35 \text{ °C}$ . No flow excursion or other perturbations occurred during the 80 day test period. The progression of fouling followed a typical sigmoidal pattern and plateau which is seen for almost any measurement of fouling progression (Characklis et al., 1981a).

The plateau fouling factor was virtually the same as for  $0.30 \text{ m s}^{-1}$ . Furthermore, the rate of fouling at  $0.50 \text{ m s}^{-1}$  is very similar to that observed at  $0.30 \text{ m s}^{-1}$ .

#### MICROBIAL CELL ACCUMULATION IN A FINNED TUBE

Biofouling of heat exchange equipment can impede the flow of heat across the surface, increase fluid frictional resistance at the surface, and increase the corrosion at the surface. In each case, energy loss results.

The need for high performance, compact heat exchange

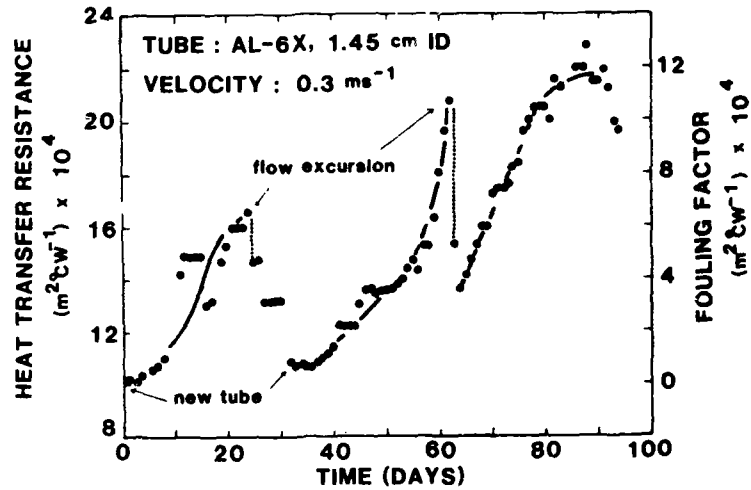


Figure IX-8. Progression of heat transfer resistance at constant flow rate ( $0.3 \text{ m s}^{-1}$ ) and constant temperature ( $35^\circ\text{C}$ ).

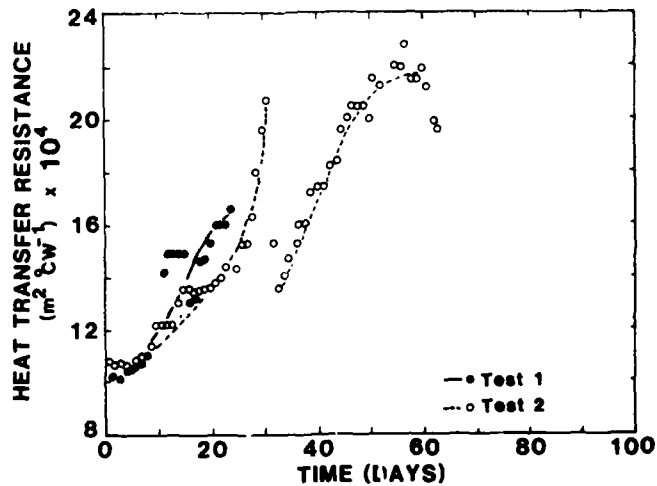


Figure IX-9. Progression of heat transfer resistance for test 1 (Figure IX-8) superimposed on test 2 at a constant flow rate ( $0.3 \text{ m s}^{-1}$ ) and constant surface temperature ( $35^\circ\text{C}$ ).

AD-A131 084

MICROBIAL FOULING AND ITS EFFECT ON POWER GENERATION  
(U) MONTANA STATE UNIV BOZEMAN DEPT OF CIVIL  
ENGINEERING AND ENGINEERING MECHANICS

2/2

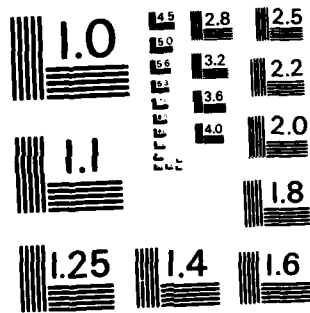
UNCLASSIFIED

W G CHARAKLIS ET AL. JUL 83

F/G 13/10

NC

END
DATE
FILMED
8 83
DTI



MICROCOPY RESOLUTION TEST CHART  
NATIONAL BUREAU OF STANDARDS-1963-A

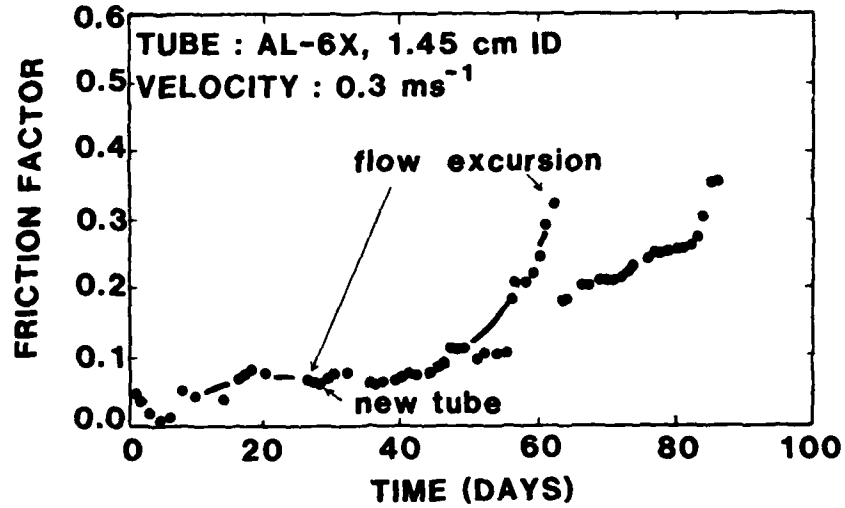


Figure IX-10. Progression of friction factor with time at a constant flow rate ( $0.3 \text{ m s}^{-1}$ ).

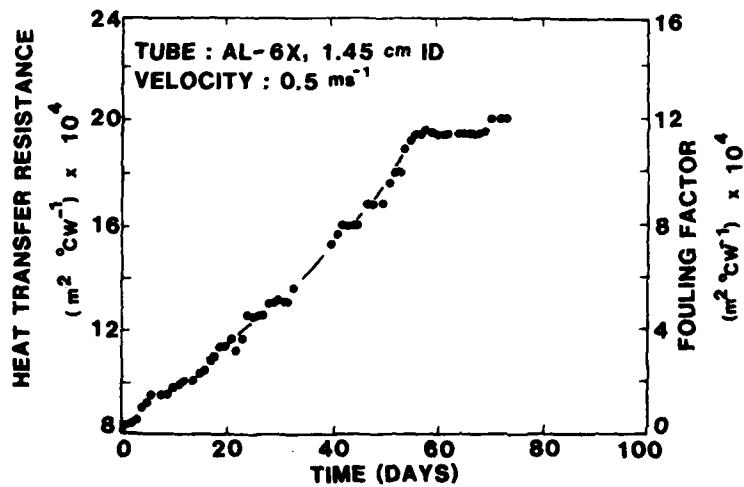


Figure IX-11. Progression of HTR at a constant flow rate ( $0.5 \text{ m s}^{-1}$ ) and constant surface temperature ( $35^\circ\text{C}$ ).

equipment has led to the development of many types of surfaces that enhance heat transfer performance of smooth tubes. Enhanced performance over smooth tubes is achieved by providing inner fins or using indented or fluted tubes. These tubes increase the heat transfer rate by modifying the flow pattern and increasing the surface area for heat transfer. The modified flow pattern in enhanced heat transfer tubes also increases the convective heat transfer. However, enhanced convective heat transfer suggests that convective mass transfer is also increased. Increased mass transfer leads to increased transport of potential fouling materials to the surface.

An experiment was conducted to compare the deposition and distribution of microorganisms on a smooth tube and a tube with inner fins in a controlled laboratory experimental system.

**EXPERIMENTAL SYSTEM AND METHODS.** The experimental results were obtained by measuring the number of bacterial cells attached on a tube section within a recirculating tubular reactor system (TR). The system consists of a mixing tank and an external recycle loop (Figure IX-12). The recycle loop consisted of 1.587 cm O.D., 70:30 Cu/Ni heat exchange tubing with wall thickness of 0.132 cm. The dilution rate,  $F_D$ , ( $0.027 \text{ l min}^{-1}$ ) was much smaller than the recycle rate,  $F_R$ , ( $7.5 \text{ l min}^{-1}$ ) therefore the entire system behaved as a continuous stirred tank reactor (CSTR). The Reynolds number in the recycle loop based on smooth tube diameter was 16600. A detailed description of the experimental system is presented elsewhere (Characklis, 1980). The experimental system included a test section (Figure IX-13c) consisting of a series of removable tubes (5 cm long) which were held in place, between teflon gaskets (fins) whose I.D. and O.D. were the same as that of tube material to form a continuous tube (Figure IX-13b).

The same test section was used to form a continuous tube with circular inner fins (height of the fin = 0.094 cm) which were placed 5 cm apart (Figure IX-13a). The circular fins were 0.06 cm thick teflon rings (I.D. = 1.135 cm. O.D. = 1.587 cm).

The experiment was initiated by inoculating a mixed population of microorganisms and operating the reactor in a batch mode (as opposed to continuous flow) for 8 hours. The dilution feed consisted of a substrate solution, dilution water, and micronutrients. The substrate was composed of glucose ( $10 \text{ mg l}^{-1}$ ) as the sole carbon and energy source. The temperature inside the reactor was maintained at  $30^\circ\text{C}$  and pH 8 - 8.2. The mean fluid velocity was  $0.91 \text{ m s}^{-1}$ .

Each tube section was machine grooved on the outside so that the tube could be broken into five (5) segments easily. The tube segments were numbered for identification. At the end of 100 hours, a tube section from the smooth tube and another from the finned tube was removed from the reactor. The tube sections were broken into five segments. The

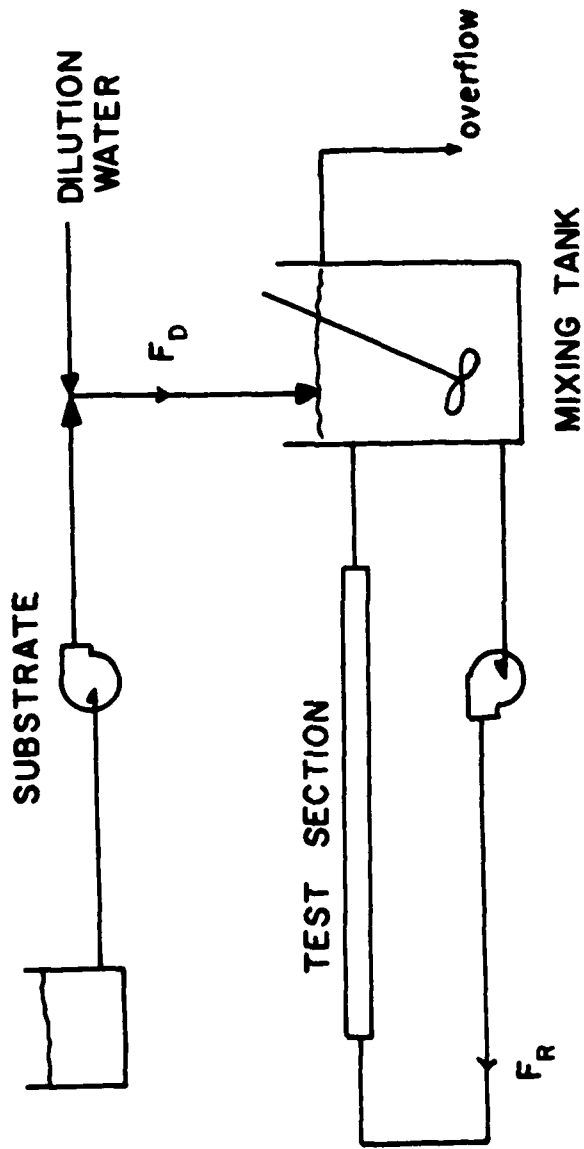


Figure IX-12. Schematic diagram of the Experimental system.

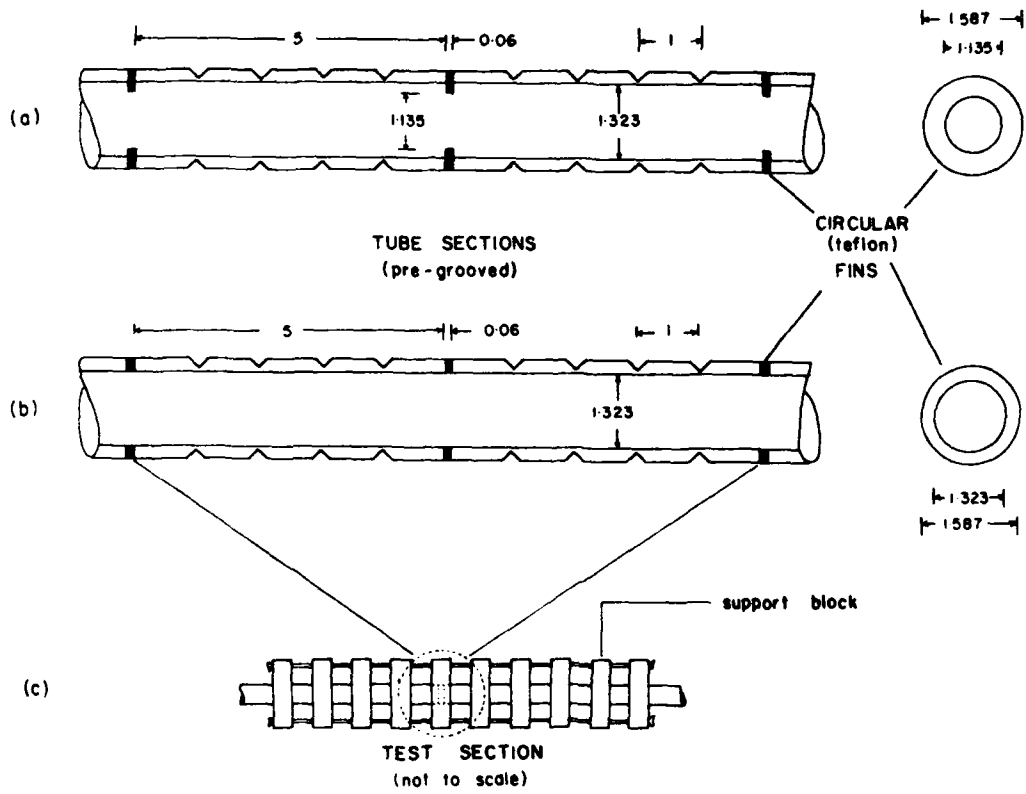


Figure IX-13. Details of test section and tube section assembly.

biofilm from these segments was scraped into 5 ml of 2 percent filtered (average pore size 0.002 cm) formalin. The total number of cells on these tube segments were measured by acridine orange direct count (AODC) epifluorescence microscopy (Hobbie et al., 1977).

RESULTS. Experiments were conducted to compare the distribution of attached bacteria on a 5 cm smooth tube section and a section of tube between two circular fins separated by a distance of 5 cm. The total number of attached cells at the end of 100 hours was measured by AODC epifluorescence microscopy.

The following observations are noteworthy:

1. There exists a significant difference in the distribution of attached cells in a tube section with two inner circular fins (Figures IX-14 and IX-15) as compared with a smooth tube section. The height of the fin protruding in the flowing fluid (7.5 l/min) was 0.094 cm. The minimum amount of attached cells was found at the center of the tube. In general, the flow pattern in the finned tube will influence the distribution of attached cells.
2. The extent of fouling in finned tube section was somewhat less than that of the smooth tube (Figures IX-14 and IX-15).

If mass and heat transfer rates are greater in the finned tube, why are fewer cells observed on the finned tube? The reported data reflect net accumulation of microbial cells. Consequently, increased turbulence in the region between the fins may decrease the attachment rate or increase detachment rate or both. The results after 100 hours can only suggest a decreased *sticking efficiency* for microbial cells under experimental conditions.

No systematic studies of biofilm accumulation in finned tubes are available. Preliminary results obtained suggest that a significantly different distribution of attached cells will form on finned tube surfaces. This single observation at the end of 100 hours cannot be extrapolated to all alloys, geometries, and operating conditions such as flow velocity and water quality. Our results suggest that more defined studies should be pursued with enhanced heat transfer surfaces to determine their performance in environments with high potential for fouling. Such studies may lead to a geometry which maximizes heat transfer while minimizing fouling.

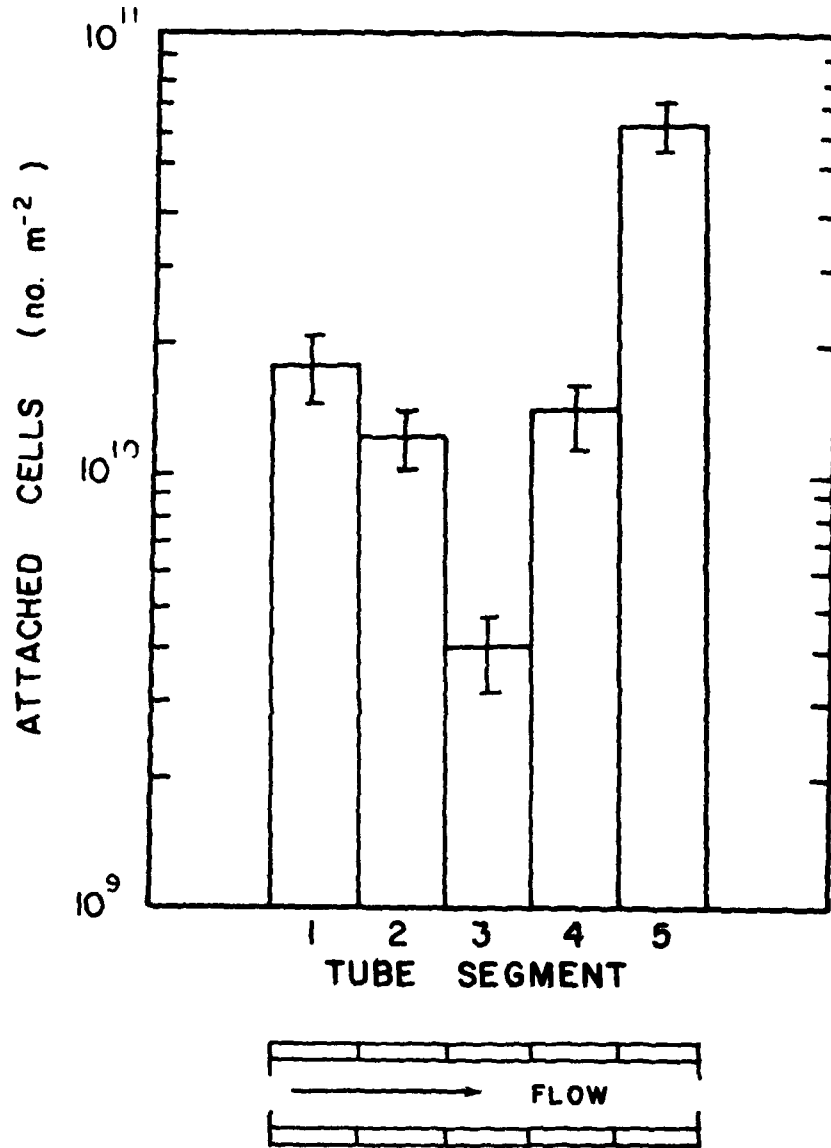


Figure IX-14. Distribution of attached microbial cells on a tube section between two circular fins separated by a distance of 5 cm (fin height = 0.094 cm) at the end of 100 hours.

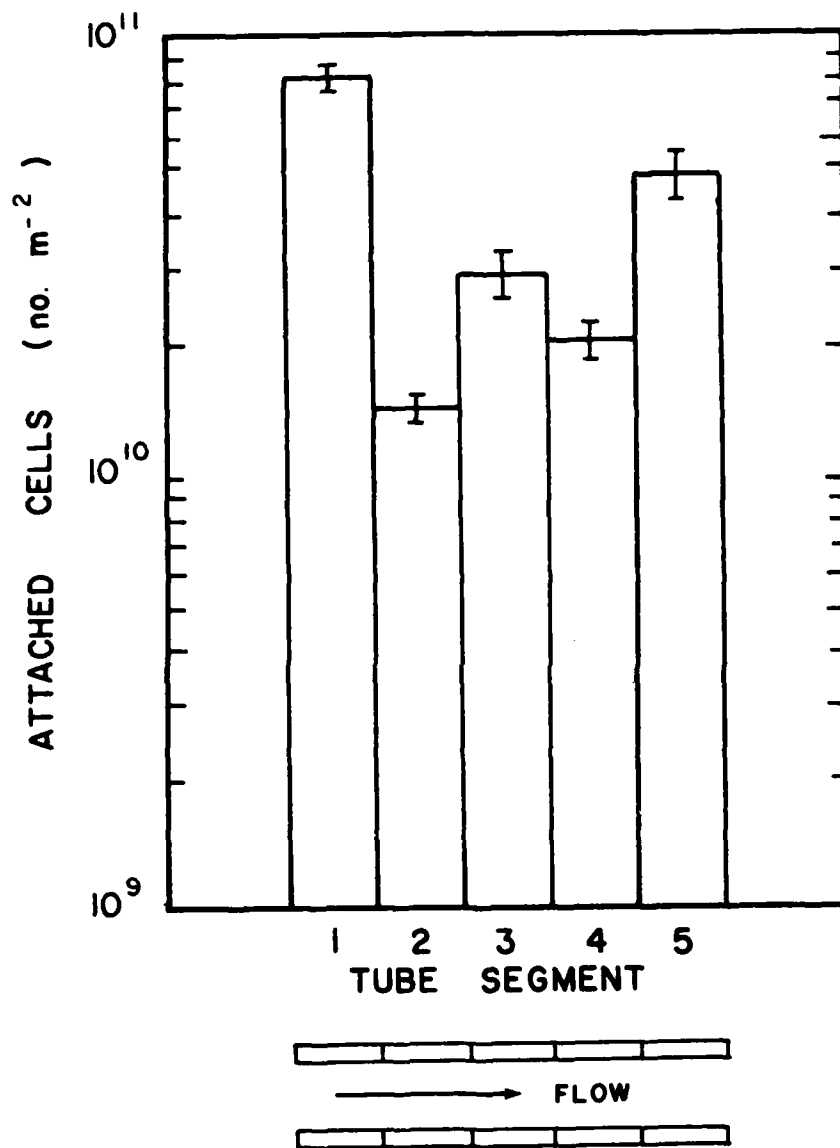


Figure IX-15. Distribution of attached microbial cells on a 5 cm smooth, 70:30 Cu/Ni tube at the end of 100 hours.

## X. MICROBIALLY-ASSISTED CORROSION

Microbially-assisted corrosion (MAC) has been a subject of significant interest to corrosion engineers and scientists for over 50 years. While solutions have been devised to minimize many problems related to MAC, the approach remains primarily empirical. The identification of specific corrosion mechanisms has remained elusive because of the complexity of the microbial processes. MAC is an extremely complex problem involving a number of processes occurring at the metal surface:

- Transport and adsorption of organics and nutrients to support growth of microorganisms.
- Transport of microbial cells to the surface.
- Attachment of microorganisms.
- Reactions of the microorganisms within the biofilm (Characklis, 1981)
  - growth or replication
  - product formation
  - cell maintenance
  - death or lysis of the cell
- Biofilm detachment.
- Reactions between the biofilm and metal surface
  - reaction of microbial products with the metal surface
  - reaction between surfaces covered with biofilm and surfaces not covered (formation of differential surface chemistries).

### PRINCIPLES OF AQUEOUS METALLIC CORROSION

The *incidence* of aqueous metallic corrosion is determined by the free energy change associated with oxidation of the metal. The electrochemical nature of the corrosion process requires that both anodic and cathodic reactions occur simultaneously on the metal or corrosion product surface (except in the case of bimetallic or galvanic corrosion). Typically, the *rate limiting step* is the slower of the two electron transfer reactions (anodic or cathodic). However, in some cases, the rate limiting step may be a chemical dissociation or recombination step (e.g. atomic hydrogen combining to form molecular hydrogen at the cathode).

Rate of corrosion is influenced by formation of a protective corrosion product film (passivation) and by physical, chemical and biological factors in the aqueous environment:

1. *Chemical constituents* affecting corrosion

rates include concentration of dissolved salts, gases, metallic ions and pH.

2. *Physical factors* include surface and water temperature, fluid velocity and transport of constituents to the surface.
3. *Biological factors* include organic product formation by bacteria, and local changes in pH and other ions.

#### INFLUENCE OF MICROBIAL PRODUCT FORMATION ON CORROSION

The influence of microorganisms on corrosion is determined by activity at the anodic and cathodic sites. A survey of possible mechanisms for the influence of microorganism on the corrosion process include:

1. *Production of Extracellular Polymeric Substances (EPS)*. EPS secreted by microorganisms is the bulk of material forming the biofilm matrix. EPS is the binding force that holds microbial cells and their products to the surface where corrosion reactions take place. EPS is composed of polyelectrolytes and may act as an electron sink.
2. *Differential Concentration Cells*. Differences in concentration of chemicals (e.g. oxygen) between areas covered by biofilm and areas left bare due to detachment of biofilm can promote corrosion.
3. *Acid Production*. Members of the genus *Thiobacillus* oxidize sulfide, producing sulfuric acid as a result of this dissimilatory process. Weaker acids (i.e. organic) are produced by a variety of microorganisms under anaerobic conditions.
4. *Sulfate Reducing Bacteria (SRB)*. SRB are often detected on corroded surfaces leading researchers to search for the mechanism by which this bacterial group may promote corrosion. A number of mechanisms have been proposed. However, a satisfactory model has yet to be developed.

**EXTRACELLULAR POLYMERIC SUBSTANCES (EPS)**. The attached bacteria produce an extracellular polymeric substances (EPS) which forms a barrier (diffusional resistance) to exchange of elements between the metal surface and the aqueous environment. Reaction between bacterial products and the metal surface take place within the biofilm matrix

consisting of bacteria and the surrounding EPS. EPS is frequently composed of polysaccharide subunits, primarily mannans, glucans and uronic acid (Stainier, 1976; Costerton, 1978). The ratio of these can vary depending on type of bacteria (Geesey, 1982). Several investigations have shown increased EPS production in nitrogen or phosphorous limited systems (Tain and Finn, 1977; Williams and Wimpenny, 1978; Mian *et al*, 1978; Williams 1978).

The mass of bacteria embedded within the biofilm is reported to be extremely small compared to the mass of EPS (Characklis, 1981, Fletcher and Floodgate, 1973; Costerton, 1978). However, the high degree of hydration (85 to 96 percent water) requires careful interpretations of these results (Geesey, 1982). Trulear (1983) demonstrated that the numbers of cells in a biofilm remained relatively constant for different substrate loading rates. However, lower substrate loading rates resulted in less production of EPS.

The role of EPS in directly influencing corrosion is unknown. Hypothetical mechanisms include:

1. EPS, being composed of mostly polyelectrolytes, acts as an electron sink for consumption of electrons at the cathode.
2. EPS affects the formation of a passive layer by creating diffusional resistance to transport of chemical species necessary for passivation.
3. EPS removes corrosion products which may include passive layers as biofilm detachment occurs.
4. EPS traps corrosion products resulting in increased energy losses in heat transfer or flow systems (heat transfer resistance or fluid frictional resistance). Characklis and Zilver (1983) showed that, not only can a biofilm trap corrosion products, but biofilms elsewhere (e.g., on inert surfaces) can trap migrating or mobile corrosion products.

The role of EPS in influencing fouling and corrosion of shipboard heat exchanger condenser tubing was studied using a Recycle Tubular Loop (RTL) constructed to simulate the corrosion process in the laboratory (Figure 1-1). Artificial sea water (1.13 percent), trypticase soy broth and glucose, and a combination of known bacteria were fed to the RTL. Fouling on both copper-nickel (70:30) and titanium tubing was studied. Progressions of frictional resistance and deposit mass were monitored. The deposit mass was analyzed for chemical and bacterial content and visually inspected by scanning electron microscopy. After removal of the fouling deposit on the copper-nickel surfaces, the surface was chemically analyzed using the Scanning Auger

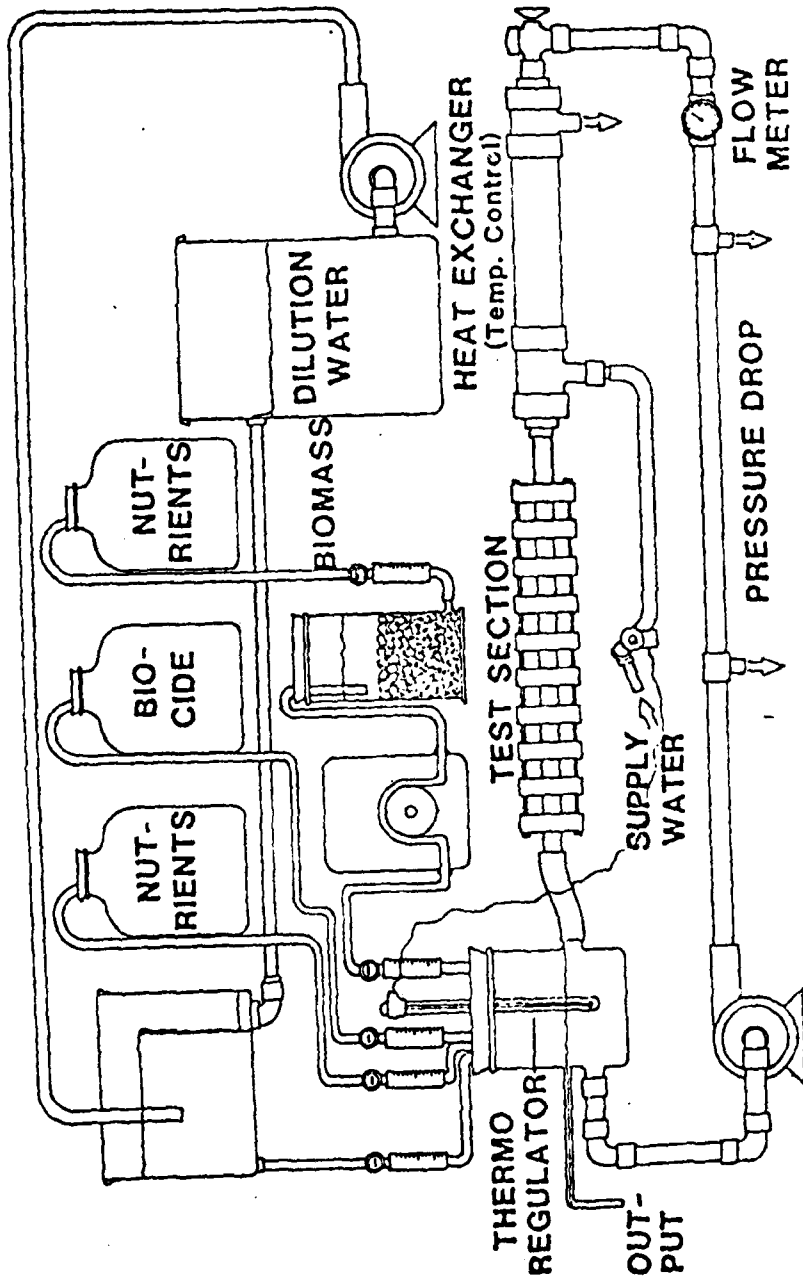


Figure X-1. One of three identical recycle tubular loops.

#### Microprobe.

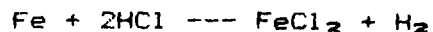
Progression of fouling on titanium and copper-nickel was compared in addition to comparison of fouling deposit compositions. Results indicate fouling on the copper-nickel is due to both biofilm and corrosion product embedded in the biofilm. Incorporation of copper-nickel corrosion products into the fouling deposit changed both the mass and chemistry of the deposit. In contrast, fouling on the titanium, where no corrosion occurred, was due only to biofilm formation.

**ROLE OF DIFFERENTIAL AERATION CELLS.** Localized corrosion on a metal surface in aerated aqueous environments is frequently associated with differential oxygen concentration cells. Oxygen reduction is typically the dominant cathodic process in aerated aqueous corrosion. As a result, any process which disturbs the uniform transfer of dissolved oxygen to the metal surface may produce areas of differential cathodic activity.

Deposition of inorganic and organic material at a surface is a frequent cause of differential oxygen transfer. The deposit impedes the transfer of oxygen resulting in a gradual depletion of dissolved oxygen beneath the deposit. As a result, the under-deposit area becomes increasingly anodic (active). The surrounding area remains cathodic, and is usually larger in area than the under-deposit anodic area. This unfavorable anode:cathode area ratio (i.e. small anode:large cathode) may result in high rates of metal dissolution and penetration beneath the deposit.

Bacterial colonization can result in formation of aeration cells when biofilms develop unevenly on the metal surface (Figure X-2). Oxygen availability at the metal surface covered by biofilm becomes limited due to oxygen consumption by bacterial metabolism. Neighboring areas, where biofilms have not formed or have detached, remain accessible to oxygen (Olsen and Szybalski, 1950; Kobrin, 1976; Tatnall, 1981; Iverson, 1981; and Miller, 1981). Greater mass and fluid shear stress result in increased detachment rates (Trulear and Characklis, 1982). Depletion of oxygen due to bacterial growth can occur to such an extent that the biofilm at the lowest depth (at the biofilm-metal interface) becomes completely anaerobic. Diffusion of oxygen to the metal surface is also dependent on biofilm mass and density and fluid shear stress at the biofilm surface. Greater mass and biofilm density results in less oxygen diffusion while greater fluid shear stress (turbulence at the surface) promotes oxygen diffusion.

**ACID PRODUCTION BY BACTERIA.** When a metal is in an acid environment, electrons combine with and reduce the positively charged free hydrogen ions. Atomic hydrogen thus formed at the metal combines to form hydrogen gas (Figure X-3). For example, iron in a hydrochloric acid solution corrodes by the following reaction:



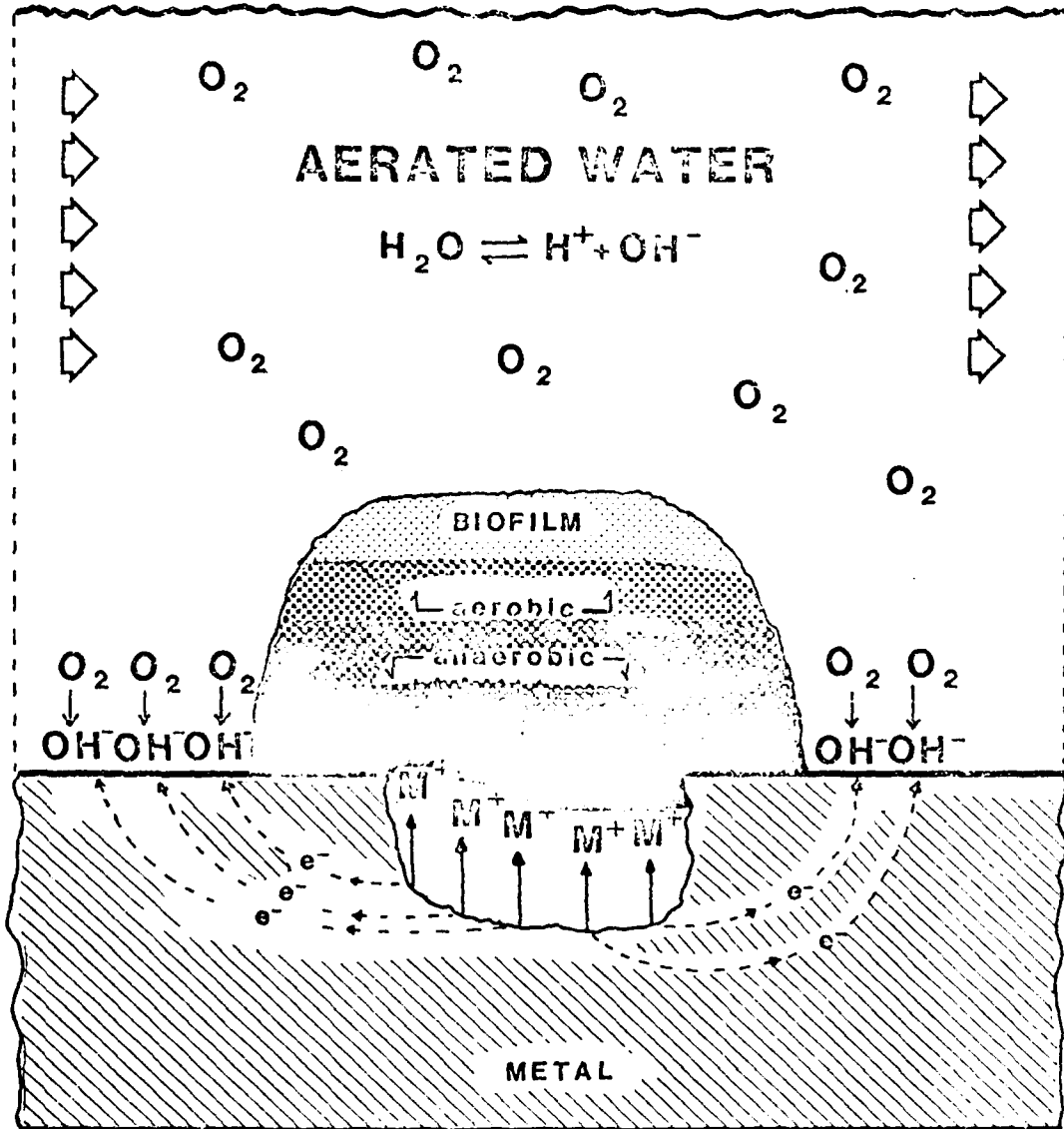


Figure X-2. Formation of corrosion causing aeration cells when biofilms develop unevenly on the metal surface.

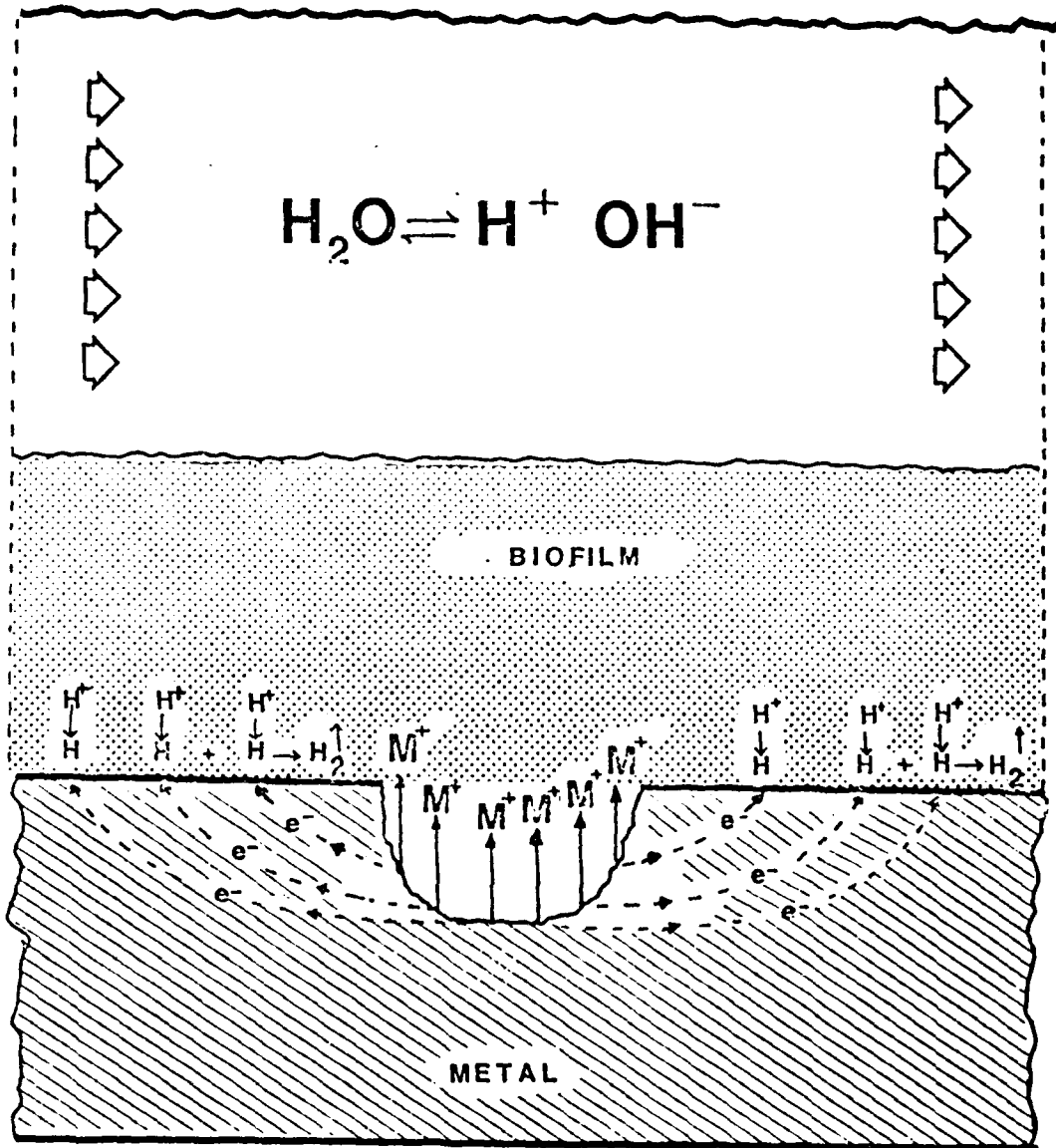


Figure X-3. Corrosion caused by microbial acid production.

In this case, a mechanism of microbially assisted corrosion is implied by the fact that bacteria produce acids (Burns et al, 1976; Kobrin, 1976; Tatnall, 1981; Miller, 1981; and Salvarezza et al, 1983). The acid-producing bacteria of the genus *Thiobacillus* are a well-defined group of strict autotrophs (Miller, 1981). These organisms share the ability to oxidize sulfur or several of its more reduced compounds to obtain energy for fixation of carbon dioxide. One member of this group, *Thiobacillus ferrooxidans*, can oxidize ferrous to ferric iron. The net result in all cases is production of highly corrosive sulfuric acid with pH values of 2 or lower. *Thiobacillus ferrooxidans* is known for its ability to leach metal ores (Lundgren and Silver, 1980) and its association with acid mine drainage. These organisms are frequently found in natural environments containing reduced forms of sulfur or in association with putrefactive microorganisms and industrial waste material. Of special interest to the corrosion engineer is the association of *Thiobacilli* with SRB whereby the *Thiobacilli* utilize the sulfide made available from sulfate reduction and produce corrosive sulfuric acid.

In natural anaerobic habitats, acetate, propionate and butyrate are the major organic acids produced during fermentation. Lactate and succinate may be produced in lesser quantities. Acetate is the strongest of the above volatile fatty acids and thus would be expected to exert the greatest influence on MAC. Furthermore, it is typically the major constituent of the volatile fatty acid (organic acid) fraction in anaerobic environments (Hungate, 1975; Kasper, and Wuhrmann, 1978; Lovely and Klug, 1982; and Mountfort, et al., 1980). Propionate and butyrate play lesser roles than acetate since they are weaker acids and occur at concentrations several times lower than acetate.

Other mechanisms of acid production by bacteria may influence corrosion such as formation of tricarboxylic acid cycle end-products or by leakage of tricarboxylic acid cycle intermediates (Miller, 1981). Although these acids are known to have the ability to corrode (Burns, et al., 1976), the production of these acids is small compared to amounts of organic acids formed during dissimilatory processes. In addition, the small concentration of bacterial cells in a biofilm indicates the influence of organic acid biosynthetic intermediates on pitting and corrosion of metals is probably minor.

**SULFATE REDUCING BACTERIA.** Ferrous metal corrosion in the presence of SRB is a problem that has plagued engineers and challenged researchers since it was identified in the 1930's. In 1934, von Wolzogen Kuhr and van der Vlugt (cited in Miller and Tiller, 1970) proposed that SRB accelerate corrosion of ferrous metals by cathodic depolarization, that is, by removing adsorbed hydrogen from cathodic surfaces. It would appear to be relatively simple to confirm this theory by conventional electrochemical corrosion techniques.

Confirmation has been obtained, however, only for very specific combinations of SRB species and experimental conditions.

One of the first studies to conclusively demonstrate cathodic depolarization with sulfate-reducers was conducted by Booth and Tiller (1962). They demonstrated that depolarization did occur with a hydrogenase positive strain of *Desulfovibrio vulgaris*, and did not occur with a pure strain of hydrogenase negative *Desulfotomaculum orientis*. A number of confusing phenomena were noted in these experiments: 1) depolarization was observed only when the culture was in active growth, 2) the stimulation of corrosion was approximately the same for both organisms, 3) a film of ferrous sulfide formed on the surface of the corrosion samples which had an apparent inhibitory effect on corrosion rates, 4) the rates of corrosion observed in the experiments were found to be much lower than corrosion rates reported for ferrous metals in natural anaerobic environments with sulfate-reducers present.

A possible explanation for the lower observed experimental corrosion rates is the relatively low bacterial activity in the batch cultures with low nutrient concentration. Booth, et al. (1967) tested this hypothesis by conducting continuous culture experiments with SRB. They observed corrosion rates of approximately 1000  $\mu\text{m}/\text{y}$  (40 mpy) and an absence of protective sulfide film formation. They noted the growth of a bulky, black envelope of corrosion product surrounding the metal specimens. Again, the results were confusing since there was no apparent correlation between corrosion rate and hydrogenase activity.

Concurrently, Booth, et al. (1967) demonstrated that ferrous sulfide itself could cause cathodic depolarization. Once the ferrous sulfide formed, its depolarizing activity continued, even in the absence of bacteria. Booth and Tiller (1962) had previously reported experimental evidence that the ferrous sulfide film structure is instrumental in the corrosion process. In the presence of a strain of halophilic *Desulfovibrio sallexigens*, cathodic depolarization was observed, but there was little polarization (or reduction in the rate) of the anodic reaction accompanying formation of the sulfide film. The anodic activity remained high, and although they could not detect a chemical difference between that film and a normally protective sulfide film, they attributed the difference to film structure.

Miller (1981) summarizes results of research on ferrous metal corrosion by SRB. He suggests the following based on research by Mara and Williams (1972), King, et al. (1973), Smith and Miller (1975), King, et al. (1976), and Smith (1980):

Precipitated ferrous sulfide may initially form a protective film on a ferrous metal surface in the presence of sulfate reducers. As the

bacterial corrosion process continues, the film thickens and changes stoichiometrically. As the ratio of  $Fe^{2+}$  to  $S^{2-}$  in the film changes from a sulfur deficient to a sulfur rich structure, the film becomes less protective and eventually spalls. Once spalled, the film does not reform and vigorous anodic activity proceeds at the exposed metal surfaces. According to Smith and Miller (1975), the sulfide film, regardless of structure, is cathodic to iron and the corrosion process continues galvanically. Smith (1980) reported that the sulfide films would not remain permanent cathodes in the absence of bacteria. The role of the bacteria, he suggests, could be either to depolarize the iron sulfide enabling it to remain cathodic, or to produce more sulfide by their continued growth.

Iverson (1981) discounts the ferrous sulfide argument. He reports corrosion rates greater than 5000  $\mu m/y$  (210 mpy) for mild steel specimens exposed to filtered media from an actively growing culture of *Desulfovibrio* (API strain). The media after nine day's incubation was filtered to remove bacteria and treated with excess ferrous ion to precipitate all free sulfide ions. Thus, the filtrate contained only soluble products from the original media and soluble metabolites from the growth of cells. Iverson concludes that the sulfate-reducing bacteria produce an unknown, highly corrosive, compound in addition to hydrogen sulfide. The outcome of the process appears to depend on whether ferrous sulfide forms a protective film before the highly corrosive product contacts the metal surface.

It is apparent that a number of factors are involved in the process of ferrous metal corrosion by SRB. As a result, measurement and control of the process parameters and variables will significantly affect the outcome of experimental results from one experiment, and one laboratory, to another. A variety of possible relevant factors are cited by Postgate (1979): 1) the nature of the metal surface, 2) the presence or absence of dissolved iron and/or organic matter capable of chelating iron in the surrounding water, 3) whether the strain of bacteria tends to form a film on the metal itself, 4) whether the iron sulfide itself forms a film which can be protective, or 5) whether other ions, such as  $Na^{+}$  and  $Cl^{-}$ , are present which can influence the protectiveness of any films that do form.

#### BIOFOULING, BIOFOULING CONTROL, AND CORROSION

Piping systems and heat transfer surfaces in the marine environment are subject to the effects of organic and inorganic fouling. The detrimental effects of these fouling deposits include increased frictional resistance for fluid flow, increased heat transfer resistance, and, under certain

conditions, an accelerating effect on corrosion of some materials.

Frictional resistance increases the power requirements for sea water pumping and reduces delivery capacity of the system. Heat transfer resistance results in a reduction in thermal efficiency of heat transfer equipment and an associated increase in energy costs.

#### BIOFOULING CONTROL METHODS

Attempts to control biofouling in marine heat exchangers and piping systems have met with varying degrees of success. Chlorination and, to a lesser extent, other chemical oxidants (ozone, hydrogen peroxide, etc.) have been effectively used to combat biofouling. Copper alloys have been widely used due to their inherent "toxicity" towards many forms of marine life.

The effectiveness of chlorine in treating biofouling, including microbial slime and macrofouling organisms such as molluscs, barnacles, bryozoa, hydroids, sponges, and tunicates, has been well established (Marine Research, 1976; Rongers and O'Conner, 1977).

Chlorine can be added directly to sea water in the gaseous form or generated electrolytically. The result in both cases is the formation of hypochlorous acid which will, depending on pH, further dissociate into hypochlorite. The reaction products of chlorine are consumed in sea water not only by the organisms for which they are intended, but also by reactions with bromide, nitrogen compounds (e.g., ammonia), organic detritus and metal surfaces. All of these factors combined contribute to the chlorine demand of the sea water system and determine the relative effectiveness and cost of chlorination as a means of controlling biofouling.

Numerous researchers have reported that copper containing alloys are toxic to marine organisms (Huguenin and Ansuini, 1980; Ritter and Sutor, 1976; Nosetani *et al.*, 1979). Dexter (1974) conducted microfouling studies in warm tropical waters of the open ocean. He demonstrated that a film 50-125  $\mu\text{m}$  thick could form in less than a month in warm surface waters. A continuous layer of diatoms and bacteria embedded in slime were observed on samples of 90-10 and 70-30 copper-nickel (70-30) in sea water and observed that attached organisms produced more extracellular proteoglycan material on the titanium surface than on the copper-nickel. Furthermore, corrosion products on the copper-nickel surface were partially embedded in the biofilm and periodic sloughing of the combined biofouling and corrosion product film occurred.

**CORROSION.** Sea water is a very complex solution of numerous salts and dissolved gases plus suspended silt, living organisms and decaying organic matter. The corrosion of metals in sea water is affected by many factors including oxygen, salinity, pH, temperature, and biological activity.

Some metals, such as titanium, form very thin, tightly adherent protective oxide films in sea water which are essentially inert. Protective corrosion product films on copper and its alloys, by comparison, grow much more slowly and are affected significantly by thermohydrodynamic conditions.

In sea water, the corrosion product on copper-nickel alloys is predominately  $\text{Cu}_2\text{O}$  (cuprous oxide) irrespective of alloy composition (North and Pryor, 1970). Often, the basic chloride atacamite ( $\text{Cu}_2(\text{OH})_3\text{Cl}$ ), a bulky, green nonprotective corrosion product, forms overlaying the  $\text{Cu}_2\text{O}$  layer. A carbonate salt, malachite ( $\text{CuCO}_3 \cdot \text{Cu}(\text{OH})_2$ ), may form competitively with the basic chloride salt depending upon local surface pH and total inorganic carbon concentration (Bianchi and Longhi, 1973). Temperature, depth, and biological activity are the main factors influencing the total inorganic carbon concentration in sea water.

The  $\text{Cu}_2\text{O}$  corrosion product is the adherent, protective film responsible for the low corrosion rates observed on Cu-Ni alloys in unpolluted, aerated, sea water. According to Efird and Anderson (1975), the corrosion rate of 70-30 CuNi in flowing sea water ( $0.6 \text{ m s}^{-1}$ ) was approximately  $2.0 \text{ um yr}^{-1}$  after 14 years exposure, but had stabilized at that value after 4 years. Efird (1975) further studied the relationship between corrosion product formation and biofouling resistance of copper base alloys. He proposed the following model to describe the process:

1. Initial formation of a protective  $\text{Cu}_2\text{O}$  film.
2. Subsequent hydrolysis of  $\text{Cu}_2\text{O}$  to a loosely adherent  $\text{Cu}(\text{OH})_2 \cdot 3 \text{ CuCl}_2$  film.
3. Fouling attachment to the  $\text{Cu}(\text{OH})_2 \cdot 3 \text{ CuCl}_2$  film.
4. Removal of the fouling organisms with the basic chloride film leaving the  $\text{Cu}_2\text{O}$  intact.

As the  $\text{Cu}_2\text{O}$  corrosion product film grows in sea water, copper ions and electrons must pass through the film to support anodic and cathodic half reactions. It has been shown experimentally (North and Pryor, 1970) that alloying additions of nickel and iron to copper improve corrosion resistance. The mechanism proposed is the incorporation of Ni and Fe ions into the highly defective p-type  $\text{Cu}_2\text{O}$  corrosion product film as "Dopants," thereby altering the defect structure. The result is a protective corrosion product film possessing relatively low electronic and ionic conductivity.

The corrosion of copper-nickel alloys in aerated, unpolluted, sea water is cathodically controlled by oxygen reduction. Dissolved oxygen retards corrosion by the promotion of a protective oxide film on the copper-nickel alloy surface, but increases the rate of corrosion by depolarizing cathodic sites and oxidizing cuprous ions to the more aggressive cupric ions. Other factors, such as

velocity, temperature, salinity and depth affect dissolved oxygen transport and content in sea water thereby influencing the corrosion rate.

Soluble complexes of cuprous ( $\text{CuCl}_2^-$ ,  $\text{CuCl}_3^-$ ) and cupric ( $\text{CuCl}^+$ ,  $\text{CuCl}_2^0$ ,  $\text{CuCl}_3^-$ ,  $\text{Cu}(\text{CO}_3)_2^-$ , etc.) ions are thermodynamically feasible in seawater. These complexes form at rates dependent upon the available concentration of  $\text{Cu}^+$  and  $\text{Cu}^{++}$  ions. Complexation with organic ligands has been studied (Compton, 1973) and is hypothesized as a mechanism for the increased corrosivity of natural sea water over equivalent saline solution. Organic complexation may be an important factor associated with biological activity and may be critical in biologically accelerated corrosion.

Polluted sea water has been cited (Gilbert, 1954) as the most important factor contributing to failure of copper alloy marine condenser tubes. The primary cause of accelerated attack of copper base alloys in polluted sea water is due to the presence of sulfide. The principal sources of sulfide in sea water are (1) the action of sulfate reducing bacteria, and (2) the putrefaction of organic sulfur compounds resulting in the formation of organic sulfides which can cause localized corrosion of copper-nickel alloys in sea water (Bates and Popplewell, 1974).

Microbiological fouling of copper-nickel alloys in sea water and its influence on the corrosion process is not well understood in comparison to the electrochemical processes. Corrosion scientists and engineers have studied the effects of organically derived sulfide and sulfur compounds, as previously mentioned, the effect of chlorination on corrosion (LaQue, 1950; Stewart and LaQue, 1952), and mechanical biofouling control methods with and without chlorination (Lewis, 1982). Sophisticated surface analytical techniques such as x-ray photoelectron spectroscopy (XPS) and scanning auger microscopy (SAM) have been utilized to study the development of inorganic and biological fouling layers on copper based alloys (Castle and Epler, 1981).

Most of these studies have been phenomenological, however, and have not adequately modelled the mechanisms of microbial attachment to copper-nickel surfaces and the role of microorganisms in the corrosion process. The following study is intended to identify some of the important aspects of microbial fouling and microbially-assisted corrosion of copper-nickel.

#### EXPERIMENTAL METHODS.

Recycle Tubular Loop (RTL). Three parallel recycle tubular loops (RTL) of the type shown in Figure X-1 were used in this research. Pertinent dimensions and materials of construction are given in Table X-1. A detailed description of the RTL system, analytical methods, and operation is presented elsewhere (Characklis and Zilver, 1983).

**Table X-1. Pertinent Dimensions and Construction of the Recycle Tubular Loop**

Liquid Volumes		V (m <sup>3</sup> )	
Tubing (CuNi or Ti, PVC and Tygon)		0.00095	
Centrifugal Pump (phenolic)		0.00018	
Flow Meter (PVC)		0.00024	
Mixing Tank (glass)		0.00035	
	Total Volume	0.00172	
Tubing Lengths and Inside Diameters		L (m)	ID (m)
Heat Exchanger (CuNi or Ti)		0.76	0.0134
Pressure Drop Section (CuNi or Ti)		1.22	0.0134
Test Section (CuNi or Ti): 10 0.051 $\mu$ m long sample tubes		0.51	0.0134
Connecting Tubing (CuNi or Ti)		1.21	0.0134
	Total Length of Metal Tubing	3.70	
Connecting Tubing (Tygon)		0.16	0.0159
Connecting Tubing (PVC)		1.30	0.0175
	Total Length	5.16	
Surface Area		m <sup>2</sup>	
	Total Area	0.2172	

Important features of the RTL include:

Each RTL is made predominantly of 0.625 in (0.0159 m) O.D. heat exchanger tubing with a wall thickness of 0.049 in (0.00124 m). Titanium or 70-30 copper-nickel tubing was used depending on the experimental design. A section of tubing is fitted with ports for measuring *pressure drop*. A polyvinyl chloride shell encloses another section of tubing to form a *heat exchanger* which is used to control bulk water temperature by removing excess heat build-up from pumping friction; a thermo-regulator detects when cooling is necessary and opens a solenoid valve to pass cold tap water over the section of tubing. A *test section* comprised of 10 removable sections of tubing each 2 in (0.051 m) long is included for surface analyses of the deposit mass and the fouled surface (Figure X-4).

A *flow meter* which measures cumulative water flow is used with a timer to calculate fluid flow velocity.

Water is recycled through the RTL by a *centrifugal* pump with a chemically resistant, phenolic head. Fluid flow rate is controlled manually by a ball valve located downstream of the flow meter.

A *pH* controller is not included but the buffering capacity of the aquarium salt maintains pH between 8.2 and 8.4.

A *glass mixing tank* is used for housing the thermo-regulator and for feed water input.

Feed Water. Feed water consists of 11,300 mg l<sup>-1</sup> *aquarium salt* (Instant Ocean) for dilution to which one or more of the following may be added:

*Trypticase Soy Broth* (TSB) nutrition for microbial growth to give a nutrient loading rate ( $R_L$ ) of either 0.44 or 4.4 mg m<sup>-2</sup> min<sup>-1</sup>.

*Bacterial cells* from a fixed film chemostat inoculated with *Pseudomonas atlanticus*, *Flavobacterium*, *Vibrio alginolyticus*, *Pseudomonas alcaligenes* and *Desulfovibrio*. The chemostat is continuously fed with 100 mg l<sup>-1</sup> *Trypticase Soy Broth* in 11,300 mg l<sup>-1</sup> salt water (Instant Ocean). Continuous analysis of chemostat output for a 7 month period shows  $4.77 \times 10^9 + 8.20 \times 10^9$  total cells per hour and  $3.37 \times 10^9 + 9.05 \times 10^9$  viable cells per hour being produced.

*Chlorine* at a loading rate of 0.44 mg m<sup>-2</sup> min<sup>-1</sup> either continuously or periodically (one hour every 24 hours).

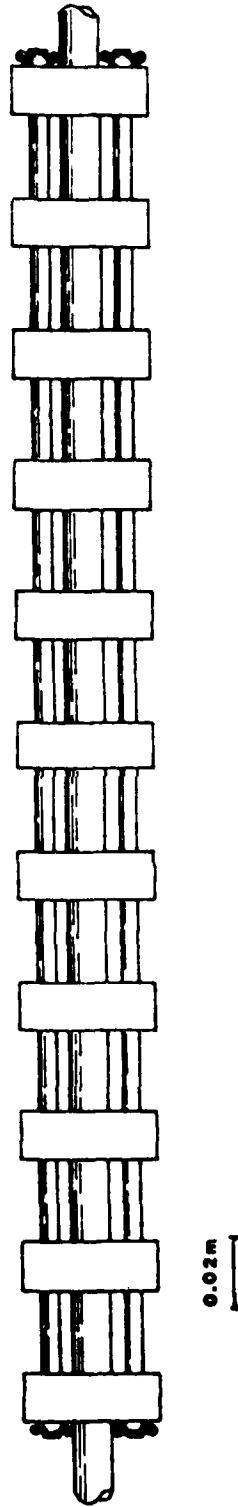


Figure X-4. Removable sampling tubes.

*Filtration* of the influent aquarium slat is used to minimize microorganisms in some experiments.

Analytical Methods. Analytical methods are described in detail elsewhere (Characklis, and Zilver, 1983; Characklis et al., 1982). Important features of these methods include:

*Sampling* for bulk water analysis is directly from the mixing tank using a sterile pipet. Surface samples are taken from the removable sample tubes by scraping the sample from the surface with a sterile rubber policeman into a beaker of sterile distilled water. All samples are homogenized with a high speed, sharp-bladed, mixer.

*Total cell counts* are measured by the AODC epifluorescence technique (Zimmerman and Meyer-Riel, 1974).

*Viable cell counts* are by the spread plate technique (APHA, 1976).

*Deposit mass* is measured by drying the removable sample tube for three hours at 100°C and then weighing the tube. The tube is then cleaned (deposit mass removed), dried and weighed again. The deposit mass is the difference between the dry fouled sample tube mass and the clean tube mass.

*Corrosion rates* are then measured from the difference between mass of the sample tube at the experiment start and the cleaned sample tube at the experiment end. The difference in mass is divided by the exposure time to determine a rate which is then converted to units of microns per day.

*Percent volatile deposit mass* is determined on deposit mass scraped from the inside tube surface. Volatile mass is the mass removed by ignition at 600°C for one hour as described in Standard Methods (APHA, 1976).

*Chemical analysis* of the deposit mass was performed by atomic absorption.

*Scanning Auger Microprobe* (SAM) measurements were performed using the Phi 595 Model (Physical Electronics).

*Chlorine* was measured by the amperometric method. RIL Operation. Table X-2 presents a summary of conditions which were the same for all experiments. Conditions which varied include *tube alloy* (70-30 copper-nickel or titanium), *substrate loading rate*

Table X-2. Summary of Conditions which were Identical for All Experiments

---

Volumetric Feed Rate	$1.9 \times 10^{-5} \text{ (m}^3 \text{ min}^{-1}\text{)}$
Hydraulic Retention Time	90 (min)
Water Temperature	30 (°C)
pH	8.2 - 8.4
Fluid Flow Velocity*	5400 (m min <sup>-1</sup> )
Fluid Shear Stress**	3.0 (N m <sup>-2</sup> )

\*Fluid flow velocity was held constant during experiments EX0-1 through EX0-2. Fluid shear stress or pressure drop was allowed to increase.

\*\*Fluid shear stress was held constant during experiments EX1-1 through EX6-3. Fluid flow velocity was allowed to decrease.

(0.44 or 4.4 mg TSB  $m^{-2} \min^{-1}$ ), and treatment (chlorination, filtration, or none).

## RESULTS

Control Experiments. Experiments where no biocide has been added are referred to as control experiments. Controls have been conducted to observe the natural progression of fouling on the condenser tube surface. Figure X-5 shows the progression of fouling for the titanium control experiments as indicated by change in Fouling Deposit Mass ( $M_D$ ). Change in  $M_D$  for substrate loadings ( $R_L$ ) of both 0.44 and 4.4 mg TSB  $m^{-2} \min^{-1}$  are indicated. Note, the rate increase in  $M_D$  at  $R_L = 4.4 \text{ mg } m^{-2} \min^{-1}$  is approximately three times the fouling rate increase at  $R_L = 0.44 \text{ mg } m^{-2} \min^{-1}$ . The progression of  $M_D$  is indicated as linear since data are presently not available to justify a more sophisticated analysis. Presumably, as suggested by other work (Characklis, 1980,  $M_D$  reaches a plateau level at some point in time. However, for the initial stages of fouling, and for comparison, the linear regression analysis is sufficient.

Figure X-6 shows the progression of  $M_D$  with time on copper-nickel tubing for the two substrate loadings. In this case, there is no significant difference between the substrate loadings.

Figure X-7 shows the progression of fouling on copper-nickel and titanium tubing as indicated by change in Volatile Deposit Mass ( $M_{VD}$ ). The rate increases in  $M_{VD}$  are calculated by multiplying the rate increases in  $M_D$  by the average percent volatile mass. At  $R_L = 0.44 \text{ mg } m^{-2} \min^{-1}$ , the rate increases in  $M_{VD}$  for copper-nickel and titanium show no significant difference. However, at  $R_L = 4.4 \text{ mg } m^{-2} \min^{-1}$ ,  $M_{VD}$  accumulates approximately four times faster on the titanium surface compared to the copper-nickel surface.

Measurements of Corrosion Loss ( $C_L$ ) for all control experiments are summarized in Table X-3.  $C_L$  is zero on the titanium tubing and averages 33 microns per year for copper-nickel at  $R_L = 0.44 \text{ mg } m^{-2} \min^{-1}$ . Average  $C_L$  at the higher substrate loading ( $R_L = 4.4 \text{ mg } m^{-2} \min^{-1}$ ) is approximately half that at the lower substrate loading.

Microbial Cell Counts. Total microbial cell counts on the copper-nickel and titanium surfaces, for all control experiments combined, show no significant difference between the two alloys (Figure X-8). Table X-4 summarizes all total and viable microbial cell counts taken for control copper-nickel and titanium experiments. No significant difference in cell counts between the two alloys is observed for measurements taken from either the tube surface of the bulk water.

Scanning Auger Microprobe. Scanning Auger Microprobe (SAM)

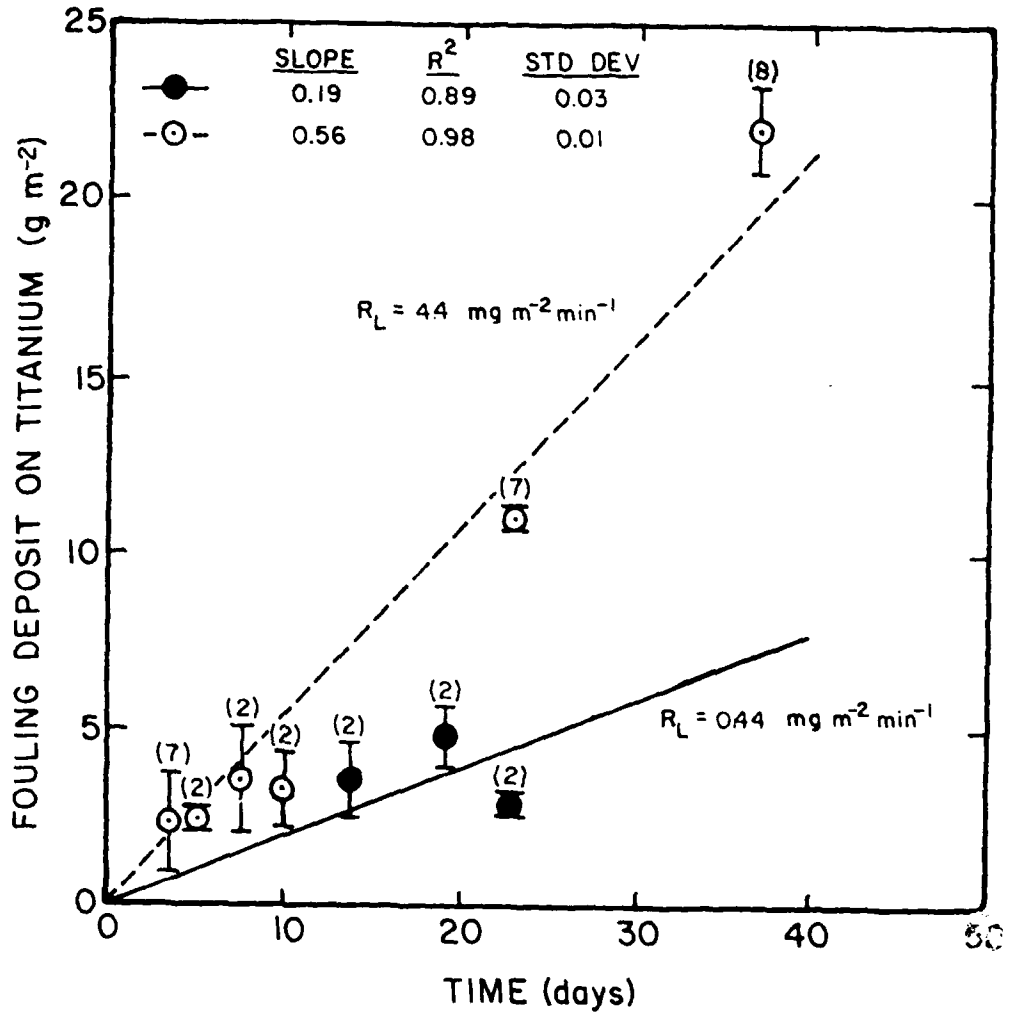


Figure X-5. Progression of total fouling deposit mass for titanium experiments.

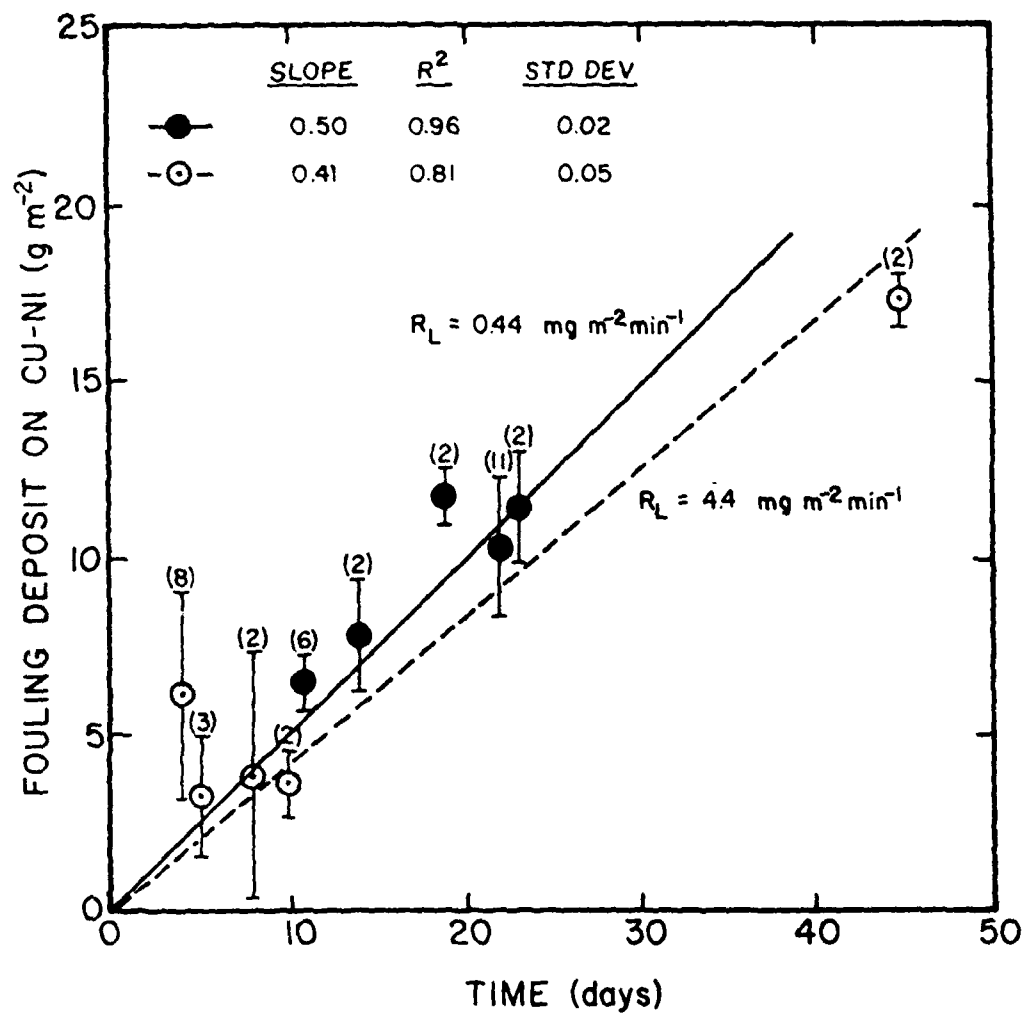


Figure X-6. Progression of total fouling deposit mass for copper-nickel.

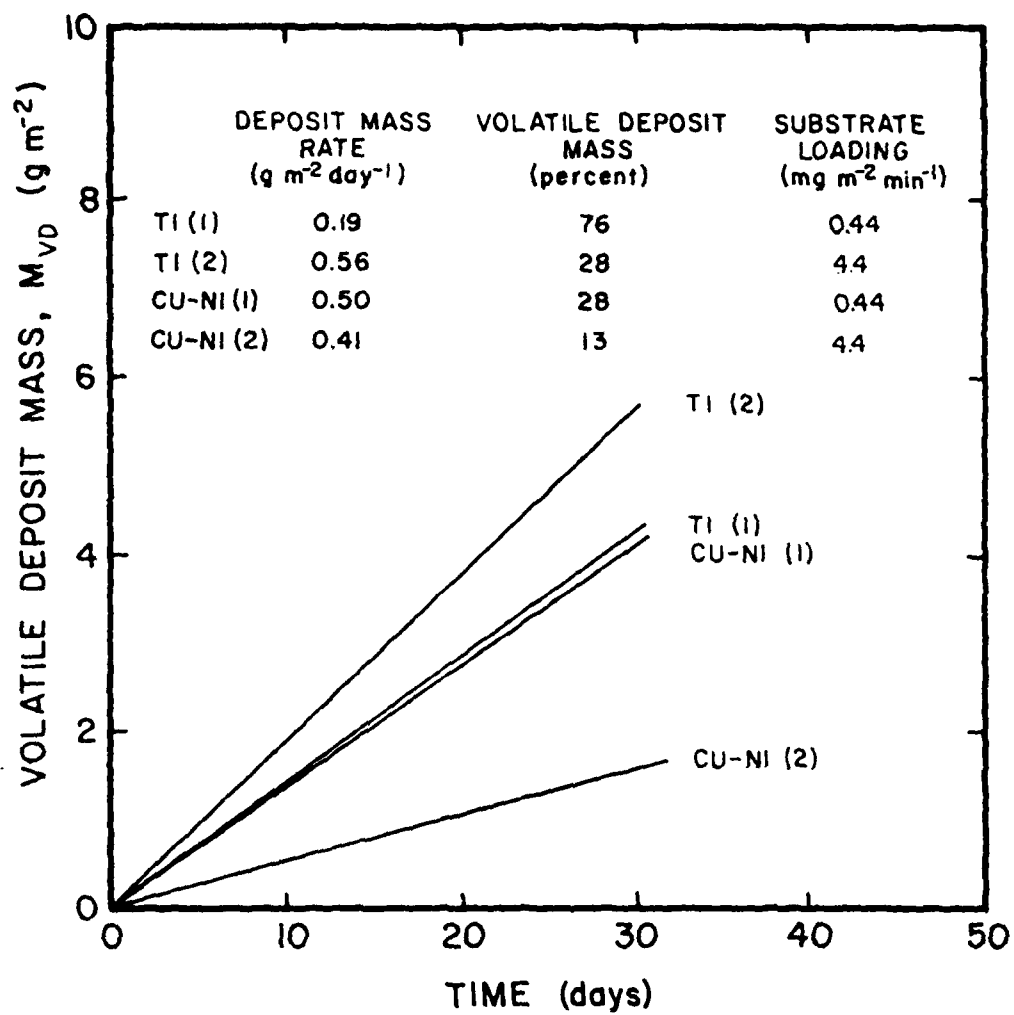


Figure X-7. Progression of volatile deposit mass.

Table X-3. Corrosion Loss and Volatile Deposit Mass for All Control Copper-Nickel and Titanium Experiments

Alloy	Substrate Loading ( $\text{mg m}^{-2} \text{min}^{-1}$ )	Corrosion* Loss ( $\mu\text{m yr}^{-1}$ )	Volatile* Deposit Mass (percent)
CuNi	0.44	$33 \pm 6$ (14)	$28 \pm 9$ (5)
Ti	0.44	$0 \pm 0$ (2)	$76 \pm 9$ (2)
CuNi	4.4	$16 \pm 9$ (4)	13 (1)
Ti	4.4	---	$28 \pm 11$ (2)

\*Values given are mean  $\pm$  one standard deviation with the number of samples given in parentheses.

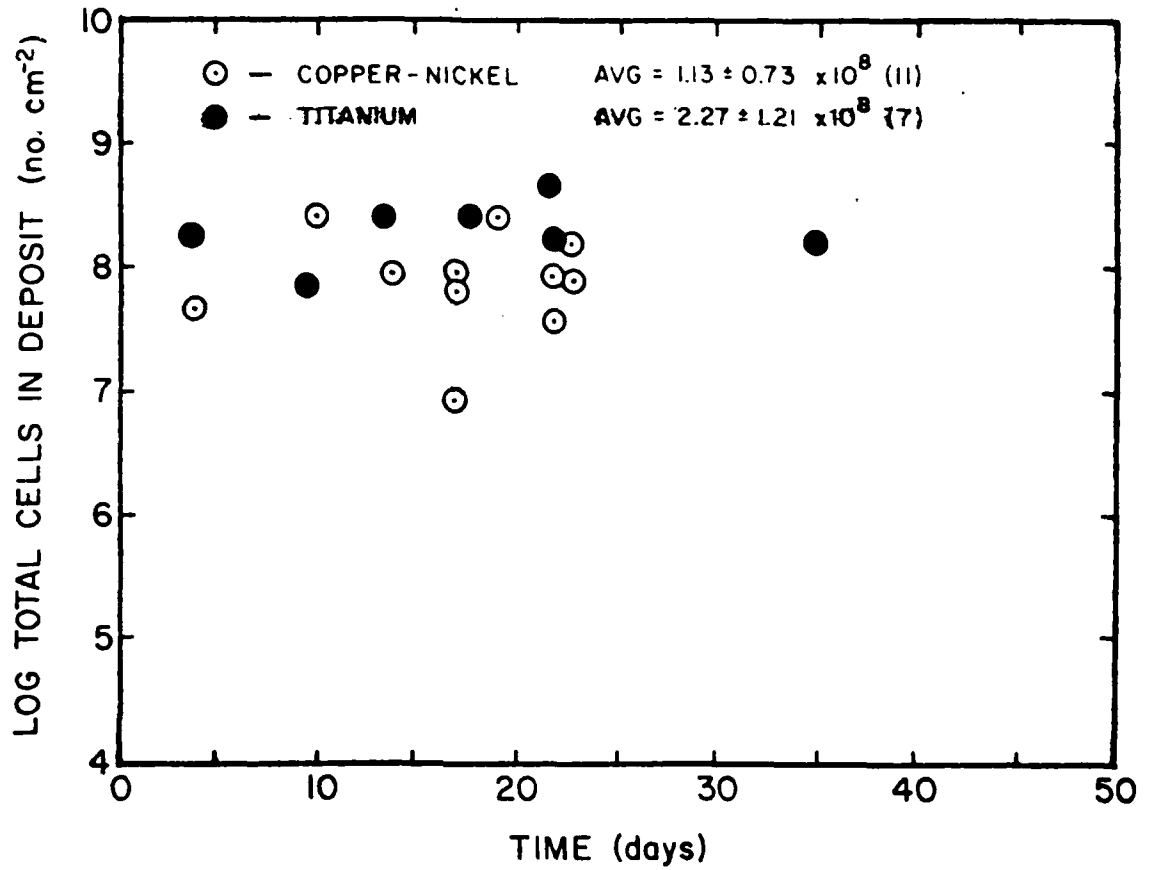


Figure X-8. Progression in numbers of total microbial cells (EPI) in the deposit for all copper-nickel and titanium control experiments.

Table X-4. Viable and Total Cell Counts in the Bulk Water and in the Deposit Mass for All Control Copper-Nickel and Titanium Experiments

Sample (alloy)	Bulk Water Cells		Attached Cells	
	<u>(10<sup>7</sup> cells hr<sup>-1</sup>)*</u>		<u>(10<sup>8</sup> cells cm<sup>-2</sup>)</u>	
	STP	EPI	STP	EPI
CuNi	2.0±2.2(26)	4.4±4.3(28)	0.4±0.32(5)	1.1±0.8(13)
Ti	1.6±1.6(12)	4.0±6.1(16)	3.9±6.9(4)	2.2±1.2(7)

Note. Values given are the mean ± one standard deviation with the number of samples given in parentheses.

STP: standard plate count (viable cells)

EPI: AODC by epifluorescence (total cells)

\*: Number of cells exiting the reactor per hour in the bulk water flow

measurements on sample tubes removed at the end of each experiment are summarized in Table X-5. The values are weight percent of each element for the overall surface analyzed. Figure X-9 shows the relationship between weight percent oxygen and the amount of volatile mass removed from the sample tube before the SAM measurement. Note, more oxygen is found on the metal surfaces containing greater attached volatile mass.

Chemical Analysis of Deposits. An analysis of elements found within the deposit is presented in Table X-6. Weight, percent of iron, and copper are measured on control copper-nickel sample and a control titanium sample. In addition, a sample of tygon tubing which connects copper-nickel tubing of the RTL to the glass tank, is analyzed to determine if any material from the copper-nickel is deposited elsewhere in the system. Results show considerably more copper in the deposit from the copper-nickel tube compared to the titanium (59 percent for CuNi versus 1.6 percent for the Ti). Weight percent iron changed little. A considerable amount of copper is found on the tygon section. Visual observation indicated a green tint to all deposits found in the RTL with copper-nickel tubing.

Filtration of Influent Water. In these experiments, the influent water is filtered and no substrate or bacteria is fed to the RTL. These experiments are designed to compare corrosion and fouling with and without bacteria. Contamination of the RTL occurred regardless of efforts to maintain aseptic conditions. However, the organism levels remain approximately an order of magnitude less on the "filtered" RTL surface compared to the control RTL (Table X-7). Note, no difference in corrosion rate of the copper-nickel is observed between the filtered and control experiments.

Chlorination of Influent Water. Chlorine was added to the influent water at a loading rate of  $4.4 \text{ mg m}^{-2} \text{ min}^{-1}$  both continuously and periodically for an hour every 24 hours. Figure X-10 indicates the chlorine demand of the copper-nickel tubing. This experiment was conducted as a batch test to observe the reaction of chlorine with copper-nickel tubing. Free chlorine ( $20 \text{ mg l}^{-1}$ ) was added to one liter of stirred solution. The amount of copper-nickel tubing added resulted in the same surface area to volume ratio as in the RTL. Chlorine in the distilled water drops to approximately  $13 \text{ mg l}^{-1}$  in the first 100 minutes and then remains constant. The chlorine exposed to the copper-nickel drops rapidly and, at 300 minutes, is no longer measurable. Combined chlorine in both solutions was always zero.

Table X-8 compares results of the chlorine experiments to corresponding control experiments. The periodic chlorination of titanium is ineffective in reducing

Table X-5. Scanning Auger Microprobe Analyses of Elements on Copper-Nickel Surface After Removal of Fouling Deposit Mass

	Cu	Ni	Fe	Mn	O	N	Ca	C	Cl	S
Control	49.7	34.4	2.4	0.7	8.4	0.3	0.4	1.1	2.4	0.6
Filtered	43.8	34.5	0.8	1.8	10.7	0.4	0.5	2.8	3.3	0.3
Chlorinated	75.0	12.3	2.1	1.1	5.2	0.2	0.6	1.4	1.1	0.3
New CuNi	67.6	26.5	1.2	1.6	0.9	0.4	0.6	1.0	2.7	0.5

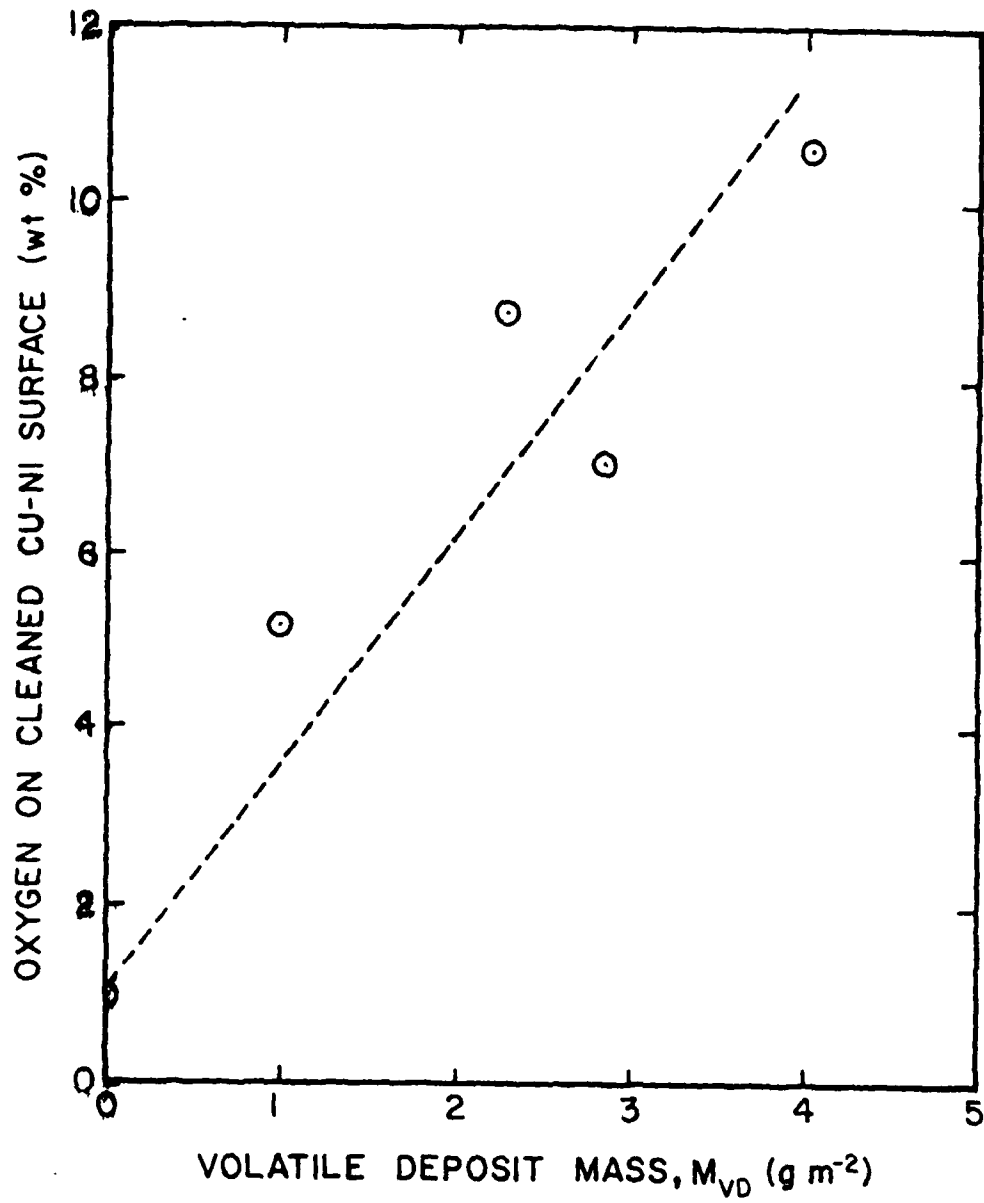


Figure X-9. Relationship between weight percent oxygen on the copper-nickel surface and the amount of volatile deposit mass removed from the surface before auger analysis.

Table X-6. Atomic Absorption Analyses of Iron and Copper Within the Fouling Deposit Mass

Sample	Exposure Time (days)	Condition	Percent of Total Deposit Mass	
			Iron	Copper
CuNi	22	Control	0.94	46
Tygon	22	Control	0.16	13
Ti	23	Control	3.2	1.3

Table X-7. Fouling Deposit Mass, Corrosion Loss, Percent Volatile, Deposit Mass and Microbial Analysis of Deposit for Control and Filtered Experiments

Sample (alloy)	Exposure Time (days)	Condition	Deposit Mass ( $\text{g m}^{-2}$ )	Corrosion Loss ( $\mu\text{m yr}^{-1}$ )	Volatile Deposit (%)	Cells in Deposit	
						STP* ( $10^3$ cells $\text{cm}^{-2}$ )	EPI** ( $10^7$ cells $\text{cm}^{-2}$ )
CuNi	45	filtered	$7.5 \pm 4.2(33)$	$14 \pm 11(4)$	53	1.3(1)	$0.32 \pm 0.02(5)$
CuNi	45	control	$12.4 \pm 6.1(3)$	$16 \pm 9(4)$	13	8.0(1)	$8.6 \pm 1.6(5)$
Ti	37	filtered	$2.0 \pm 3(8)$	---	---	9.3(1)	$2.5 \pm 7.0(5)$
Ti	37	control	$22.1 \pm 1.2(8)$	---	36	---	$1.5 \pm 5.0(5)$

Note. Values given are the mean  $\pm$  one standard deviation with the number of samples given in parentheses.

\*STP: standard plate count (viable cells)

\*\*EPI: AODC by epifluorescence (total cells)

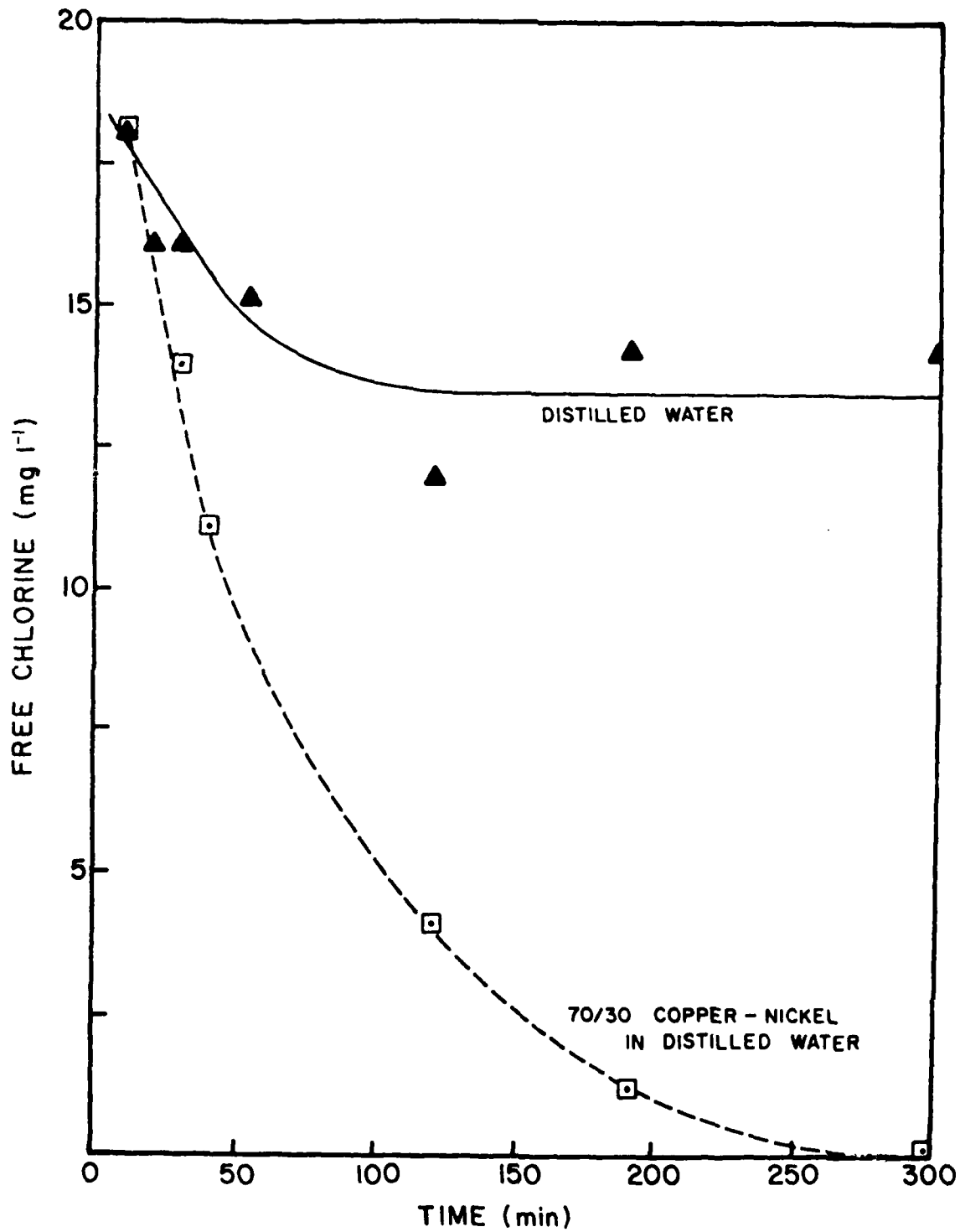


Figure X-10. Free chlorine versus time for one liter distilled water with and without submerged copper-nickel samples.

**Table X-8. Fouling Deposit Mass, Corrosion Loss, Percent Volatile Deposit Mass and Microbial Analyses for Control and Chlorine Experiments**

Sample (alloy)	Exposure Time (days)	Condition	Deposit Mass ( $\text{g m}^{-2}$ )	Volatile Deposit		Corrosion Loss		Deposit Cells ( $10^6 \text{ cells cm}^{-2}$ )		Bulk Water Cells ( $10^6 \text{ cells cm}^{-3}$ )	
				Mass (%)	Mass ( $\text{g m}^{-2}$ )	( $\mu\text{m yr}^{-1}$ )	STP*	EPI**	STP*	EPI**	
Ti	10	control	3.3±1.4(2)	---	---	---	6.1±5.4(2)	118±59(2)	6.3 ±2.3(2)	30 ±17(2)	
Ti	10	5 mg $\ell^{-1}$ $\text{Cl}_2$ (periodic for 1 hr each 24 hr)	5.0±0.5(2)	---	---	---	62 ±75(2)	168±185(2)	8.4 ±.8(2)	39 ±6.3(2)	
CuNi	45	5 mg $\ell^{-1}$ $\text{Cl}_2$ (continuous)	10.0±6.4(3)	10(1)	13±10(4)	85(1)	17(1)	0.96±.61(5)	3.2±1.3(10)		
CuNi	45	control	12.4±6.1(3)	13(1)	16±9(4)	80(1)	86(1)	2.7 ±2.0(5)	6.3±4.3(10)		
Ti	37	5 mg $\ell^{-1}$ $\text{Cl}_2$ (continuous)	4.5±1.3(8)	---	---	0.10(1)	6.2(1)	0.37±.39(4)	4.0±3.2(7)		
Ti	37	control	22.1±1.2(8)	---	---	---	150(1)	0.90±0.50(4)	3.6±1.5(7)		

Note. Values given are the mean ± one standard deviation with the number of samples given in parentheses.

\*STP: standard plate count (viable cells)

\*\*EPI: AODC by epifluorescence (total cells)

accumulation of deposit mass. However, continuous chlorination of titanium reduces  $M_b$  at 37 days from 22 g  $m^{-2}$  to 4.5 g  $m^{-2}$ . Surface cell numbers are reduced on the titanium surfaces exposed to both continuous and periodic chlorination. No significant difference in cell numbers is observed in the bulk water organisms. Only continuous chlorination is applied on the copper-nickel RTL. The results show no significant difference in deposit mass, corrosion rate, or in surface and bulk water organisms.

**DISCUSSION.** The results of this study do not justify the development of a new theory for microbially-mediated corrosion in Cu-Ni alloys. However, the results are useful for proposing a model to describe the process which may serve as a hypothesis for further experimentation.

**A Conceptual Model.** The processes of major concern in this experimental system are corrosion of the metal surface and accumulation of fouling biofilm deposit. The processes occur simultaneously and interact with each other. Figure X-11 is a schematic representation of the individual processes contributing to the corrosion and fouling processes. Table X-9 identifies each of the processes designated by a number in Figure X-11.

Initially, the metal surface is exposed to water containing substrate (an energy source for microbial growth), biomass (microbial cells), and dissolved oxygen. The corrosion process begins with the transport and reaction of oxygen at the metal surface (Process no. 1) which forms a protective oxide layer of insoluble corrosion products on the metal surface (Process no. 2). The events leading to corrosion of Cu-Ni alloys and the resulting composition of the surface oxide layer is complex and has been mentioned briefly in an earlier section. Random detachment and attachment of the insoluble corrosion products from the metal surface may occur due to the fluid motion and resulting shear stress (Processes no. 4 and no. 5). The detachment of insoluble corrosion products may initiate pit growth in the metal surface due to electrochemical corrosion (Process no. 3). Soluble corrosion products also diffuse into the bulk fluid (Process no. 13). The microbial cells (biomass) entering the system are suspended in the bulk fluid and consume substrate (Process no. 8) and dissolved oxygen (Process no. 9) resulting in cellular growth and reproduction. Some fraction of the suspended microorganisms attach to the metal surface (Process no. 11) and continue to consume substrate (Process no. 7) and dissolved oxygen (Process no. 10) resulting in growth and reproduction within the fouling deposit. The attached cells also produce extracellular polymers which further enhance attachment and adsorption of more cells, corrosion products, and other debris. The combined cellular and extracellular mass is termed the *biofilm*. A portion of the detached insoluble corrosion products become entrapped in the biofilm (Process no. 6). The biofilm continues to increase in

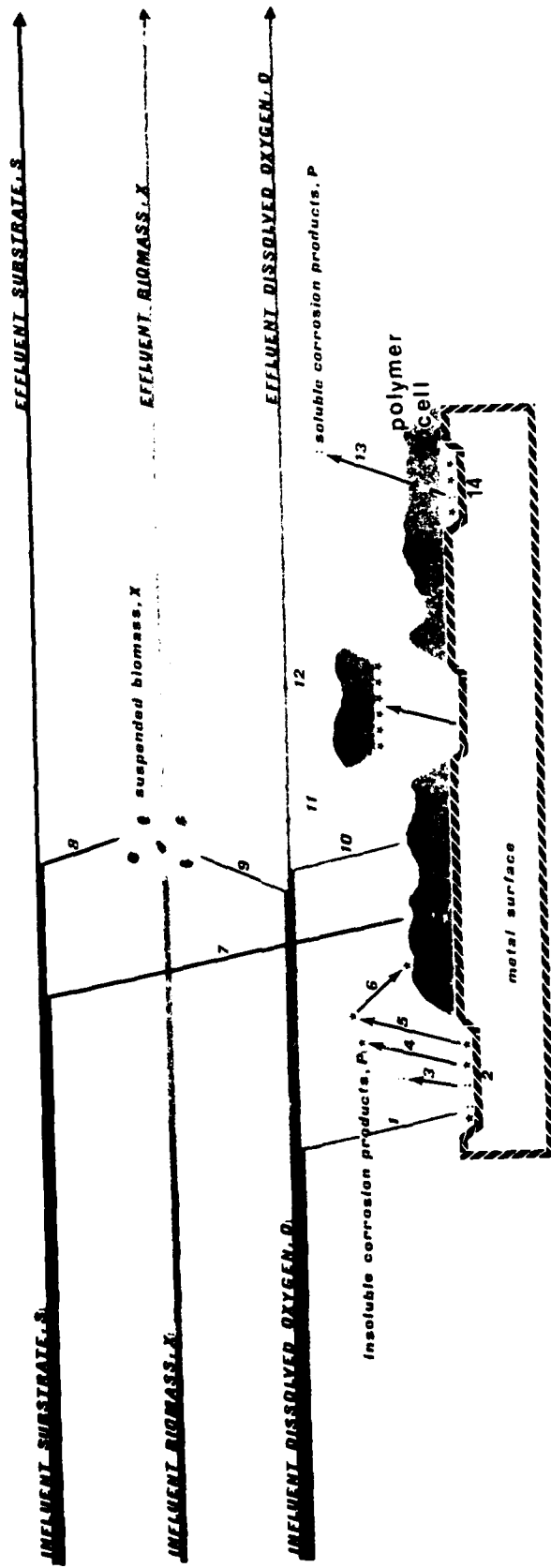


Figure X-11. Schematic of conceptual model for microbially mediated corrosion.

Table X-9. Explanation of Process Terms Used in Corrosion Model

- 
- 1) Dissolved oxygen removal by metal surface
  - 2) Corrosion product formation
  - 3) Soluble corrosion product detachment from metal surface
  - 4) Insoluble corrosion product detachment from metal surface
  - 5) Insoluble corrosion product attachment to metal surface
  - 6) Insoluble corrosion product attachment to biofilm
  - 7) Substrate removal by biofilm
  - 8) Substrate removal by suspended biomass
  - 9) Dissolved oxygen removal by suspended biomass
  - 10) Dissolved oxygen removal by biofilm
  - 11) Suspended biomass attachment to biofilm
  - 12) Biofilm and insoluble corrosion product detachment from metal surface
  - 13) Soluble corrosion product diffusion through biofilm
  - 14) Anaerobic corrosion product formation
-

density and thickness until fluid shear stress causes partial detachment (Process no. 12). Insoluble corrosion products may also detach with the biofilm (Process no. 12) thus leaving the metal surface more susceptible to corrosion processes. Soluble corrosion products are able to diffuse directly out of the biofilm and enter the bulk fluid. After the biofilm has reached a certain thickness, anaerobic conditions form in the lower layers. These conditions are favorable for proliferation of sulfate-reducers which form sulfide and may lead to accelerated corrosion (Process no. 14).

A mathematical model has been developed to simulate this system and is presently being tested. The equations are an approximation of the processes occurring in the system. The initial calculations can serve to identify the dominate processes or rate-controlling processes. The results can be used to formulate hypotheses for experimental testing and for experimental design.

Influence of Substrate Loading Rate on Deposition. The accumulation of fouling deposit on a condenser tube surface is the net result of production and depletion processes. Prominent among the production processes are microbial metabolic processes and adsorption. Detachment or sloughing of deposit is perhaps the most important depletion process. Detachment may be quite important in explaining behavior in Cu-Ni alloys which are continuously releasing corrosion products into the bulk water.

An increase in substrate loading rate,  $R_L$ , significantly increased the amount of deposit accumulating on the titanium alloy as indicated in Figure X-5. The volatile fraction of the deposit (organic component, including microbial cells, plus carbonates), however, decreased with increasing  $R_L$  (Table X-3). The results suggest that at higher loading rates, dissolved oxygen was depleted in the lower layers of the biofilm and anaerobic microenvironments existed. Anaerobic metabolism generally results in a lower volatile solids content.

$R_L$  had no effect on total deposit accumulation on the Cu-Ni alloy (Figure X-6). The volatile content of the deposit in the Cu-Ni was higher at the lower  $R_L$  as observed in the Ti alloy. The volatile deposit mass was significantly lower in the Cu-Ni as compared to the Ti tube at the high substrate loading (Figure X-7). At low substrate loading, volatile deposit mass was essentially the same in both alloys. The relative ratio of volatile-to-total solids in the two alloys is predominantly influenced by the corrosion products observed in the Cu-Ni fouling deposits. The lower volatile deposit mass on the Cu-Ni is not easy to rationalize. One possibility is that the microorganisms' metabolism is altered by the Cu or Ni in the deposit, e.g., the organisms' extracellular polymer substance (EPS) production may be influenced by the presence of Cu.

The total and viable number of microbial cells in the

deposit varied little between experiments or between alloys (Figure X-8). These preliminary results suggest that Cu-Ni alloys are not very "toxic" to microorganisms (in contrast to macroorganisms). On the other hand, Cu-Ni may influence certain microbiological metabolic functions.

The influence of substrate loading rate on deposition can be summarized as follows:

- Deposit mass increases with increasing  $R_L$  in the Ti alloy because more nutrients are available for microbial metabolism (Figure X-5).
- Deposit mass in the Cu-Ni alloy does not increase with  $R_L$  (Figure X-6) because much of the deposit consists of corrosion products as evidenced by the low deposit volatile fraction as compared to the Ti alloy.
- The change in deposit volatile fraction with different substrate loading rates may be due to increases in extracellular polymer substances (EPS) since cell numbers did not change.
- At higher  $R_L$ , dissolved oxygen may not penetrate the entire depth of the biofilm resulting in anaerobic microbial activity in the lower layers. Anaerobic biofilms generally exhibit lower volatile solids content (Metcalf and Eddy, 1972).

The hypothesis regarding oxygen is apparently contradicted by results of the scanning auger Microprobe (Table X-5) which indicated elevated oxygen contents on the metal surface with increasing deposit mass (Figure X-9). However, the oxide layer on the alloy most probably forms early in the experiment prior to biofilm formation. Consequently, the oxide layer may determine the amount of biofilm deposit which forms (Figure X-9). Metal oxides vary in the degree to which they affect microbial processes and may not be nearly as active as the pure metal. Therefore, the oxidized Cu-Ni surface, although not "toxic," may provide an "inhospitable" surface for the microorganisms.

Increased  $R_L$  resulted in decreased corrosion rates in the Cu-Ni alloy (Table X-3). However, the influence of  $R_L$  on corrosion is most probably an indirect effect. The influence of the deposit mass and its constituents (volatile mass and microorganisms) on corrosion, however, is probably more consequential and is discussed below.

#### Influence of Deposit Mass on Corrosion Rate of Cu-Ni.

Increasing  $R_L$  has no effect on deposit mass in the Cu-Ni alloy but decreases the volatile content of the deposit. This is related to the fact that more corrosion occurs at low loading rates (Table X-3) and a significant portion of the deposit consists of corrosion products (Table X-6). Since total and viable cell numbers are relatively constant,

several alternative hypotheses are advanced to explain the increased corrosion rate at low  $R_L$ :

- At low  $R_L$ , microbial cells produce more EPS (Trulear, 1982) and, thereby, increase the deposit volatile content although the deposit cell numbers remain relatively constant. The EPS, composed essentially of polyelectrolytes, acts as an electron source or sink to perpetuate or accelerate corrosion.
- At higher  $R_L$ , a significantly lower dissolved oxygen flux reaches the Cu-Ni surface (as a result of microbial activity) thus reducing corrosion rate.
- At higher  $R_L$ , metabolism of the deposit microorganisms changes in some other unknown manner resulting in decreased corrosion rate.

More experiments are necessary to reproduce and convincingly explain the increased corrosion rate of Cu-Ni at lower substrate loading rate. The precision and accuracy of total and viable cell enumeration must be improved to quantitatively prove any mechanism. Experiments with monocultures or defined microbial communities may be necessary to improve such measurements.

Influence of Microbial Cell Numbers on Corrosion Rate of Cu-Ni. The experiment conducted with filtered sea water may help reduce the choices among hypotheses. The filtered sea water contained no microorganisms nor any trypticase soy broth (TSB) as a microbial energy source. Thus, any organisms in the system were biological contaminants which grew on chemical contaminants in the artificial sea water or dilution water. The result was a deposit with dramatically lower viable cell counts and significantly lower total cell counts (Table X-7). Despite the reduced number of microorganisms in the deposit, no difference in corrosion rate was observed. Several explanations for these observations are possible including the following:

- The number of microorganisms in the deposit does not influence corrosion rate.
- The dissolved oxygen concentration in the filtered experiment was much higher and increased corrosion rate enough to cancel any effect due to decreased level of microbial activity.
- The deposit organisms in the filtered experiment were significantly different from those in other experiments.
- The absence of organic substrate increased corrosion rate in the filtered experiment as much as microorganism increased corrosion rate in the control

experiments.

Detachment of the Fouling Deposit and Corrosion Rate in Cu-Ni. The model for microbially-mediated corrosion described above includes a term for detachment of fouling biofilm deposit from the tube surface. This process may influence corrosion rate substantially. When a portion (or a "patch") of deposit detaches, the metal surface left exposed will be subject to a considerably different microenvironment from the bare metal (i.e., metal surface with little or no deposit). As a consequence, a differential electrolytic cell may form increasing the potential for localized corrosion.

Chlorine Treatment and Corrosion of Cu-Ni Alloys. Chlorine is a very reactive compound and, hence, an effective bactericide. Chlorine is a strong oxidant which oxidizes many organic compounds and is known to depolymerize polymers of microbial origin (Characklis and Dydek, 1976). Therefore, chlorine has been used as an anti-microbial fouling treatment for many years. Recently, environmental concerns have encouraged searches for new, effective, yet environmentally safe, treatments. Nevertheless, chlorine is still widely used as a cooling water treatment.

Because of its reactive nature, chlorine treatment is frequently ineffective because it is consumed in undesirable side reactions, i.e., "Chlorine demand" reactions. Usually, the chlorine demand is due to reduced inorganic compounds or organic compounds in the cooling water. However, Cu-Ni alloys also present a chlorine demand.

This study was conducted in artificial sea water. When chlorine is added to sea water containing bromide ion, the bromide is rapidly oxidized to bromine and the chlorine reduced to chloride. The chemistry of the reaction has been described elsewhere. As a result, and because no distinction was made between chlorine and bromine in our measurements, the combined chlorine and bromine will be referred to as "halogen" below.

*Halogen demand.* Figure X-9 presents data from a halogen demand experiment. The results clearly indicate a high halogen demand for the Cu-Ni tube section. A halogen residual was never observed in the chlorination experiments as a result of the halogen demand presented by the metal tube, the sea water, and the trypticase soy broth.

*Influence of halogen on deposit mass.* Halogen treatment, in general reduced deposit accumulation. The more dramatic effect was observed in the Ti tubes. Halogen treatment had little effect on deposit mass in the Cu-Ni tube nor did it influence microbial cell counts in the deposit or in the bulk water. The high halogen demand of the Cu-Ni tube surface area, ISB, and the artificial sea water resulted in no measurable halogen residual and, hence, partially explains the negligible effect of halogen on the accumulation of fouling deposit.

In the Ti tubes, the influence of halogen on total

deposit mass was much more dramatic for at least two reasons:

1. The deposit mass in the Ti tubes contained significantly greater amounts of volatile components, i.e., microbial mass.
2. The Ti tube had little, if any, halogen demand.

Total and viable cell numbers in the deposit as well as in the bulk water were reduced significantly in the Ti system as a result of halogen treatment. The lack of halogen demand at the tube surface may influence the bactericidal nature of the halogen as compared to its effect in the Cu-Ni system. However, the influence of the Cu-Ni corrosion products trapped in the deposit may have also influenced the reactivity of the halogen.

*Influence of halogen treatment on corrosion rate in Cu-Ni.* Table X-8 indicates no significant effect of halogen treatment on corrosion rate of Cu-Ni. If halogen had significant contact with the Cu-Ni surface, considerable corrosion would be expected due to its high halogen demand. Since no significant corrosion was observed, chlorine may have been consumed in undesirable side reactions and may not have been penetrating the fouling deposit to the Cu-Ni surface. Additionally, Cu-Ni may serve as a catalyst for halogen reduction and, if so, little corrosion would occur as a result of a halogen reduction. More experiments are necessary to determine if a higher halogen loading rate would reduce fouling but, at the same time, increase corrosion rate.

**SUMMARY.** A conceptual model has been proposed to describe the interrelationship between biofouling and corrosion in a Cu-Ni alloy. Laboratory results have been presented which are consistent with the proposed model. The experimental results suggest several mechanistic hypotheses requiring further experimental testing which is currently underway.

## XI. BIOFOULING CONTROL

All practical methods for controlling fouling biofilms or, for that matter, any other type of fouling, must operate under the following constraints:

- 1) Economics
- 2) Material limitations
- 3) Environmental and health considerations
- 4) Process limitations

Consequently, there may be as many fouling control strategies as there are fouling situations.

### FUNDAMENTAL FOULING PROCESSES

A useful way to look at biofouling control is to see how various practical methods affect fouling biofilms. Fouling in general can be understood in terms of the following sequence of fundamental processes:

- 1) Transport of material to the fouling surface
- 2) Attachment or adsorption of material to the surface
- 3) Reaction and accumulation of deposit at the surface
- 4) Detachment or sloughing of deposit from the surface

This same sequence applies whether the deposit is biological, organic, inorganic, or a combination of these (Table XI-1).

Transport is a physical process described by the laws of hydrodynamics. Diffusion and turbulent eddies are the primary mechanisms of transport. Transport carries material away from the surface just as readily as it brings material to the surface. It is influenced by the concentration gradient and diffusion rate of material in the fluid, and fluid flow rate, viscosity, and temperature.

Attachment is a physico-chemical process where particulate or soluble material bonds to the surface with an accompanying reduction in free energy. It is a continuous phenomenon which involves relatively weak bonding. It can be as tenuous as the weak hydrogen bonding forces which account for adsorption of some organics, or as strong as the electrostatic forces which initially attract ions to a crystalline surface. Initial attachment may prepare a clean surface for further fouling. For example, adsorption of an organic film has been postulated to be a prerequisite for biofouling (Loeb and Neihof, 1975; Baier, 1972).

Reaction is the process whereby the deposit accumulates, hardens, and develops structure. Material which was loosely attached to the surface becomes more firmly bound. Structure begins to appear in the form of, for example, a microbial mat surrounded by extracellular polysaccharide, or a familiar crystalline calcium carbonate

scale.

Finally, detachment occurs when the deposit structure breaks down. It either dissolves or fragments and is swept away by fluid shear forces.

For the specific case of fouling biofilms, the four fundamental processes reduce to the following (Characklis, 1981):

- Transport of organics and cells to the wetted surface
- Adsorption and firm adhesion of the cells to the wetted surface
- Microbial cell growth and EPS formation at the wetted surface and within the biofilm
- Detachment of biofilm material primarily due to fluid shear forces

#### BREAKING THE CHAIN

Fouling control involves interrupting any of the fundamental fouling processes. In Table XI-2 common fouling control methods are categorized according to their effect on fundamental processes.

Decreasing transport to the surface is common in control of biofouling (filtration), scaling (water softening), and corrosion (deoxygenation). They all work by reducing the concentration of deposit promoting material in the feed water. It is an expensive technique since large volumes of relatively high quality water must be produced to be effective. One way around this is to find the weakest link in the transport process; the essential fouling promoting substance which is lowest in concentration. Since both biofouling and, indirectly, microbially mediated corrosion require a number of micronutrients this might be a fruitful place to start. Once an effective method is found, it can be implemented using the well developed technology found in the water softening industry.

Other generalized ways to reduce transport to the surface would be to reduce flow rate, reduce turbulence, or increase viscosity. While these may not seem practical in general, for some systems they may work.

Interrupting the interfacial process of adsorption-attachment can be used to reduce both biofouling (and thus indirectly corrosion) and scaling. This is accomplished by reducing the energy of attraction between the particles and the surface. It can occur when the fouling surface is at an optimum surface energy (Dexter, 1977) or, when the fouling particle surface charge is changed by adding polyelectrolytes or surfactants to the water (Drew Chemical Corp., 1979). By occupying bonding sites on particle or surface or both, the fouling process is interrupted.

Inhibiting growth or accumulation is widely used in industry to control fouling. Biocides, such as chlorine, inhibit the development of microbial slimes, crystal growth inhibitors interfere with the development of the crystalline lattice in inorganic scale deposits (Drew Chemical Corp., 1979), and protective paints and cathodic protection inhibit development of corrosion deposits. A significant disadvantage with active growth inhibitors such as the quaternary ammonium biocides is that they must be applied continuously. Otherwise, since they do not remove accumulated deposits, growth resumes where it left off when application is interrupted (Characklis, unpublished results).

Finally, the most often used method for fouling control is enhancement of detachment. Both physical and chemical methods are used which disrupt bonding to the surface or destroy cohesiveness of the deposit. Mechanical methods, such as increasing the flow rate, or scraping the surfaces, remove fouling deposits but must be used at infrequent intervals since they disrupt normal plant operation. Chemicals are also often used at infrequent intervals to remove accumulated fouling deposits. For example, chlorine is applied in "shock" doses to strip microbial slimes from fouled surfaces. Likewise, acids or chelating agents are used to remove inorganic scale deposits. These intermittent methods are generally simple to implement but often create other problems:

- 1) When used to control biofouling, they can cause rapid regrowth. The rate of deposit accumulation after "shock" dosing with chlorine is often greater than before treatment. This may result from incomplete removal of the deposit leaving either some viable microorganisms on the surface or a more attractive surface for microbial attachment.
- 2) It is costly to apply chemicals in the high concentrations necessary to be completely effective.
- 3) The high concentrations of chemicals used in intermittent control of fouling are toxic in the environment
- 4) The plant often operates at a borderline efficiency until it is deemed necessary to clean.

Nevertheless, while traditional biofouling control methods have addressed each of these processes, for the most part, they have concentrated on enhancing detachment through use of chlorine.

#### BIOFOULING CONTROL WITH CHLORINE

Biofouling is controlled by a wide variety of physical and chemical means (Marine Research, Inc., 1976; Battaglia et al., 1981; Graham, 1982; Roe and Characklis, 1982). However, the most effective and most commonly used method for controlling and/or preventing biofouling is chlorination. Recent concern over the toxicity of chlorine (Hall et al., 1981) and some of its reaction products (Trabalka and Burch, 1978) has stimulated a search for alternatives (Battaglia et al., 1981; Waite and Fagan, 1980; Burton, 1980). Nevertheless, chlorination is still widely practiced in power plants and in process plants for minimizing the negative effects of biofouling (Battaglia et al., 1981).

Chlorine itself is used in a variety of ways to control biofouling. It is applied as chlorine gas, hypochlorite ion, chlorine dioxide, and is electrochemically generated in sea water. Chlorine is used in once-through systems or in recirculating cooling towers; applied continuously or in shock dosages. It is used in fresh water systems and sea water; in clean water and in contaminated water containing high levels of oxidizable materials.

Constraints placed on the use of chlorine have often limited its success in biofouling control. These constraints include:

- 1) Cost effectiveness. This may be a factor in once-through systems where extremely high chlorine demand exists.
- 2) Limitations in condenser materials which lead to corrosion. High chloride levels often develop in recirculating cooling tower systems operating at high cycles of concentration.p.
- 3) Environmental regulations which limit effluent levels of chlorine in receiving waters.

The latter has been the principal constraint on use of chlorine in once-through cooling water systems since discovery of its diverse affect on health and the environment. Chlorine and chlorine-produced oxidants have been found to be toxic to aquatic life (Brungs, 1973). In addition, chlorine reacts with waterborne organic compounds to produce potentially carcinogenic chlorinated organics (Jolley et al., 1978; Bean et al., 1980). Briley (1980) showed that chlorination of the alga *Anabena cylindrica* and its extracellular products formed trihalomethanes (THMs). This suggests that chlorination of biofilms and their associated extracellular polymeric material may contribute to THMs in the aquatic environment.

Chlorine has been widely used as a disinfectant in the water treatment industry. It was originally presumed that this was the only way it controlled biofouling. Recently, however, experimental results have indicated that chlorine also oxidizes and depolymerizes the EPS in the biofilm

causing destruction of the biofilm matrix and its detachment from the surface (Characklis and Dydek, 1976). There is still some controversy over which mechanism is responsible for chlorine's superior effectiveness in fouling control (Bongers *et al.*, 1977). It is probable that both mechanisms operate to varying degrees depending on process conditions.

Control of biofouling with chlorine in turbulent flow is perceived to occur as a result of the following processes consistent with either mechanism (Figure XI-1):

- Chlorine species entering the pipe segment react with chlorine-demanding components (viable cells and chemical compounds) in the bulk water.
- Chlorine species are transported through the bulk fluid to the water-biofilm interface.
- Chlorine species diffuse and react within the biofilm.

Since both "solid" and liquid phases are present, the chlorine-biofilm reaction can be termed a heterogeneous process. In heterogeneous systems such as this, there is a high probability that transport rates will limit the overall rate of reaction. This includes transport of reactants and products in each phase and across phase boundaries. McIntire *et al* (1983) have developed a mathematical model describing the combined effect of transport and reaction on the effectiveness of chlorine in controlling biofouling in a circular tube.

#### TRANSPORT OF CHLORINE

Water Phase. The rate at which chlorine is transported to the biofilm depends on the concentration of chlorine in the bulk water and the intensity of turbulence.

The concentration of chlorine in the bulk water is related to its rate of application minus the rate of chlorine demand of the water. If the chlorine concentration at the biofilm interface is the same as its concentration in the bulk water, then the concentration in the water drives the reactions of chlorine within the biofilm. If chlorine reacts with the biofilm relatively rapidly, the concentration at the interface will be low and physical transport of chlorine to the interface may limit the rate of the overall process within the biofilm.

By increasing the intensity of turbulence through increased flow rate, both the transport rates in the bulk water and the concentration at the interface will increase. In the bulk water, chlorine is transported primarily by eddy diffusion. Several investigators have observed that increasing turbulence results in increased chlorine reaction rates (Norrman *et al.*, 1977; Novak, 1982; Miller and Bott, 1981). Novak (1982) observed a first order rate with

respect to chlorine concentration which indicates either a first order reaction or a mass transfer limitation.

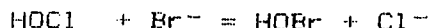
**Biofilm.** The transport of chlorine in biofilms occurs primarily by molecular diffusion. Since the composition of biofilms is from 96 to 99 percent water, the diffusivity of chlorine in biofilm is probably similar to its diffusivity in water. In biofilms of higher density, or in those containing microbial matter associated with inorganic scales, tubercules, or sediment deposits, diffusion of chlorine may be relatively slow.

#### REACTION OF CHLORINE

**Water Phase.** The reaction of chlorine in the water phase is generally referred to as the "chlorine demand" of the water. The chlorine demand is due to oxidizable inorganic compounds, organic compounds, microbial cells, and other particulates in the water. These oxidizable species compete with the biofilm for available chlorine and often reduce the effectiveness of biofouling control. Both the extent and rate of chlorine demand determine the amount of chlorine available for biofouling control. Present methods for obtaining chlorine demand measure only how much chlorine is consumed, i.e., a stoichiometric quantity. The rate of chlorine demand (i.e., how fast chlorine is consumed) would be a more useful quantity for assessing its effect on biofouling control.

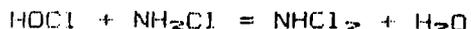
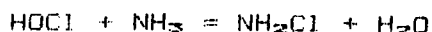
Bongers (1977) measured the rate of decay of chlorine in estuarine waters and found it to occur in three phases. He found that during phase one free chlorine rapidly dropped to about half of its original concentration in 30 seconds. Two successive but distinct phases had rates of decay which were significantly slower. These data imply that reactions in the water phase cannot necessarily be modeled by a single simple first order rate expression.

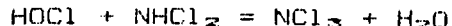
In marine or estuarine waters, bromide ion may represent a significant fraction of the chlorine demand. Bromine (hypobromite ion) is rapidly formed from reaction of chlorine with bromide ion:



Hypobromite is a strong disinfectant and is probably effective at destroying biofilm EPS as well.

The amines are a class of compounds, ubiquitous in nature, which are often responsible for chlorine demand in cooling water sources. Ammonia, the parent compound for the amines, reacts with chlorine to form mono-, di-, and trichloramine:





Where other amines are present and in sea water where bromide is present, the number of possible reactions and cross reactions increase very quickly (Haag and Lietzke, 1980). It is not known to what extent halogenated amines, often referred to as "combined chlorine", can disrupt microbial films.

Temperature has been shown to significantly affect both the rate and extent of chlorine consumption in sea water (Wong, 1980). Consequently, fluid temperature may affect fouling control where there is significant chlorine demand.

**Biofilm.** Chlorine reacts with various organic and reduced inorganic components within the biofilm. It can disrupt cellular material and inactivate cells (disinfect). In well developed biofilms, its greatest apparent effect is reaction with EPS (primarily polysaccharides) which are responsible for the physical integrity of the biofilm (Characklis and Dydek, 1976). A series of studies (Characklis, 1971; Characklis and Dydek, 1974; Characklis *et al.*, 1980) have estimated the process rate and process stoichiometry of the reaction of chlorine with immobilized biofilm. However, these data reflect variations resulting from poorly defined chlorine demand and microbial populations.

Bacterial flocs and biofilms that are rich in EPS exhibit a more rapid and ultimately greater chlorine demand (Characklis and Dydek, 1976). One possible explanation is derived from the observation that hypochlorite ion attacks glucose polysaccharides with extensive oxidation at the C<sub>2</sub> and C<sub>3</sub> positions of D-glucose units, which results in cleavage of the C<sub>2</sub>-C<sub>3</sub> bond (Hullinger, 1964; Whistler *et al.*, 1956). Depolymerization can result from the inductive effects of this oxidation, from direct oxidative cleavage of the glucosidic bond, or from degradation of the intermediate carbonyl compound.

Most of what is known about chlorine disinfection is derived from water treatment studies. It is generally agreed that chlorine disinfects by inhibiting enzymatic processes within the bacterial cell (White, 1972; Wyss, 1962). Chlorine has been found to be more effective as a disinfectant at pH 6.0 to pH 6.5 (White, 1972). Hypochlorous acid predominates at these pH values. It is postulated that the hypochlorous acid molecule, which is electrically neutral and has a smaller solvation shell than the hypochlorite ion, can readily pass through cellular membranes while the hypochlorite ion cannot.

**Condenser Surface.** The condenser surface may also exert a chlorine demand. Characklis and Zilver (1983)

have documented the chlorine demand of a copper-nickel alloy. Titanium, on the other hand, exerted no such demand. Lewis (1982a) also found that Cu-Ni reacts with chlorine. The chlorine demand may be directly related to the significant corrosion observed in sea water studies when copper-nickel alloys are chlorinated regularly (Fischer, 1980). This may be due to stoichiometric reaction of the tube alloy with chlorine, or removal of a protective oxide coating from the alloy, rendering the underlying metal vulnerable to other corrosion reactions. Metal ions such as Cu(II) have been shown to catalyze chlorine decomposition (Lister, 1956).

**BIOFILM REMOVAL AND/OR DESTRUCTION.** The reaction of chlorine with biofilm produces an immediate response in the bulk water by increasing turbidity and the soluble organic constituents (Characklis and Dydek, 1976). A significant removal of biofilm is evidenced by a decrease in biofilm thickness (Characklis *et al.*, 1980; Miller and Bott, 1981) and a decrease in fluid frictional resistance (Characklis, 1980; Characklis and Dydek, 1976; Norman *et al.*, 1977). Inactivation of the biofilm with a nonoxidizing poison does not result in any biofilm removal (Characklis and Dydek, 1976). The results suggest that hypochlorite ion oxidizes EPS within the biofilm resulting in depolymerization, dissolution, and detachment.

Characklis *et al.* (1980) reported that biofilm detachment resulting from chlorination is much higher between pH 7.5 and 8.5 than between pH 6 and 7 where disinfection is optimum. These data are consistent with data for chlorination of polysaccharides such as starch, which is optimum at pH > 7 (Whistler and Schweiger, 1957). Similar data are not available for monochloramine, dichloramine, or other N-chloro compounds.

Chlorine "enhancers" are sometimes added to improve chlorination performance. Supposedly, these compounds increase penetration of chlorine into the biofilm.

Chlorine concentrations as high as 20 mg/l applied several times a day may be needed to effectively control biofouling at a power plant (Battaglia *et al.*, 1981). The criterion for dosage is frequently the residual concentration in the outlet water. By maintaining a residual at the outlet, chlorine demand in the water is presumably nullified. Typical chlorine residuals in the outlet range from 0.1 to 0.5 mg/l for effective performance.

Fluid shear forces may play a major role in the removal of biofilm. Several investigators (Norman *et al.*, 1977; Miller and Bott, 1981; Novak, 1982; Characklis, 1980) measured a higher rate of chlorine uptake by biofilms and a greater amount of biofilm

removed when the fluid shear stress was greater. The authors suggest that greater shear force may have the following effect:

- Increases mass transfer of chlorine from the water to the biofilm
- Disrupts the biofilm during chlorination, reentraining reaction products in the water phase and exposing new surfaces for chlorine attack
- Increasing shear force (fluid velocity) also reflects a thinner viscous sublayer in the tube. The viscous sublayer is a region of low shear force and biofilm within the viscous sublayer will not be disrupted to a great extent. Timperley (1981) has commented on this effect of mean flow velocity on the cleaning of biofouled tubes.

Observations indicate that a residual biofouling deposit remains after removal through intermittent chlorine treatment. This has important consequences for subsequent regrowth of the biofouling deposit.

**BIOFOULING CONTROL THROUGH DISINFECTIONS.** Low level chlorination can significantly reduce viable microbial cells in water and destroy some of the nutrients necessary for cell growth. It is effectively used to maintain drinking water quality at residual concentrations as low as 0.03 mg/l (Biros, 1980). It is also effective in controlling attachment and growth of epifaunal animals in heat exchanger systems (White, 1972; Bongers, 1977). Low level chlorination, however, is not sufficient to prevent attachment of surviving viable cells to heat exchanger walls. Low level, continuous chlorination can be used to slow down microbial fouling but not eliminate it. Concentrations of chlorine high enough to make these systems aseptic would be prohibitively expensive and create unacceptable environmental damage.

**BIOFILM REGROWTH.** Numerous investigators (Characklis, 1980; Norrman *et al*, 1977; Novak, 1982; Miller and Bott, 1981; Lewis, 1982a) and plant operators have observed a rapid resumption of biofouling immediately following chlorine treatment and have termed this phenomenon "regrowth". Figure XI-2 (Lewis, 1982a) illustrates this phenomenon. Regrowth may be due to one or all of the following reasons:

- The remaining biofilm contains enough viable organisms to preclude any lag phase in fouling biofilm formation observed on clean tubes.
- The remaining biofilm is relatively rough and enhances transport of microbial cells and other

compounds to the surface. The roughness of the deposit also provides a "stickier" surface.

- The chlorine simply removes EPS and leaves biofilm cells more exposed to nutrients.
- EPS is rapidly created by surviving organisms as a protective response to irritation by chlorine.
- There is selection for a chlorine resistant organism (e.g., one which normally produces excessive amounts of EPS) which proliferates on successive chlorinations.

Rapid regrowth has also been observed on walls of water distribution systems (Fidgeway and Olson, 1982; Berg et al., 1982). These authors both demonstrated that bacteria previously exposed to chlorine were more resistant to chlorine than those never exposed. This is consistent with the latter two hypotheses.

After extended periods of repeated chlorination, a residual refractory material has been noted in several investigations (Characklis, 1980; Mangum and Shepherd, 1973; Lewis, 1982b). The deposit increases in ash content with repeated chlorination and, in several cases, and inordinately high content of manganese has been observed. The refractory deposit has an inhibitory effect on biofouling (Mangum and Shepherd, 1973). This refractory material may accumulate to such an extent that it impedes heat transfer and will not be affected by chlorine.

#### DISCUSSION

Chlorine is a superior microbial fouling control agent because it can effectively disrupt and loosen fouling deposits. Chlorine, in the water phase, can also inactivate microbial cells (disinfect) and oxidize nutrients. When chlorine contacts biofilm, the following occurs: detachment of biofilm, dissolution of biofilm components, and disinfection. Chlorine is consumed in all of these reactions. Limited observations suggest that the following factors influence the rate of the chlorine-biofilm reaction:

- 1) Transport of chlorine from the water to the water-biofilm interface. Transport rate increases with increasing chlorine concentration and turbulence.
- 2) Transport of chlorine within the biofilm or deposit. Transport rate can be increased by increasing the chlorine concentration at the water-biofilm interface.
- 3) Reaction of chlorine within the biofilm,

especially the abiotic components.

- 4) Detachment and reentrainment of reacted biofilm primarily due to fluid shear stress.
- 5) The hypochlorous acid-hypochlorite ion equilibrium, which on the one hand favors disinfection ( $\text{HOCl}$ ) and on the other favors detachment ( $\text{OCl}^-$ ).
- 6) Disinfection, which is effective at low chlorine concentrations but unfavorably competes with the EPS of well-developed biofilms for available chlorine.

Consequently, a chlorination treatment program may be improved by the following measures:

- Increase chlorine concentration at the water-biofilm interface. Most practically, this is accomplished by increasing chlorine concentration in the water phase. However, another possibility is to target chlorination at the water-biofilm interface.
- Increase fluid shear stress at the water-biofilm interface. This requires increasing fluid flow rate.
- Reduce chlorine demand of the water, sometimes a difficult, costly task. If chlorine can be injected in the viscous sublayer region, the chlorine demand of the water will have significantly less effect on the process.
- Use pH control to favor hypochlorite ion promoted detachment with well developed biofilms and hypochlorous acid disinfection with thin films. Alternate between continuous chlorination at pH 6.5 and "shock" chlorination at pH 8.

While these recommendations, based on observations from the literature, may lead to more effective use of chlorine for biofouling control, they are, for the most part, just speculation. In fact, the processes contributing to the short and long-term effectiveness of a chlorination program for biofouling control are not well understood since *fundamental research* on the topic has never been conducted.

#### RESEARCH NEEDS

There are two primary questions that should be addressed in order to develop a rational approach to using chlorine in heat exchanger biofouling control:

- 1) Can we predict, based on readily measurable parameters, when chlorination will be effective or when some other method should be selected?
- 2) Once chlorine has been chosen, what control strategy will optimize its use? Can effective dosage be continually determined using simple methods?

A principal tool in answering these questions will be an accurate predictive model for describing the influence of chlorine on fouling biofilms.

Considerable work has appeared in the literature on predicting the fate of chlorine in cooling water based on laboratory studies and equilibrium or kinetic models (Zielke and Macey, 1980; Sugam and Helz, 1980; Haag and Lietzke, 1980; Helz et al., 1978). These studies have concentrated on equilibrium or kinetic chlorine demand of the cooling water and have assumed insignificant reaction at the heat exchanger surfaces. The results have not always been successful (Helz et al., 1978) and chlorine minimization programs are still relied on in most cases (Moss et al., 1979). Minimization studies are costly and cannot account for seasonal changes in water quality and variations in power demand. The model developed by McIntire et al (1983) describes the chlorine-biofilm reaction in a circular tube under turbulent flow conditions, and takes into account both transport and reaction of chlorine in the water and biofilm. The principal relationships in the model are derived from the following equation of continuity expressed in cylindrical coordinates (figure XI-3):

$$\frac{1}{r} \frac{\partial}{\partial r} \left( D_r r \frac{\partial C}{\partial r} \right) + \frac{\partial}{\partial z} \left( D_z \frac{\partial C}{\partial z} \right) + R = V_z \frac{\partial C}{\partial z} + V_r \frac{\partial C}{\partial r} + \frac{\partial C}{\partial t} \quad \text{eq XI-1}$$

It is assumed that:

- Net flow of fluid into the film is negligible.
- Radial concentration gradients of chlorine are much greater than axial concentration gradients.
- Mass transport is solely by radial diffusion and axial convection.

With these assumptions, equation 1 reduces to equation 2 (processes occurring in the fluid phase), and to equation 3 (processes occurring in the biofilm):

$$V_z \frac{\partial C}{\partial z} = \frac{1}{r} \frac{\partial}{\partial r} \left( D_f r \frac{\partial C}{\partial r} \right) + R_f \quad \text{eq XI-2}$$

$$\frac{1}{r} \frac{\partial}{\partial r} \left( D_b r \frac{\partial C}{\partial r} \right) = R_b \quad \text{eq XI-3}$$

where:

$C$  = chlorine concentration

$D_f, D_b$  = effective diffusivity of chlorine in the fluid and biofilm

$V_z$  = axial time-smoothed fluid velocity

$V_r$  = radial time-smoothed fluid velocity

$R_f, R_b$  = reaction rate of chlorine in the fluid and biofilm

Reactions in the fluid and in the biofilm are approximated by two first order kinetic expressions. Boundary conditions are as follows:

$C = C_0$  at  $z = 0$ , the entrance to the tube.

$dC/dr = 0$  at  $r = r_1$ , the tube wall.

$dC/dr = 0$  at  $r = 0$ , due to symmetry of the tube.

$D_f dC/dr|_{r_1} = D_b dC/dr|_{r_1}$ , fluxes into and out of the biofilm-fluid interface are equal.

$C|_{r_1} = \alpha C_f|_{r_1}$  at  $r = r_1$ , the concentration of chlorine in the fluid must be in equilibrium with the concentration of chlorine in the film (interface partition coefficient =  $\alpha$ ).

Biofilm removal is described by a simple mass balance, i.e., a constant proportion of chlorine entering the biofilm results in removal of biomass from the surface.

The results of the computer simulation are presented in Figures XI-4 to XI-6 in dimensionless form. The results clearly indicate the significant effect that chlorine demand in the fluid can have on the performance of a chlorination program intended to minimize biofouling.

Figure XI-4 indicates that a chlorine demand in the fluid will deplete the water of active chlorine much sooner than if chlorine demand were absent. Figure XI-6 indicates how biofilm removal progresses with time with and without chlorine reaction in the fluid.

Clearly, there is a need to better define the reaction rate expressions which describe the rate of chlorine demand in cooling waters. Is the assumed first order expression in this model sufficient? Are the rate

coefficients satisfactory? Does temperature, which varies significantly in heat exchanger tubes (radially and axially), significantly influence the rate of chlorine demand?

Table XI-1. Fundamental Fouling Processes.

Transport	- soluble material - particulate material
Attachment	- adsorption - adhesion
Reactions	- particulate - precipitation - corrosion - microbiological
Detachment	- desorption - sloughing - spalling

Table XI-2. Current Fouling Control Methods Categorized by the Fundamental Processes Affected.

## FOULING CONTROL METHODS

<u>FUNDAMENTAL</u>					
<u>PROCESS</u>	<u>BIOFOULING</u>	<u>SCALING</u>	<u>CORROSION</u>		
TRANSPORT	—	• FILTRATION/ COAGULATION	• WATER SOFTENING	• OXYGEN REMOVAL	
INTERFACIAL PROCESS	—	• BIODISPERSANTS • BIOCIDES	• DISPERSANT	—	
REACTION	—	• TUBE ALLOY • BIOCIDES	• CRYSTAL GROWTH INHIBITOR	• COATINGS • ELECTROLYTIC PROTECTION	
DETACHMENT	—	• OXIDIZING BIOCIDES • PHYSICAL	• CHELANT • ACID	—	

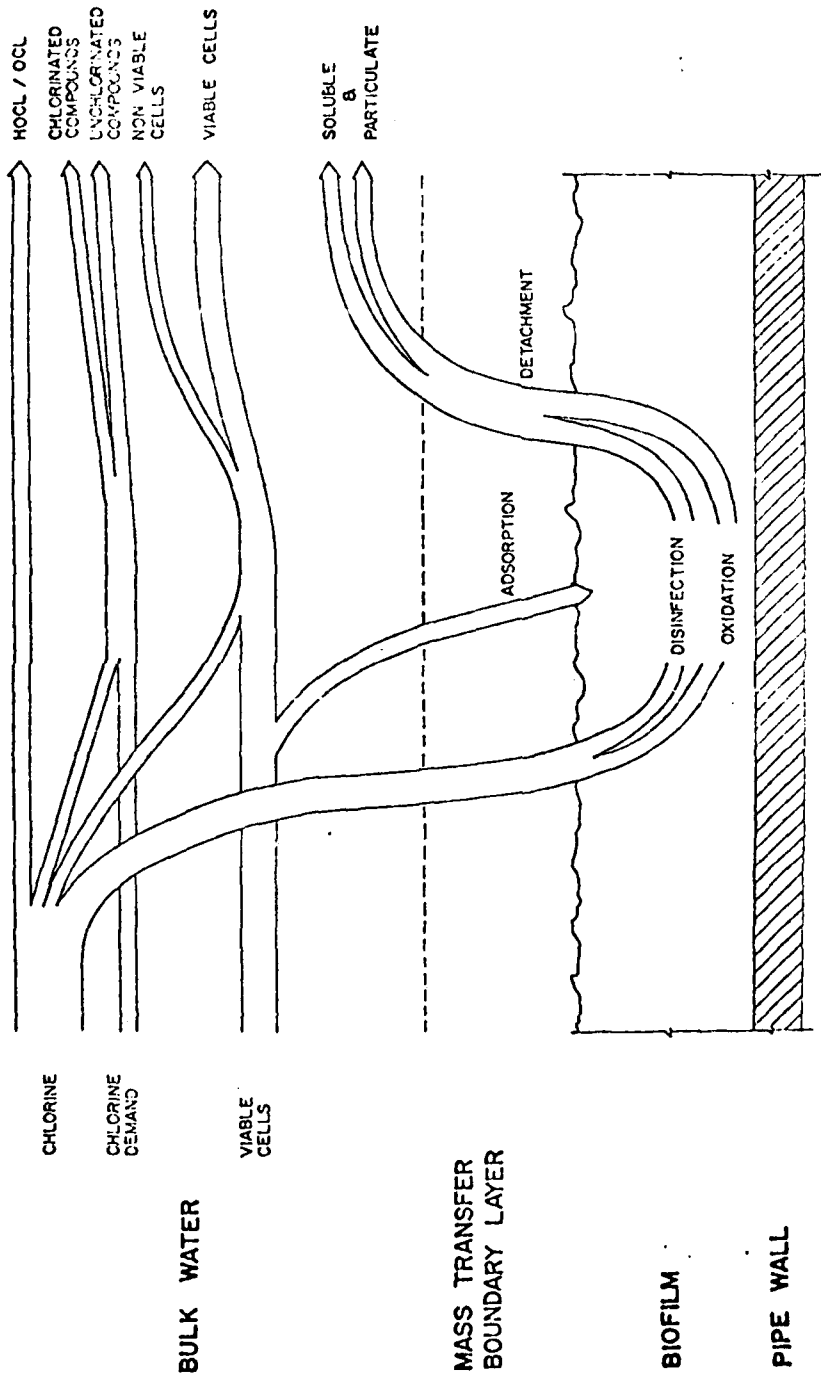


Figure XI-1. Processes Occurring in Regulating Control with Chlorine.

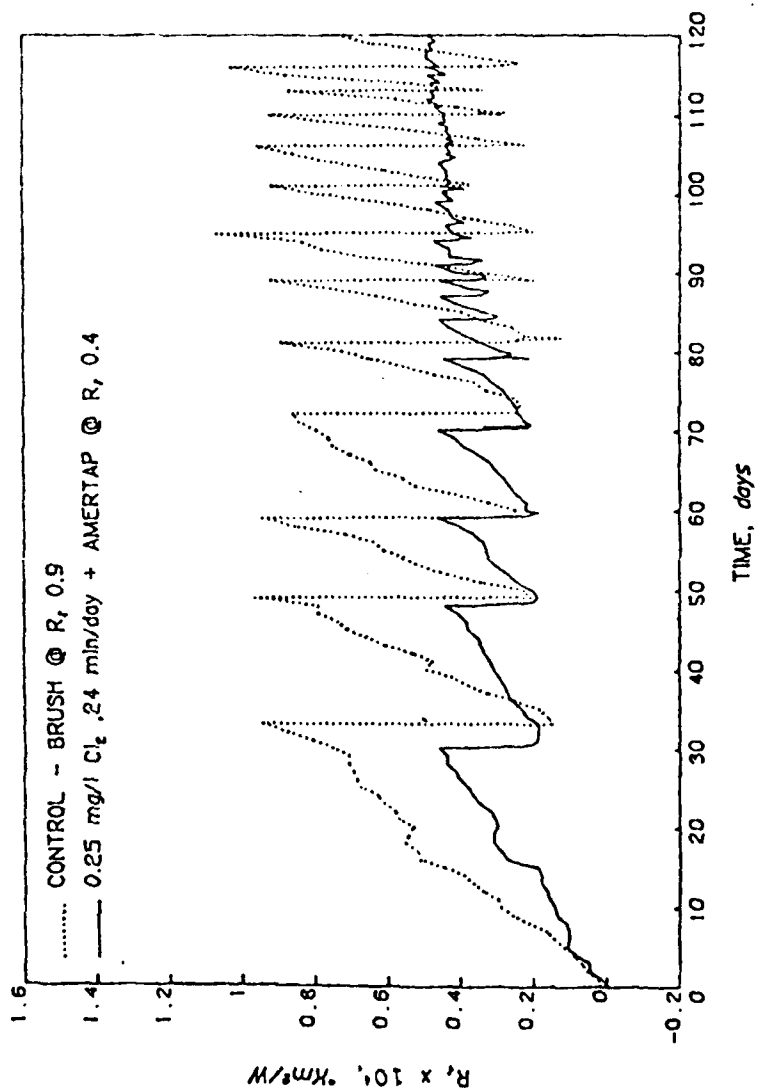


Figure XI-2. Fouling Resistance on Aged 3003 Aluminum Tubes Treated as Shown when  $R_f$  Reached the Maximum Desired Level (0.4 or 0.9) (Lewis, 1982a).

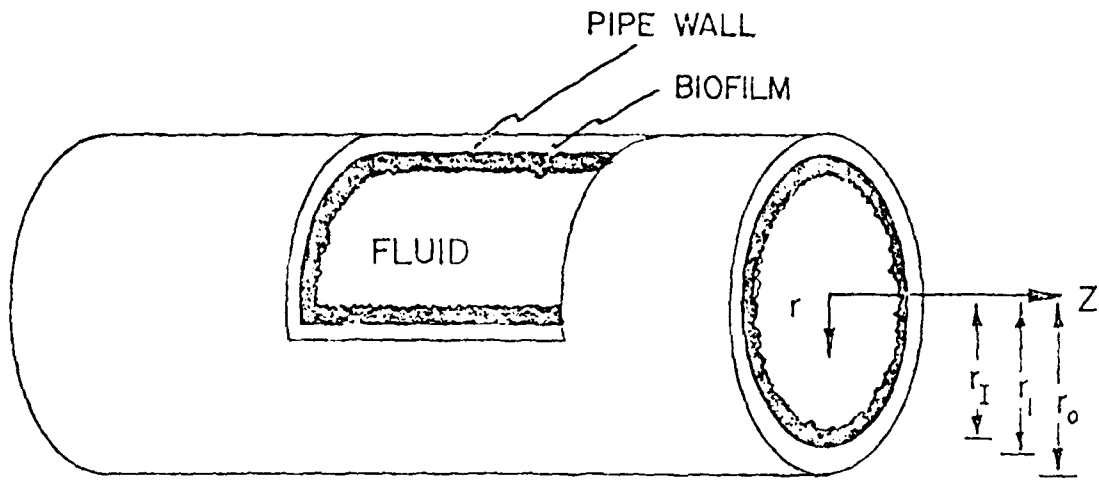


Figure XI-3. Geometry of Modeled System (McIntire et al., 1983).

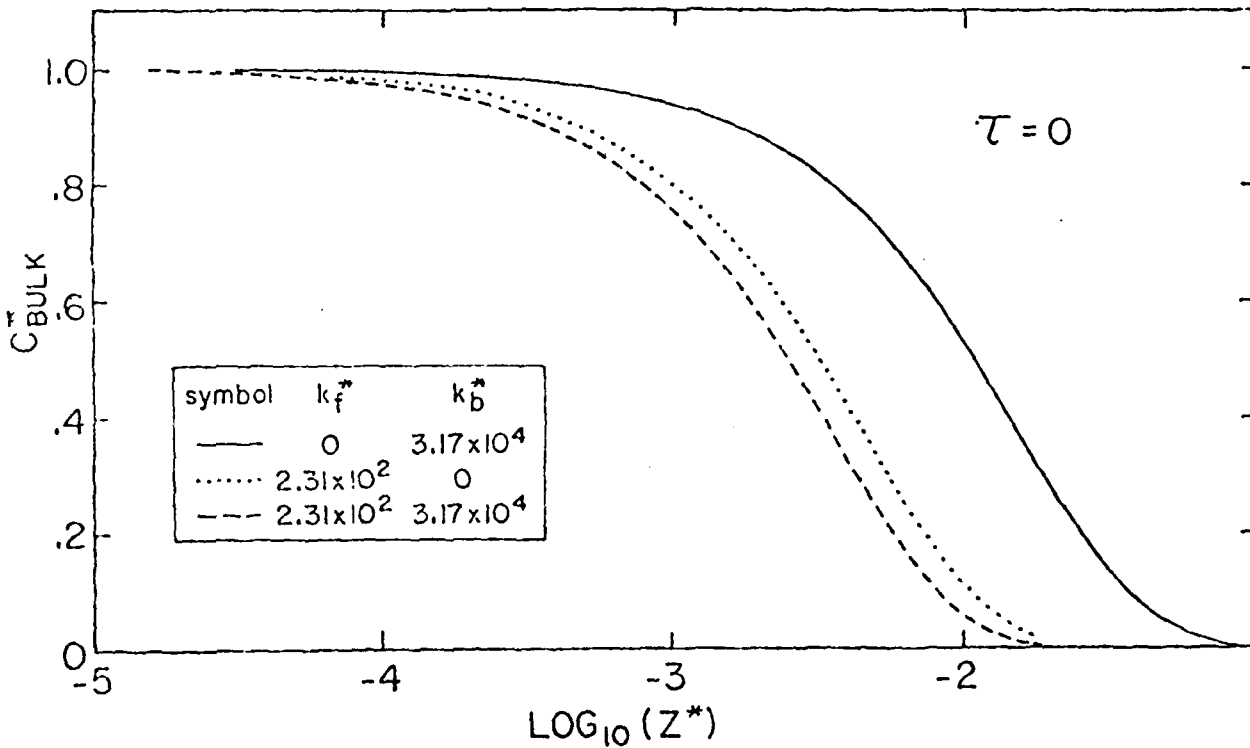


Figure XI-4. Dimensionless Fluid Chlorine Concentration Along the Length of a Tube (dimensionless units) With Reaction in the Fluid ( $k_f^*$ ) and REACTION in the Biofilm ( $k_b^*$ ) for the Described Model (McIntire et al., 1983).

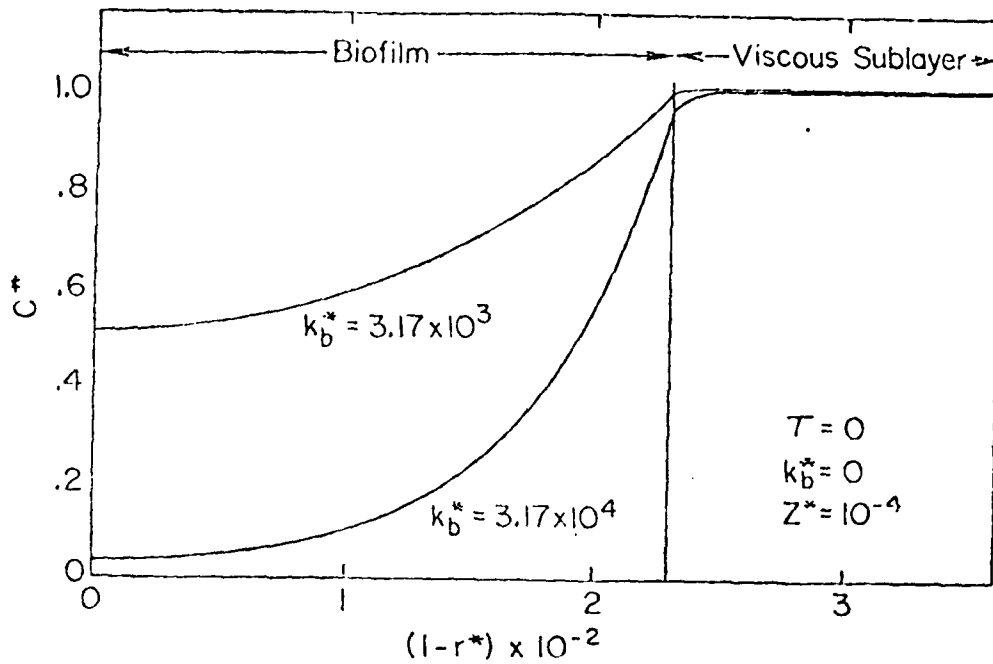


Figure 14. Dimensional Concentration (dimensionless units) as a function of Radial Distance into the Biofilm with Two Different Biofilm Reaction Rates ( $k_b^*$ ), for the Described Model (McIntire et al., 1983).

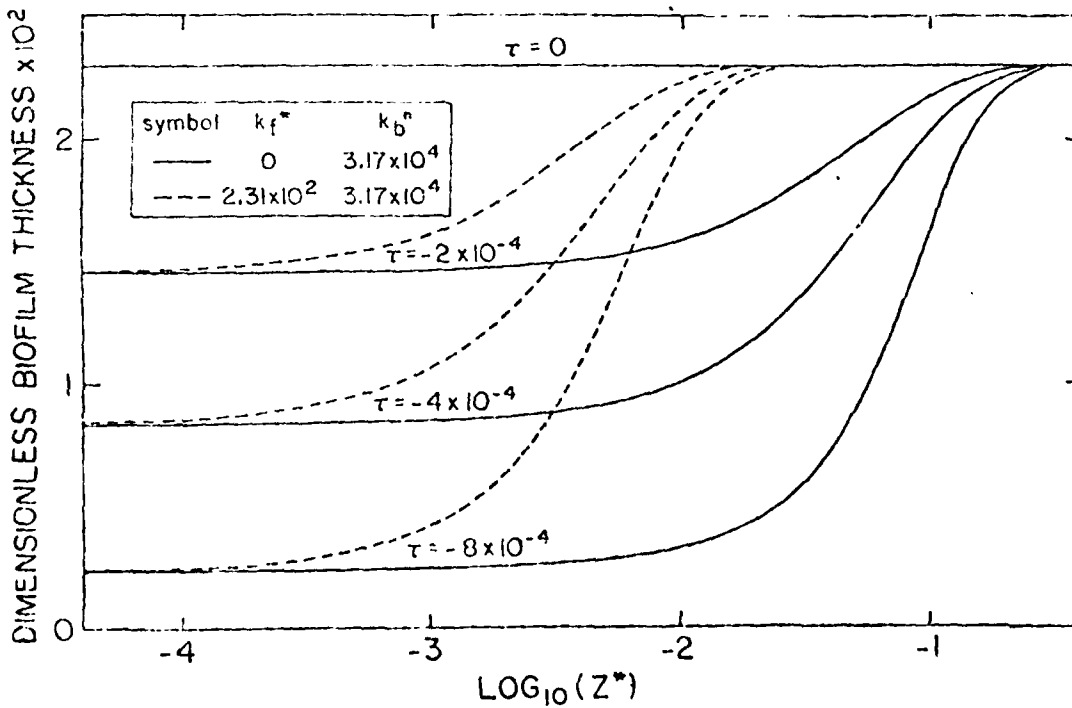


Figure 15. Thickness of the Biofilm (dimensionless units) along the length of a tube (dimensionless units) as a function of Time ( $\tau$ ) During Chlorination for the Described Model (McIntire et al., 1983).

## REFERENCES

- APHA. 1976. Standard Methods for the Examination of Water and Wastewater, 14th Edition, APHA, Washington, DC, .
- Arnold, G.E. 1963. Engineering News Record, Vol. 116, pp 774-775.
- Baier, R.E. 1972. In Proceedings: Third International Congress On Marine Corrosion and Fouling, Ed. R.F. Acker et al, Gaithersburg, MA, pp633-640.
- Baier, R.E. 1975. In Applied Chemistry at Protein Interfaces. (R.E. Baier, Ed.) pp. 1-25. Advances in Chemistry Series 145. American Chemical Society, Washington, DC.
- Baier, R.E. 1980. In Adsorption of Microorganisms to Surfaces. (G. Bitton and K.C. Marshall, Eds.) pp. 59-104. Wiley, NY.
- Baier, R.E. and Weiss, L. 1975. In Applied Chemistry at Protein Interfaces. (R.E. Baier, Ed.) pp. 300-307. Advances in Chemistry Series, 145. American Chemical Society, Washington, DC.
- Bailiod, R.D., and W.C. Boyle. 1970. J. Sault. Engrg. Div., American Society of Civil Engineers. 96 (SA4):525-545.
- Bakke, R. 1983. M.S. Thesis, Montana State University (MSU), Bozeman, MT., 53 pp.
- Bates, J.F. and J.M. Popplewell. 1974. Paper No. 100 presented NACE Corrosion/74, Chicago, IL.
- Battaglia, F.J., D.P. Bour, and R.M. Burd. 1981. Biofouling Control Practice and Assessment. Electric Power Research Institute, EPRI CS-1976, Project 1132-1, Final Report, Palo Alto, CA, 212 pp.
- Beal, S.K. 1970. Nucl. Sci. Engrg. 40, 1-11.
- Bean, R.M., D.C. Mann, B.W. Wilson, R.C. Riley, E.W. Lusty, and T.O. Thatcher. 1980. In Water Chlorination: Environmental Impact and Health Effects, Vol. 3, R.L. Jolley, W.A. Brungs, and R.B. Cumming, Eds. (Ann Arbor, MI: Ann Arbor Science Publishers, Inc.), pp.369-377.
- Berg, J.D., A. Matin, and P. Roberts. 1982. "Effect of Antecedent Growth Conditions on Sensitivity of *Escherichia coli* to Chlorine Dioxide," Applied and Environmental Microbiology, October, pp.814-819.
- Bianchi, G. and P. Longhi. 1973. Corrosion Science, Vol.

- 13., pp. 853-864.
- Biros, J.L. and H. Lamblin. 1980. In Water Chlorination: Environmental Impact and Health Effects, Vol.3, R.L. Jolley, W.A. Brungs, and R.B. Cumming, Eds. (Ann Arbor, MI: Ann Arbor Science Publishers, Inc.), pp.743-755.
- Bongers, L.H. and D.T. Burton. 1977. "Bromine Chloride - An Alternative to Chlorine for Fouling Control in Condenser Cooling Systems", U.S. Environmental Protection Agency (Washington, DC, EPA-600/7-77-053).
- Booth, G.H. and A.K. Tiller. 1960. Transactions Faraday Society, 56:1689-1696.
- Booth, G.H. and A.K. Tiller. 1962. Transactions Faraday Society, 58:2510-2516.
- Booth, G.H., A.W. Copper, and P.M. Cooper. 1967. Chemistry and Industry, 86:2084-2085.
- Bowles, J.A. and D.H. Marsh. 1982. American Society Microbiology News, 48 p. 295.
- Brash, J.L. and Samak, G.M. 1978. J. Colloid, Interface Sci., Vol. 65, pp. 495-504.
- Brauer, H. 1963. Chemische Zeitung, 87:199-210.
- Briley, K.F., R.F. Williams, K.E. Longley, C.A. Sorber. 1980. In Water Chlorination: Environmental Impact and Health Effects, Vol.3, R.L. Jolley, W.A. Brungs, and R.B. Cumming, Eds. (Ann Arbor, MI: Ann Arbor Science Publishers, Inc.), pp.117-129.
- Browne, L.W.B. 1974. Atmospheric Environment, 8:801.
- Brungs, W.A. 1973. J. Water Pollut. Control Fed., 45, 2180-2193.
- Bryers, J.D. 1979. Ph.D. Thesis, Rice University, Houston, TX, 196 pp.
- Bryers, J.D. and W.G. Characklis, 1979. In "Condenser Biofouling Control," (Garey, J.F. Ed.), pp. 169-184, Ann Arbor Science, Ann Arbor, MI.
- Bryers, J.D., and W.G. Characklis. 1981. Water Res. 15:483.
- Bryers, J.D. and W.G. Characklis. 1982. Biotech. Bioeng., 24, 2451-2476.
- Burns, J.M., E.E. Staffeldt, and O.H. Calderon. 1976. Develop. Ind. Microbiol. 8:327-334.

- Burrill, K.A. 1981. In Fouling of Heat Transfer Equipment. (Somerscales and Knudsen, Eds.), pp. 227-247, Hemisphere Publishing Corp., Washington DC.
- Burton, D.T. 1980. In Condenser Biofouling Control (J.F. Garey, et al., eds.), Ann Arbor Science, Ann Arbor, MI, 251-266.
- Castle, J.E. and D.C. Epler. 1981. "The Development of Inorganic and Biological Fouling Layers on Copper Based Alloys," paper presented at the Inst. Corrosion Science TECHNOL/Inst. Chemical Engineering conference on Progress in the Prevention of Fouling in Industrial Plant, Univ. of Nottingham, UK.
- Chamberlain, A.H.L. 1976. In Proc. Third Int. Biodegradation symp. (J.M. Sharpley and A.M. Kaplan Eds.), pp. 417-432. Applied Science, London.
- Characklis, W.G. 1971. Proc., 26th Industrial Waste Conf., Purdue University, 171-181.
- Characklis, W.G. 1973. Water Res. 7:1249-1258.
- Characklis, W.G. 1980. Biofilm Development and Destruction. Electric Power Research Institute, EPRI CS-1554, Final Report, Palo Alto, CA 311 pp.
- Characklis, W.G. 1981. Biotech. Bioengrg., 23, 1923-1960.
- Characklis, W.G. and Dydek, S.T. 1976. Water Research, 10, 515-522.
- Characklis, W.G. et al., 1981. Proc., International Wat. Conf., p. 229.
- Characklis, W.G. et al., 1981. Heat Transf. Engrg. 3:23.
- Characklis, W.G. et al., 1982. Wat. Res. 16:1207.
- Characklis, W.G. et al., 1983. "Influence of Biofouling and Biofouling Control Techniques on Corrosion of Copper-Nickel Tubes," presented at CORROSION/83, Anaheim, CA.
- Characklis, W.G., M.J. Nimmons, and B.F. Picologlou. 1981. Heat Transfer Engineering, 3:23-37.
- Characklis, W.G., F.L. Roe, and N. Zilver. 1982. "Method and Apparatus for Determining the Heat Transfer Characteristics of a Tube." U.S. Patent Application Serial No. 249.466.
- Characklis, W.G., M.G. Trulear, N. Stathopoulos, and L.C.

- Chang. 1980. In Water Chlorination: Environmental Impact and Assessment, Vol. 3 (Jolley, R.L., ed), Ann Arbor Science, Ann Arbor, MI, 349-368.
- Characklis, W.G. and N. Zilver. 1983. Biofilm Development and Control in Simulated Shipboard Condenser Tubes. Final report submitted to David Taylor Naval Ship Research and Development Center, 203 pp.
- Characklis, W.G., N. Zilver, and M. Turakhia. 1981a. "Microbial Films and energy Losses," Symposium on Marine Biodeterioration, Office of Naval Research, Bethesda, MD.
- Characklis, W.G., N. Zilver, M. Turakhia, and F.L. Roe. 1981b. Proc. 42nd Int. Water Conference, Pittsburgh, PA.
- Chenoweth, J.M. and M. Impagliazzpio (Eds.). 1981. Fouling in Heat Exchange Equipment, ASME, HTD-Vol; 17, New York, NY.
- Cleaver, J.W. and B. Yates. 1975. Chem. Engrg. Sci. 30:983-992.
- Cleaver, J.W. and B. Yates. 1976. Chem. Engr. Sci. 31:147-151.
- Colburn, A.P. 1933. Trans. A.I.Ch.E., Vol. 29, p. 174.
- Compton, K.G. 1973. "Corrosion Reactions in Natural Sea Water as Compared to Reactions in Various Synthetic Saline Corrosive Media," paper No. 9 presented NACE Corrosion/73, Anaheim, CA.
- Cooksey, K.E. 1981. Appl. Environ. Microbiol., 41:1378-1382.
- Cooksey, B., and K.E. Cooksey. 1980. Plant Physiol., 65:129-131.
- Corpe, W.A. 1970. In "Adhesion in Biological Systems," (R.S. Manly, Ed.) pp. 73-87. Academic Press, New York.
- Corpe, W.A., L. Matsuuchi, and B. Armbuster. 1976. In Proc. Third Int. Biodgr. Symp. (J.M. Sharpley and A.M. Kaplan, Ed.) pp. 433-442. Applied science, London.
- Corpe, W.A. 1977. In Proceedings of the Ocean Thermal Energy Conversion (OTEC) Biofouling and Corrosion Symposium, Ed. R.H. Grey, DOE, Washington, DC, pp.31-34.
- Costerton, J.W., G.G. Geesey, and K.J. Cheng. 1978. Sci. American. 238:86-95.

- Costerton, J.W., R.T. Irwin, K.J. Cheng. 1981. Annu. Rev. Microbiol., 35:299-324.
- Cowan, J.C. and D.J. Weintritt. 1976. Water-Formed Scale Deposits, Gulf Publishing Corp., Houston, TX.
- Culp, L.A. and P.H. Black. 1972. Biochem., 11:2161-2172.
- Culp, L.A. R.A. Murray, and B.J. Rollins. 1979. J. Supramole. Struct., 11:401-427.
- Daniel, G.F., A.H.L. Chamberlain, E.B.G. Jones. 1980. Helgolander Wiss. Meeresunters. 34:123-149.
- Daniels, S.L. 1980. In Adsorption of Microorganisms to Surfaces. (G. Bitton and K.C. Marshall, Eds.) pp. 8-58. Wiley, New York.
- Dehart, R. 1979. Personal communication.
- DePalma, V.A., D.W. Goupil, and C.K. Akers. 1979. Paper presented at 6th OTEC Conf., Washington, DC.
- Derby, R.L. 1947. Journal of American Water Works Association, 39:1107-1114.
- Derjaguin, B.V., and L. Landau. 1971. Acta Physicochim. (USSR), 14:633-662.
- Dexter, S.C. 1974. Microbiological Fouling and Its control in Coastal Water and the Deep Ocean, Woods Hole Oceanographic Institution Report No. WHOI-74-64.
- Dexter, S.C., J.D., Sullivan, J. Williams, and S.W. Watson. 1975. Appl. Microbiol. 30:298-308.
- Dexter, S.C. 1977. "Some New Possibilities for Biofouling Control", OTEC Biofouling and Corrosion Symposium, Seattle, WA.
- Drew Chemical Corp. 1979. Publishers, "Principles of Industrial Water Treatment", pp. 79-96.
- Disalvo, L.H. 1973. Limnol. Oceanogr., 18:165-168.
- Dolowy, K. 1980. In "Cell Adhesion and Motility." (A.S.G. Curtis and J.D. Pitts, Eds.) pp. 39-63. Cambridge University Press, Cambridge, U.K.
- Edgar, L.A. and J.D. Pickett-Heaps. 1982. Protoplasma. 113:10-22.
- Efird, K.D. 1975. "The Interrelation of Corrosion and Fouling of Metals in Sea Water," paper presented NACE

Corrosion/75, Toronto.

- Efird, K.D. 1977. CORROSION, Vol. 33, No. 1.
- Efird, K.D. and D.B. Anderson. 1975. Materials Performance, Vol. 14, No. 11.
- Epstein, N. 1981. In Fouling of Heat Transfer Equipment (Somerscales and Knudsen, Eds.) pp. 31-53, Hemisphere Publishing Corp., Washington, DC.
- Fischer, E. 1980. Unpublished results.
- Fletcher, M. and G.D. Floodgate. 1973. J. Gen. Microbiology, 24:325.
- Fletcher, M. 1976. J. Gen. Microbiol., 94:400:404.
- Fletcher, M. 1980. In Bacterial Adherence, (E.H. Beachey, Ed.) pp. 347-374. Chapman and Hall, London.
- Fletcher, M. and K.C. Marshall. 1982. Appl. Environ. Microbiol., 44:184-192.
- Friedlander, S.K. and H.F. Johnstone. 1957. Ind. Engrg. Chem. 49:1151-1156.
- Fowler, H.W. and A.J. McKay. 1980. In Microbial Adhesion to Surfaces, (Berkeley, Lynch, Melling, Rutter, and Vincent, Eds.). Ellis Horwood Ltd., Chichester, England.
- Garey, J.F., R.M. Jordan, A.H. Aitken, D.J. Burton and R.H. Gray (Eds.). 1980. Condenser Biofouling Control, Ann Arbor Science Publisher, Inc., Ann Arbor, MI.
- Geesey, G.G. American Society for Microbiology News, 48:9-14.
- Gibbons, R.J. 1980. In Microbial Adhesion to Surfaces, (R.C.W. Berkeley, J.M. Lynch, J. Melling, P.R. Rutter and B. Vincent, Eds.), pp. 351-388. Ellis-Horwood, Chichester.
- Gingell, D. and S. Vince. 1980. In Cell Adhesion and Motility, (A.S.G. Curtis and L.D. Pitts, Eds.) pp. 1-37. Cambridge University Press, Cambridge, UK.
- Graham, J. 1982. Biofouling Control Assessment-A Preliminary Data Base Analysis. Electric Power Research Institute, EPRI CS-2469, Contract TPS 80-739, Final Report, Palo Alto, CA, 235 pp.
- Grinnell, F., M. Milam, and P.A. Srere. 1972. Arch. Biochem. Biophys., 153:193-198.

- Haag, W.R. and M.H. Lietzke. 1980. In Water Chlorination: Environmental Impact and Health Effects, Vol. 3, R.L. Jolley, W.A. Brungs, and R.B. Cumming, Eds. (Ann Arbor, MI: Ann Arbor Science Publishers, Inc.), pp.415-426.
- Hall, L.W.Jr., G.R. Helz, and D.T. Burton. 1981. Power Plant Chlorination: A Biological and Chemical Assessment, Ann Arbor, MI: Ann Arbor Science Publishers in cooperation with Electric Power Research Institute (EPRI EA-1750).
- Harper, M.A. 1977. In "The Biology of the Diatoms," (D. Werner, Ed.) pp. 224-249. California University Press, Berkeley, CA.
- Harper, M.A. and Harper, J.F. 1967. Br. Phycol. Bull., 3: 195-207.
- Harrick, N.J. 1967. Internal Reflection Spectroscopy. Interscience, New York.
- Harty, D.W.S. and Bott, T.R. 1981. In Fouling of Heat Transfer Equipment (Somerscales, E.F.C. and Knudsen, J.G., Eds.), Hemisphere Publishing Corp., Washington, D.C., 334-344.
- Hasson, D. 1981. In Fouling of Heat Transfer Equipment (Somerscale and Knudsen, Eds.), p. 527, Hemisphere Publishing Corp., Washington, DC.
- Helz, G.R., R. Sugam, and R.Y. Hsu. 1978. In Water Chlorination: Environmental Impact and Health Effects, Vol. 2, R.L. Jolley, H. Gorchev, and D.H. Hamilton, Jr., Eds. (Ann Arbor, MI: Ann Arbor Science Publishers, Inc.), p209.
- Herbert, D. 1961. Symp. Soc. Gen. Microbiol. 11:391-416.
- Heukelekian, H. 1956. Sewage Ind. Wastes, 28:206-210.
- Hobbie, J.E., J.E. Daley, and S. Jasper. 1977. App. Environ. Microbiol. 33:1225-1228.
- Hopkins, J.T. and R.W. Drum. 1966. Br. Phycol. Bull. 3:63-67.
- Howell, J.A. and B. Atkinson. 1976. Water Res. 10:307-315.
- Huguenin, J.E. and F.J. Ansuini. 1980. "The Design, Construction, Testing and Evaluation of Copper Based Commercial Prototype Equipment for Use in Marine Aquaculture," International Copper Research Association, Inc. Technical Paper, NY.

- Hullinger, C.H. 1963. In Methods in Carbohydrate Chemistry, R.L. Whistler and M.L. Wolfram, Eds. Vol. II, Academic Press, New York, pp. 313-315.
- Humphrey, B.A., M.R. Dickson, and K.C. Marshall. 1979. Arch. Microbiol., 120:231-238.
- Hungate, R.E. 1975. Annu. Rev. Ecol. Syst. 6:29-66.
- Huntsman, S.A. and H.H. Stonecker. 1971. J. Phycol. 7:261-264.
- Iverson, W.F. 1981. "An Overview of the Anaerobic Corrosion of Underground Metallic Structures, Evidence for a New Mechanism," ASTM Special Technical Publication 741, pp. 33-52.
- Jolley, R.L., W.W. Pitt, Jr., F.G. Taylor, S.J. Hartmann, G. Jones, Jr., and J.E. Thompson. 1978. In Water Chlorination: Environmental Impact and Health Effects, Vol. 2, R.L. Jolley, H. Gorchev, and D.H. Hamilton, Jr., Eds. (Ann Arbor, MI: Ann Arbor Science Publishers, Inc.), pp.695-706.
- Jones, H.C., I.L. Roth, and W.M. Sanders. 1969. J. Bacteria, 99:316-325.
- Kaspar, H.F. and K. Wuhrmann. 1978. Appl. Environ. Microbiol. 36:1-7.
- Kern D.O. and R.G. Seton. Chemical Engineering Progress, 55:59-65, No. 6.
- King, R.A., C.K. Dittmer, and J.D.A. Miller. 1976. British Corrosion Journal, 11:105.
- King, R.A., J.D.A. Miller, and J.S. Smith. 1973. British Corrosion Journal, 8:137.
- Kobrin, G. 1976. Materials Performance pp. 38-43.
- Kreith, F. 1973. Principles of Heat Transfer, 3rd ed., pp. 571-573, Harper and Row, Publishers, Inc., New York.
- LaQue, F.L. 1950. Discussion Corrosion, 6.
- Lewin, J.C. 1955. J.Gen. Microbiol., 13:162-169.
- Lewin, J.C., R.A. Lewin, and D.E. Philpott. 1958. J. Gen. Microbiol. 18:418-426.
- Lewin, R.A. 1965. Canad. J. Microbiol., 11:77-86.
- Lewis, R.O. 1980. "Biofouling Control for OTEC: A. Test of

a Macro-Fouling Control Device; B. Selection of Promising Methods for Maintaining Heat Transfer Surface," presented at the 7th Ocean Energy Conference, Washington, DC.

- Lewis, R.O. 1982a. Material Performance, September, pp.31-38.
- Lewis, R.O. 1982b. Personal communication.
- Lin, C.S., R.W.Moulton, and G.L. Putnam. 1953. Ind. Engrg. Chem. 45:636-640.
- Lister, M.W. 1956. Can. J. Chem. 34, 479-488.
- Lister, D.H. 1979. In Fouling of Heat Transfer Equipment, (E.F.S. Somerscales, and J.G. Knudsen, Eds.) pp. 135-200. Hemisphere, Washington, DC.
- Loeb, G.I., and Neihof, R.A. 1975. In Applied Chemistry at Protein Interfaces (R.E. Baier, ed.), Washington, D.C., American Chemical Society, pp. 319-335.
- Lovely, D.R., D.F. Dwyer, and M.J. Klug. 1982. Appl. Environ. Microbiol. 43:1373-1379.
- Lund, D. and C. Sander. 1981. In Fouling of Heat Transfer Equipment (Somerscales and Knudsen, Eds.) pp. 437-476, Hemisphere Publishing corporation, Washington, DC.
- Lundgren, D.G. and M. Silver. 1980. Ann. Rev. Microbiol., 34, 263-283.
- Mangum, D.C. and Shepherd, B.F. 1973. Methods of Controlling Marine Fouling in Sea Water Desalination Plants. Office of Saline Water, U.S. Dept. of Interior, Final Report, Contract No. 14-30-2829, 124 pp.
- Mara, D.D. and D.J.A. Williams. 1972. In Biodeterioration of Materials, (A.H. Walters and E.H. Hueck-Van der Plas, Eds.) 2:103-113, Applied Science Publishers Ltd., London.
- Marine Research, Inc. 1976. Final Report on Possible Alternatives to Chlorination for Controlling Fouling in Power Station Cooling Water Systems, Marine Research, Inc., April.
- Marshall, K.C. 1979. In Strategies of Microbial Life in Extreme Environments, (M. Shilo, Ed.) 13:281-290. Dahlem Konferenzen Life Sciences Research Report. Verlag Chemie.
- Marshall, K.C. 1980. In Adsorption of Microorganisms to Surfaces, (G. Bitton and K.C. Marshall, Eds.) pp. 1-5.

- Wiley, New York.
- Marshall, K.C. R. Stout, and R. Mitchell. 1971. J. Gen. Microbiol. 68:337-348.
- Matson, J. V., and W.G. Characklis. 1967. Water Res., 10, 877-885.
- Matson, J.V., and W.G. Characklis. 1982. Cooling Tower Institute, TP-250-A.
- Matson, J.V. and W.G. Characklis. 1983. J. Cooling Tower Inst., 4:27-32.
- McIntire, L.V., Kirkpatrick, J.P. and Characklis, W.G. 1983. Manuscript in preparation.
- Meadows, F.S. 1971. Arch. Mikrobiol., 75:374-381.
- Metcalf and Eddy. 1972. Wastewater Engineering, McGraw Hill, Inc.
- Mian, F.A., et al. 1978. J. Bacteriology, pp. 134-418.
- Miller, J.D.A. 1978. In Economic Microbiology, (A.H. Rose, Ed.) 6:150-202, Academic Press, London and New York.
- Miller, P.C. and T.R. Bott 1981. The Removal of Biological Films using Sodium Hypochlorite Solutions. Progress in the Prevention of Fouling in Industrial Plant, Corrosion Science Div., Institution of Corrosion Science and Technology, Nottingham University, Nottingham, England, 121-136.
- Minkus, A.J. 1954. Journal of New England Water Works Association, 68:1-10.
- Moss, R.D., H.B. Flora II, R.A. Hiltunen, C.V. Seaman, N.D. Moore, S.H. Magliente. 1979. "A Chlorine Minimization/Optimization Study for Condenser Fouling Control," presented at the Third Conference on Water Chlorination: Environmental Impact and Health Effects, Colorado Springs, CO, October.
- Mountfort, D.O., R.A. Asher, E.L. Mays, and J.m. Tiedje. 1980. Appl. Environ. Microbiol. 39:686-694.
- Mueller, J.A., et al. 1966. Proc. 21st Annu. Purdue Industrial Waste Conf. pp.962-995.
- Nikuradse, J. 1932. Ver Deutsch. Ing. Forsch. 356,21.
- Nimmons, M.J. 1979. M.S. Thesis, Rice University, Houston, 1979.

- Nishikawa, S. and M. Kuriyama. 1968. Water Res., 2:811-812.
- Norrman, G., W.G. Characklis, and J.D. Bryers. 1977. Dev. Ind. Microbiol. 18, 581-590.
- North, R.F. and M.J. Pryor. 1970. Corrosion Science. 10:297-311.
- Nosetani, T. et al. 1979. In Fouling of Heat Transfer Equipment (Somerscales and Knudson, Eds.) pp. 345-353.
- Nosetani, T.S., K. Sato, and J. Kashiwada. 1979. Effect of Marine Biofouling on the Heat Transfer Performance of Titanium condenser Tubes, Suitomo Light Metal Industries Ltd., Technical Research Laboratories.
- Novak, L. 1982. J. Heat Transfer, 104, 663-669.
- Olden, K., L.H.E. Hahn, and K.M. Yamada. 1980. In Cell Adhesion and Motility, (A.S.G. Curtis and J.D. Pitts, Eds.) pp. 257-287. Cambridge University Press, Cambridge.
- Olsen, E. and W. Szybalski. 1950. Corrosion, 6:405-414.
- Olson, R.M. 1973. Essentials of Engineering Fluid Mechanics, Intest Educational Publishers, New York, NY.
- Pethica, B.A. 1961. Expt. Cell. Res., Supp. 8, pp. 123-140.
- Pethica, B.A. 1980. In Microbial Adhesion to Surfaces, (R.C.W. Berkeley, J.M. Lynch, J. Melling, F.R. Rutter and B. Vincent, Eds.) pp. 19-45. Ellis-Horwood, Chichester.
- Picologlou, B.F., et al. 1980. Biofilm Growth and Hydraulic Performance, J. Hyd. Div., ASCE 106, p. 733.
- Postgate, J.R. 1979. The Sulphate-Reducing Bacteria, Cambridge University Press, Cambridge.
- Powell, M.S. and N.K.H. Slater. 1982. Biotech. Bioeng., 24:2527-2537.
- Powell, M.S. and N.K.H. Slater. 1983. Biotech. Bioeng., in press.
- Ridgway, H.F. and B.H. Olson. 1982. Chlorine Resistance Patterns of Bacteria from Two Drinking Water Distribution Systems, Applied and Environmental Microbiology, October, pp.972-987.

- Ritter, R.B. and J.W. Sutor. 1976. Fouling Research on Copper and Its Alloys-Sea Water Studies, International Copper Research Association, Inc. Technical Paper.
- Roe, F.L. and W.G. Characklis. 1982. A Systematic Approach to Fouling Control. Presented at International Conference on Fouling of Heat Exchange Surfaces, White Haven, PA, 18 pp.
- Rogers, H.J. 1979. In Adhesion of Microorganisms to Surfaces, (D.C. Ellwood and S. Melling, Eds.) pp. 29-55. Academic Press, London.
- Rosen, J.J. and L.A. Culp. 1977. Exp. Cell Res., 107:139-149.
- Rosenberg, M., E.A. Bayer, J. Delarea, E. Rosenberg. 1982. Appl. Environ. Microbiol., 44:929-937.
- Rouhiainen, P.O. and J.W. Stachiewicz. 1970. J. Heat Transfer (Trans. ASME), 92:169-177.
- Roux, W. 1894. Arch. Entwickl. Merch. Org. 1:43-68.
- Rutter, P.R. 1980. In Cell Adhesion and Motility. (A.S.G. Curtis and J.D. Pitts, Eds.) pp. 103-135. Cambridge University Press, Cambridge.
- Rutter, P.R. and B. Vincent. 1980. In Microbial Adhesion to Surfaces, (R.C.W. Berkeley, J.M. Lynch, J. Melling, P.R. Rutter and B. Vincent Eds.) pp. 79-92. Ellis-Horwood, Chichester.
- Salvarezza, R.C., M.F.L. DeMele, and H.A. Videla. 1983. Corrosion, NACE, Vol. 39, No. 1.
- Schaechter, M, O. Maaløe, and N.O. Kjeldgaard. 1958. J. Gen. Microbiol. 19:592-606.
- Schlichting, H. 1968. Boundary Layer Theory, McGraw-Hill Book Co., New York, N.Y.
- Schuster, H. 1971. Ph.D. thesis, Johns Hopkins University, Baltimore, MD.
- Slots, J. and R.J. Gibbons. 1978. Infection and Immunity, 19:254-264.
- Smith, J.S. 1980. Ph.D. thesis, University of Manchester, England.
- Smith, J.S. and J.D.A. Miller. 1974. British Corrosion Journal, 10:136.
- Stainier, R.Y., E.A. Adelberg and J.L. Ingraham. 1976. The

- Microbial World, 4th ed., Prentice-Hall, NJ.
- Somerscales, E.F.C. 1981. In Fouling in Heat Exchange Equipment, ASME HTD 17, p. 17.
- Somerscales, E.F.C. and J.G. Knudsen (Eds.). 1981. Fouling of Heat Transfer Equipment, Hemisphere Publishing Corporation, Washington, DC.
- Stathopoulos, N. 1981. M.S. Thesis, Rice University, Houston, TX, 107 pp.
- Stewart, W.C. and F.L. LaQue. 1952. Corrosion, Vol. 8, No. 8.
- Sugam, R. and G.R. Helz. 1980. In Water Chlorination: Environmental Impact and Health Effects, Vol. 3, R.L. Jolley, W.A. Brungs, and R.B. Cumming, Eds. (Ann Arbor, MI: Ann Arbor Science Publishers, Inc.), pp.427-433.
- Sutherland, I.W. 1980. In Microbial Adhesion to Surfaces, (R.C.W. Berkeley, J.M. Lynch, J. Melling, F.R. Rutter, and B. Vincent, Eds.) pp. 329-336. Ellis-Horwood, Chichester, U.K.
- Taborek, J., T. Aoki, R.B., Ritter, J.W. Palen and J.G. Knudsen. 1972. Chemical Engineering progress, Vol. 68, No. 2, pp. 59-67.
- Tain K.T. and R.K. Finn. 1977. In Extracellular Microbial Polysaccharide, pp. 58-80, (P.A. Sandford and A. Laskin, Eds.) A.C.S. Symposium series 45 Washington, DC.
- Tatnall, R.E. 1981. "Fundamentals of Bacteria Induced Corrosion," Materials Performance.
- Terry, A.H. and L.A. Culp. 1974. Biochem. 13:414-425.
- Thomas, T.R. (Ed.). 1982. Rough Surfaces, Longman Group Limited, London., 261 pp.
- Timperley, D. 1981. Proceedings, Fundamentals and Applications of Surface Phenomena Associated with Fouling and Cleaning in Food Processing (B. Hallstrom, D.B. Lund, Ch. Tragardh, Eds.), Dept. of Food Science, University of Wisconsin, Madison, WI, 402-412.
- Trabalca, J.R., and M.B. Burch. 1980. In Water Chlorination: Environmental Impact and Health Effects, Vol. 2, R.L. Jolley, H. Gorchev and D.H. Hamilton, Jr., Eds. (Ann Arbor, MI: Ann Arbor Science Publishers, Inc.), pp.163-173.
- Trulear, M.G. 1980. M.S. thesis, Rice University, Houston

Tx.

- Trulear, M.G. 1983. Ph.D. thesis Montana State University.
- Trulear, M.G. and W.G. Characklis. 1982. Journal WQCF. 54:1288-1301.
- Tunahia, M. 1982. Unpublished results.
- Verwey, E.J.W. and J.T.G. Overbeek. 1948. Theory of the Stability of Lyophobic Colloids, Elsevier, Amsterdam.
- Waite, T.D. and Fagan, J.R. 1980. In Condenser Biofouling Control (J.F. Garey, et al., Eds.), Ann Arbor Science, Ann Arbor, MI, 441-462.
- Watkinson, A.P. and N. Epstein. 1969. Chem. Eng. Prog. Symposium Series, Vol. 65, No. 92.
- Webster, D.R., D.E. Cooksey and R.W. Rubin. 1982. American Society for Cell Biology, Abstracts of Annual Meeting, Baltimore, MD.
- Weiss, G.B. 1974. Annu. Rev. Pharmacol., 14:343-354.
- Weiss, L., and J.P. Harlos. 1977. In Intercellular Communications, (W.C. DeMello, Ed.) pp. 33-59. Plenum, NY.
- Wells, A.C. and Chamberlain, A.C. 1967. Br.J. Appl. Phys., 18:1793-1799.
- Whistler, R.L., Linke, E.G. and Kazeniak, S. 1956. Journal of American Chemical Society, Vol. 78, No. 18, pp. 4704-4709.
- Whistler, R.L. and Schweiger, R. 1957. Journal of American Chemical Society, Vol. 79, No. 24, Dec., pp. 6460-6464.
- White, G.C. 1972. In Handbook of Chlorination, Van Nostrand-Reinhold, New York.
- Widerhold, W. 1949. Gas Wass Fach., 90:634-641.
- Williams, A.G. and J.W.T. Wimpenny. 1978. J. Gen. Microbiology, 47:107.
- Williamson, K.J., and P.L. McCarty. 1976. J. Water Poll. Control Fed., 48:281-296.
- Wilson, E.E. 1915. trans. A.S.M.E., 37:47.
- Wong, G.T.F. 1980. In Water Chlorination: Environmental Impact and Health Effects, Vol. 3, R.L. Jolley, W.A. Brungs, and R.B. Cumming, Eds. (Ann Arbor, MI: Ann

- Arbor Science Publishers, Inc.), pp.395-406.
- Wyss, O. 1962. Water and Sewage Works, 109 (12), R155-R158
- Zelver, N. 1979. M.S. Thesis, Rice University, Houston, TX.
- Zelver, N. et al. 1981. "Biofouling Control with UV/Peroxide," presented at AWWA "Water Reuse Symposium II," Washington, DC.
- Zelver, N., J.R. Flandreau, W.H. Spataro, K.R. Chapple, W.G. Characklis, and F.L. Roe. 1982. "Analysis and Monitoring of Heat Transfer Tube Fouling," ASME Paper No. 82-JPGC/Pwr-7.
- Zielke, R.L. and S.K. Macey. 1980. In Water Chlorination: Environmental Impact and Health Effects, Vol.3, R.L. Jolley, W.A. Brungs, and R.B. Cumming, Eds. (Ann Arbor, MI: Ann Arbor Science Publishers, Inc.), pp.445-451.
- Zimmerman, R. and Meyer-Reil. 1974. Kiel Meeresforsch, 30:24-27.
- Zisman, W.A. 1964. In (F.M. Fowkes, Ed.). Advances in Chemistry Series, 43. pp. 1-51. American Chemical Society, Washington, DC.
- Zobell, C.E. 1943. J. Bacteriol., 46:39-59.

## DISTRIBUTION LIST

### HEAT TRANSFER/BIOLOGICAL FOULING

Mr. M. Keith Ellingsworth  
Power Program  
Office of Naval Research  
800 N. Quincy Street  
Arlington, VA 22217  
\*5

CDR Ronald C. Tipper  
Director, Ocean Biology Program  
Office of Naval Research  
NSTL Station, MS 39529  
\*5

Defense Documentation Center  
Bldg. 5, Cameron Station  
Alexandria, VA 22314  
\*12

Technical Information Division  
Naval Research Laboratory  
4555 Overlook Avenue SW  
Washington, DC 20375  
\*6

Professor Paul Marto  
Chairman, Mechanical Engineering Dept.  
U.S. Naval Post Graduate School  
Monterey, CA 93940

Professor Eugene C. Haderlie  
Department of Oceanography  
U.S. Naval Post Graduate School  
Monterey, CA 93940

Professor Bruce Rankin  
Naval Systems Engineering  
U.S. Naval Academy  
Annapolis, MD 21402

Office of Naval Research Eastern/Central  
Regional Office  
Bldg. 114, Section D  
666 Summer Street  
Boston, MA 02210

Office of Naval Research Branch Office  
536 South Clark Street  
Chicago, IL 60605

Office of Naval Research  
Western Regional Office  
1030 East Green Street  
Pasadena, CA 91106

Dr. George I. Loeb  
Marine Biology Branch  
Ocean Sciences Division  
Naval Research Laboratory  
4555 Overlook Avenue  
Washington, DC 20375

CDR Bill Marsh  
Code 05DC3  
Naval Sea Systems Command  
Washington, DC 20362

Mr. Charles Miller, Code 05R13  
Crystal Plaza #6  
Naval Sea Systems Command  
Washington, DC 20362

Heat Exchanger Branch, Code 5223  
National Center #3  
Naval Sea Systems Command  
Washington, DC 20362

---

\*One copy except as noted.

Mr. Ed Ruggiero, NAVSEA 08  
National Center #2  
Washington, DC 20362

Dr. Eugene Fischer, Code 2853  
David Taylor Ship R&D Center  
Annapolis, MD 21402

Mr. Wayne Adamson, Code 2722  
David Taylor Ship R&D Center  
Annapolis, MD 21402

Mrs. Brenda J. Little  
Naval Oceanographic R&D Activity  
NSTL  
Bay St. Louis, MS 39522

Mr. John Depalma  
Bldg. 1105  
Naval Oceanographic Division  
NSTL  
Bay St. Louis, MS 39520

Mr. Daniel F. Lott  
Code 793  
Naval Coastal Systems Laboratory  
Panama City, FL 32407

Dr. Win Aung  
Heat Transfer Program  
National Science Foundation  
Washington, DC 20550

Mr. Michael Perlsweig  
Department of Energy  
Mail Station E-178  
Washington, DC 20545

Dr. W. H. Theilbahr  
Chief, Energy Conservation Branch  
Dept. of Energy, Idaho Operations Office  
550 Second Street  
Idaho Falls, ID 83401

Professor Ephriam M. Sparrow  
Department of Mechanical Engineering  
University of Minnesota  
Minneapolis, MN 55455

Professor J. A. C. Humphrey  
Department of Mechanical Engineering  
University of California, Berkeley  
Berkeley, CA 94720

Professor Brian Launder  
Thermodynamics and Fluid Mechanics Div.  
University of Manchester  
Institute of Science & Technology  
PO88 Sackville Street  
Manchester M601QD England

Professor Shi-Chune Yao  
Department of Mechanical Engineering  
Carnegie-Mellon University  
Pittsburgh, PA 15213

Professor K. E. Cooksey  
Rosenthal School of Marine and Atmospheric  
Science  
University of Miami  
Miami, FL 33149

Professor Stephen C. Dexter  
College of Marine Studies  
University of Delaware  
Lewes, DE 19958

Professor Sol M. Gerchakov  
School of Medicine  
University of Miami  
Miami, FL 33152

Professor Arthur E. Bergles  
Mechanical Engineering Department  
Iowa State University  
Ames, IA 50011

Professor Kenneth J. Bell  
School of Chemical Engineering  
Oklahoma State University  
Stillwater, OK 74074

Dr. James Lorenz  
Component Technology Division  
Argonne National Laboratory  
9700 South Cass Avenue  
Argonne, IL 60439

Dr. David M. Eissenberg  
Oak Ridge National Laboratory  
PO Box Y, Bldg. 9204-1, MS-0  
Oak Ridge, TN 37830

Dr. Jerry Taborek  
Technical Director  
Heat Transfer Research Institute  
1000 South Fremont Avenue  
Alhambra, CA 91802

Dr. Simion Kuo  
Chief, Energy Systems  
Energy Research Laboratory  
United Technology Research Center  
East Hartford, CN 06108

Mr. Jack Yampolsky  
General Atomic Company  
PO Box 81608  
San Diego, CA 92138

Mr. Ted Carnavos  
Noranda Metal Industries, Inc.  
Prospect Drive  
Newtown, CN 06470

Dr. Ramesh K. Shah  
Harrison Radiator Division  
General Motors Corporation  
Lockport, NY 14094

Dr. Ravi K. Sakhuja  
Manager, Advanced Program  
Thermo Electron Corporation  
101 First Avenue  
Waltham, MA 02154

Professor Charles B. Watkins  
Chairman, Mechanical Engineering Dept.  
Howard University  
Washington, DC 20059

Professor Adrian Bejan  
Department of Mechanical Engineering  
University of Colorado  
Boulder, CO 80309

Professor Donald M. McEligot  
Dept. of Aerospace and Mechanical  
Engineering  
Engineering Experiment Station  
University of Arizona  
Tucson, AZ 85721

Professor Paul A. Libby  
Dept. of Applied Mechanics and Engineering  
Sciences  
PO Box 109  
La Jolla, CA 92037

Professor C. Forbest Dewey, Jr.  
Fluid Mechanics Laboratory  
Massachusetts Institute of Technology  
Cambridge, MA 02139

Professor William G. Characklis  
Dept. of Civil Engineering and Engineering  
Mechanics  
Montana State University  
Bozeman, MT 59717

Professor Ralph Webb  
Department of Mechanical Engineering  
Pennsylvania State University  
208 Mechanical Engineering Bldg.  
University Park, PA 16802

Professor Warren Rohsenow  
Mechanical Engineering Department  
Massachusetts Institute of Technology  
77 Massachusetts Avenue  
Cambridge, MA 02139

Professor A. Louis London  
Mechanical Engineering Department  
Bldg. 500, Room 501B  
Stanford University  
Stanford, CA 94305

Professor James G. Knudsen  
Associate Dean, School of Engineering  
Oregon State University  
219 Covell Hall  
Corvallis, OR 97331

Mr. Robert W. Perkins  
Turbotec Products, Inc.  
533 Downey Drive  
New Britain, CN 06051

Dr. Keith E. Starnes  
York Division, Borg-Warner Corp.  
PO Box 1592  
York, PA 17405

Mr. Peter Wishart  
C-E Power Systems  
Combustion Engineering, Inc.  
Windsor, CN 06095

Mr. Henry W. Braum  
Manager, Condenser Engineering Dept.  
Delaval  
Front Street  
Florence, NJ 08518

Dr. Thomas Rabas  
Steam Turbine-Generator Technical  
Operations Division  
Westinghouse Electric Corporation  
Lester Branch  
PO Box 9175 N2  
Philadelphia, PA 19113

Professor Daryl Metzger  
Chairman, Mechanical & Energy Systems  
Engineering  
Arizona State University  
Tempe, AZ 85281

ATE  
LMED  
8